PRECLINICAL PHARMACOKINETICS OF ANTI-INFECTIVE AGENTS

By

DAWEI LI

(Under the Direction of Catherine A. White)

ABSTRACT

Pharmacokinetics is the characteristic interactions of a drug and the body in terms of its absorption, distribution, metabolism and excretion (ADME). Pharmacokinetic related evaluations have been widely applied as one powerful tool to enhance the information gain and the efficiency of the decision making process during drug development. Preclinical pharmacokinetics refers to all *in vivo* and *in vitro* pharmacokinetic evaluations supporting drug development, which plays a major role in candidate compounds screening in early stage of drug development. In this dissertation, preclinical pharmacokinetic evaluations were performed to investigate pharmacokinetic properties of anti-infective agents, including an anti-parasitic agent ((1-Decyl)triphenylphosphonium bromide, dTPP), an anti-tuberculosis agent (Two-(Hydroxymethyl)phenylboronic acid cyclic monoester, OH49) and an anti-viral agent (L-β-5-Bromovinyl-[2-(2'-amino-3'-methtyl-butanoyloxy)methyl]-1, 3-(dioxolanyl) uracil, L-BHDU). Simple, rapid, and sensitive HPLC methods were developed and validated for the quantification of these compounds in plasma and tissues. The *in vivo* pharmacokinetic

and tissue distribution studies of dTPP and OH 49 were performed in mice. These pharmacokinetic studies showed that both dTPP and OH49 have low bioavailability, short elimination half-life, rapid clearance from the plasma and wide tissue distribution. The *in vitro* stability study showed that L-BHDU is substrate of esterase, which may affect pharmacokinetic profiles of L-BHDU *in vivo*. These pharmacokinetic study results would offer supportive information for the decision making of further drug development.

INDEX WORDS Preclinical pharmacokinetics Anti-infective agents Anthelmintics Anti-tuberculosis Antivirus

PRECLINICAL PHARMACOKINETICS OF ANTI-INFECTIVE AGENTS

By

DAWEI LI

B.S., Xiamen University, China, 2000

M.S., Peking Union Medical College, China, 2004

A Dissertation Submitted to the Graduate Faculty of the University of Georgia in Partial Fulfillment of the Requirements for the Degree

DOCTOR OF PHILOSOPHY

ATHENS, GEORGIA

2014

PRECLINICAL PHARMACOKINETICS OF ANTI-INFECTIVE AGENTS

By

DAWEI LI

Major Professor: Catherine A. White

Committee: James V. Bruckne

Jason Zastre

Randall L. Tackett

Electronic Version Approved

Maureen Grasso

Dean of the Graduate School

The University of Georgia

May 2014

DEDICATION

I would like to dedicate this dissertation to my loving and supportive parents, Shengli Li and Shuzhi Liang, my wife, Yin Gu.

ACKNOWLEDGEMENTS

First of all, I am greatly appreciative of my parents, Shengli Li and Shuzhi Liang for their endless love and support throughout my life. To Yin Gu, thank you for your encouragement and being such a wonderful wife. I would like to thank other relatives and friends for their love and support. I am also thankful to my major professor Dr. Catherine A. White for her guidance and support throughout my PhD program. I am very grateful to my committee members: Dr. James V. Bruckner, Dr. Jason Zastre and Dr. Randall L. Tackett for their advice and encouragement. I would also like to thank many of my friends in PBS and my lab-mates; Shawn, Liang, Bo for their assistance, encouragement, and stimulating conversations.

TABLE OF CONTENTS

Page

CHAPTER 1

INTRODUCTION

(1-Decyl)triphenylphosphonium bromide (dTPP) is an analog of MitoQ, which is a widely proven mitochondria-targeted antioxidant, consisting of a quinone moiety linked to a triphenylphosphonium (TPP) moiety by a 10-carbon alkyl chain. *In vitro* studies indicate that dTPP is a potential, broad-spectrum anthelmintic, with low toxicity and a novel mechanism of action. *In vivo* pharmacokinetic and tissue distribution study is described in chapter 3, including the development of an HPLC assay for quantification of dTPP in mouse plasma and tissues; and the pharmacokinetic evaluation of dTPP in mouse following oral, IV and subcutaneous administration.

Two-(Hydroxymethyl)phenylboronic acid cyclic monoester (OH49) is an analog of aryl boronic acid, some of which showed excellent antifungal, anti-inflammatory, antibiotic activity, and antiprotozoal activity. *In vitro* studies suggest that OH49 is a potential anti-tuberculosis agent. Chapter 4 describes an *in vivo* pharmacokinetic and tissue distribution study in the mouse. In this study, a simple, rapid and sensitive HPLC assay was developed for quantification of OH49 in mouse plasma and tissues. A pharmacokinetic evaluation of OH49 following IV and oral administration was performed in the mouse.

L-β-5-Bromovinyl-[2-(2'-amino-3'-methtyl-butanoyloxy)methyl]-1, 3-(dioxolanyl) uracil (L-BHDU) is a pro-drug of the anti-viral agent, L-β-5-Bromovinyl-(2-hydroxymethyl)-

1, 3-(dioxolanyl) uracil (L-BVOddU). Both of these compounds are L-nucleoside analogs. L-BHDU is designed to improve the metabolic activation of the parent compound (L-BVOddU). In chapter 5, a simple, rapid and sensitive HPLC assay was developed for the quantification of L-BHDU and L-BVOddU simultaneously in rat plasma. An *in vitro* stability study of L-BHDU was performed in human, rat and mouse plasma by using the validated HPLC assay.

CHAPTER 2

LITERATURE REVIEW

Preclinical Pharmacokinetics in Drug development

Introduction

Drug discovery and development is a very complex, costly, and time-consuming process. It requires a major investment of money, human resources and technological expertise. The search for new drugs can be divided functionally into two stages: discovery and development [1]. The discovery stage includes the identification of drug targets-typically through an understanding of the biological pathways of health and disease, medicinal chemistry, in which molecules are structured to attack such targets, establishment of suitable models to test biological activities, and screening new drug molecules for *in vitro* and/or *in vivo* biological activities. In the development stage, efforts are focused on the evaluation of the toxicity and efficacy of new drug candidates. The new drug development process can also be divided into four sequential stages, including discovery stage, preclinical development, clinical development and post-approval stage.

Recent statistics reveal that for every 5,000-10,000 potential compounds only 250 will progress to pre-clinical development, and of these, 5 will move forward into clinical development of which only a single compound will be approved by regulatory authorities for human use [2, 3]. Drug development from the synthesis of a compound to New Drug Application approval can take 10-20 years, with an estimated average of about 9-12 years. In addition, the length of this process has increased in the past 20 years [4, 5]. Data from

a variety of sources indicate that in the past two decades, the total R&D investment in pharmaceutical industry increased more than two fold, and biomedical research has progressed at a faster pace putting more and more new molecular entities on the drug development pathway, however, the rate of marketing approval has shown a declining trend [6-10]. As a result, the R&D cost per new drug has increased dramatically. In 1987, the R&D cost of a new drug was only $237 million as opposed to $802 million in 2000. Until 2003, this number increased to $1,700 million, and now, the estimated R&D cost per new drug is as high as $3.5-5.3 billion [2, 11-13]. One of the most apparent cost drivers in the R&D process is the failure to identify poor candidate compounds early in the development process, and the failure identification attributes to overall 75% of the total R&D costs [14]. Improving failure detection by even 10% before clinical trials could reduce R&D costs by $100 million per drug [15].

One important attribute of a drug is its pharmacokinetic profile. Suboptimal pharmacokinetics is stated to be one of main reasons for failures during drug development [16]. Pharmacokinetics is the study of the time course of drug ADME, and the multiple interrelationships affecting ADME, such as incomplete absorption, saturability in transport, biotransformation, or binding. [17]. Now, pharmacokinetic related evaluations have been widely applied in all stages of preclinical and clinical drug development (Fig 2.1), and has become one potential tool to enhance information gain and efficiency of the decision making process during drug development [18,19].

Pharmacokinetic study can broadly be divided into two areas: preclinical and clinical pharmacokinetics. Traditionally, “preclinical pharmacokinetics” referred to pharmacokinetics in animals. Today, the definition is expanded to all *in vivo* and *in vitro*

pharmacokinetic activities supporting drug development. Therefore, preclinical pharmacokinetic activities can be further divided into *in vitro* preclinical pharmacokinetics and *in vivo* preclinical pharmacokinetics.

In vitro Preclinical Pharmacokinetics

High-throughput Screening

High-throughput screening is a relevant, effective, fast, robust and accurate process to evaluate the physicochemical characteristics of a large number of chemicals, and obtain appropriate "drug-like" lead candidates for further pharmacokinetic evaluation [20]. There are several parameters or rules that can be applied as criteria for the high-throughput screening process:

Modified Absorption Potential (MAP)

In1985, Dressman et al. first introduced the concept of absorption potential, a dimensionless number indicating the fraction of an oral dose available to human liver via passive diffusion. Sanghvi et al (2001) developed this model as

$$MAP = \log [K_{ow} * S_w * V_L / D]$$

where, K_{ow} is the partition coefficient, S_w is the intrinsic solubility in water at 37°C, V_L is the volume of fluid in the gastric lumen (which is assumed to be 0.25 L), and D is the dose administered [21,22]. In practice, the analogs with the largest MAP are chosen for further development.

Polar Surface Area (PSA)

Polar surface area of a molecule is defined as the surface sum over all polar atoms, primarily oxygen and nitrogen, also including their attached hydrogens. It is another parameter that helps identify compounds with poor absorption potential. Analyzing

twenty compounds, Palm et al. found a highly predictive sigmoidal relationship between the fraction of dose absorbed in humans and the PSA of the molecule. Compounds with a PSA more than 140 $Å^2$ showed poor absorption potential [23, 24]. Kelder et al. further limited the PSA value to 120 (80) $Å^2$ for good oral bioavailability, by analyzing 1,590 orally administered non-CNS drugs and 776 orally administered CNS drugs [25].

Other rules

By studying the physicochemical properties of thousands of drugs from the World Drug Index (WDI), Lipinski et al. developed the so-called "Rule of Five" to predict oral bioavailability (intestinal absorption) of a compound [26, 27]. Based on this rule, poor absorption or permeability is more likely if the drug possesses any of the following properties or characteristics:

1. More than five H-bond donors (NH's or OH's)
2. The molecular weight is more than 500
3. The LogP (lipophilicity) is greater than 5
4. More than H-bond acceptors (N's or O's)

In addition, the solubility of the compound is considered as an additional rule, which requires the solubility of the drug in water to be greater than100 ug/mL. If two or more parameters are out of range, the candidate will not be selected for further development. One drawback of this method is that the Rule of Five is based on the physicochemical properties of the compounds and assumes drug absorption follows Fick's first law of diffusion. Therefore, if transporters facilitate the absorption of the compounds, these rules might not apply to them.

Another criterion for drug-likeness is the presence or absence of particular chemical groups and the amount of these groups. Veber et al. observed that compounds with ten or fewer rotatable bonds have a high gastrointestinal permeability rate indicating that compounds with lower molecular flexibility are more likely to have better oral absorption [28]. Oprea et al. analyzed compounds from the MDDR, Comprehensive Medicinal Chemistry (CMC), Current Patents Fast Alert, New Chemical Entities, and Available Chemicals Database (ACD) and limited the number of rotatable bonds as equal or less than 8, or rings in a molecule equal or less than 4 for high gastrointestinal permeability [29]. As a summary, table 2.1 shows a list of boundaries of prominent counting parameters mentioned above and some others such as, molar refractivity, heavy atoms, net charge.

In-Vitro Permeability assays

Oral delivery is without question the preferred route of administration for patients. Therefore successful therapy requires good intestinal absorption to ensure that sufficient drug can enter the systemic circulation. Permeability, together with solubility, are two major factors affecting the intestinal absorption of oral drugs. Solubility can be improved by formulation means. Permeability depends on the physicochemical properties of the molecule and is difficult to fix by formulation. Therefore, permeability evaluation is more important for candidate compound screening, especially at early stages in drug discovery and development.

Permeability models serve as tools in the drug candidate selection for further *in vitro* and *in vivo* studies. To obtain accurate prediction of the absorption profile of lead compounds, reliable and appropriate screening methods to assess intestinal permeability

are necessary (30-32). A variety of methods have been developed over the past decade to assess drug permeation across the gastrointestinal tract, including Caco-2 cells, artificial membranes and tissue-based assays. Each method has its own advantages and limitations to be considered when choosing models for permeability evaluation.

Caco-2 cell Assay

The Caco-2 system is one of the most extensively utilized assays for assessment of permeability. Although originally derived from a human colon adenocarcinoma, Caco-2 cells exhibit many primary-like qualities of enterocytes, both functional and morphological. When cultured as a monolayer, Caco-2 cells differentiate to form a brush border (microvilli) membrane with tight junctions between cells. In addition, this cell line has been shown to express various efflux transporters, microvillar transporters, hydrolases, and Phase II conjugation enzymes which are more representative of enterocytes of the small intestine. Caco-2 cells also express enzymes such as membrane peptidases and disaccharidase [33]. Therefore, the Caco-2 cell line is one of the most popular assays to model a variety of transcellular pathways as well as the metabolic transformation of test substances.

In many respects, the Caco-2 cell monolayer mimics the human intestinal epithelium. The Caco-2 system has some limitations, due to the minor difference from *in vivo* enterocytes. Firstly, in Caco-2 cells the expression of the cytochrome P450 isozymes is low or nonexistent, and in particular, CYP3A4, which is normally expressed at high levels in the intestine. Expression of CYP 3A4 in Caco-2 cells can be induced by treatment with vitamin D3 [34]. As a result, the gut wall metabolism of some compounds will be severely underestimated in the Caco-2 system. In addition, the tight junctions

formed in the Caco-2 system are less permeable than those in human intestinal epithelium. P-gp efflux pump is overexpressed in Caco-2 cells compared to levels measured *in vivo* with primary enterocytes [35]. Therefore, these minor differences between Caco-2 cells and *in vivo* enterocytes may cause the permeation of some compounds to be underestimated or overestimated, resulting in poor correlation of *in vitro/in vivo* data [35].

Artificial Membrane Assays

The parallel Artificial Membrane Permeability Assay (PAMPA) was initially developed in 1998 as a high-throughput screening tool to model the gastrointestinal epithelium passive permeability [36]. This system involves artificial lipid membranes formed by a mixture of lecithin and an inert organic solvent on a filter support, the donor compartment containing buffer solution with new chemical entities and the acceptor compartment with only fresh buffer. Despite the absence of enzymes and transporters, PAMPA is able to measure the relative passive transcellular diffusion of compounds with reasonable accuracy [37-39]. The simplicity, low cost, high-throughput, and wide pH range make PAMPA technology popular within the pharmaceutical industry. In addition, by optimizing the membrane composition, PAMPA can be easily prepared and applied to mimic different biological barriers, such as blood brain barrier (BBB) or skin [40-42].

Animal tissue-based Assays

Excised animal tissue models have been used since the 1950s to explore the mechanism of absorption of nutrients from the intestine. Tissue flux chambers, everted gut sacs, non-everted gut sacs and other tissue-based assays have been developed for the study of intestinal absorption and assessing the intestinal absorption potential of drug candidates [43-44]. Compared to cell or artificial membrane-based assays, these tissue-

based assays offer more accurate predictions, in terms of intestinal absorption of the drug candidates. The drawbacks of these assays are also obvious, such as, low-throughput and labor-intensive. In addition, the viability of the excised tissues is difficult to maintain since the tissues are devoid of a direct blood supply and need constant oxygenation [43].

All these *in vitro* permeability assays represent a compromise between high-throughput with low predictive potential and low-throughput with high predictive potential [45]. Therefore, no single method will be sufficient for evaluating drug absorption, but most likely a combination of systems is needed. Higher throughput, less reliable methods could be used to discover 'loser' compounds, whereas lower throughput, more accurate methods could be used to optimize the absorption properties of lead compounds [46].

In-Vitro Metabolism Studies

Metabolism is the irreversible transformation of parent compounds into metabolites. It is part of the body's natural defense mechanism to eliminate unwanted xenobiotics. By enzymatic transformation, chemicals are metabolized into polar, more water-soluble products that can be readily excreted from the body. Metabolism constitutes the most important aspect during drug discovery and development. Metabolic studies provide information about metabolites, enzymatic pathways, and inhibition or induction of a metabolizing enzyme. All of these studies can be used to understand potential toxicity, drug-drug interactions, toxicological differences between species and dosage issues associated with a drug candidate [47].

The liver is the major organ involved in the metabolism of drugs and performs enzymatic transformation in two distinct phases: phase I and phase II reactions.

Evaluation of liver metabolism *in vitro* is critical when selecting drug candidates [48]. A number of *in vitro* systems have been developed for drug metabolism studies, including liver microsomes, S9 homogenates, hepatocytes, liver slices, cDNA expressed enzymes, isolated perfused livers and some preclinical animal models [47, 49]. While considering the simplicity, availability, cost and ease of automation, liver microsomes and S9 homogenates are the most widely applied systems in the pharmaceutical industry.

Recently, some metabolism *in silico* screening systems, such as, homology modeling, pharmacophore modeling, QSAR modeling, metabolism information systems, and metabolite prediction systems have been reported to provide supportive information for the decision making process in drug discovery [47, 50]. Several approaches that use databases to predict metabolism are available, including MetabolExpert (Compudrug), META (MultiCASE), Meteor (Lhasa), the databases Metabolite (MDL) and Metabolism (Accelrys) [51].

Plasma Protein Binding

Plasma protein binding is another important factor that affects pharmacokinetics (ADME) and pharmacological activities of drugs. Only the fraction of drug unbound from plasma proteins is available to be transported from the vascular system into the tissues, and interacts with therapeutic targets. In addition, only unbound drug can be cleared from the body. Therefore, the extent of drug binding to plasma proteins can have a significant impact on pharmacokinetic parameters, such as, clearance and volume of distribution, and pharmacodynamic properties of a compound [52]. In addition, the extent and linearity of plasma protein binding are highly associated with potential drug-drug interactions and toxicity. The free fraction of drug in plasma is also an important input

parameter in physiologically based pharmacokinetic and allometric scaling models and in pharmacokinetic/ pharmacodynamic (PK/PD) models [53].

Binding Proteins in Plasma

Drugs commonly bind to albumin, alpha-1-acid glycoprotein, or lipoproteins. Among them, albumin is the most abundant protein in plasma. It contributes about half of the total plasma protein. Albumin is highly water soluble and flexible, resulting in the ability to bind a large array of molecules. There are at least two high affinity drug binding sites, site I (warfarin binding site) and site II (benzodiazepine binding site) as well as many low affinity sites [54]. Albumin is a basic protein and preferentially binds to acidic and neutral drugs.

The next most important plasma protein responsible for drug binding is alpha-1-acid glycoprotein. It has one binding site selective for basic drugs such as disopyramide and lignocaine. Alpha-1-acid glycoprotein is an acute-phase protein. Therefore, the extent of binding to alpha-1-acid glycoprotein will be altered by certain pathological conditions such as cancer, cardiovascular disease, inflammatory disease, kidney disease, liver disease and infections. For instance, alpha-1-acid glycoprotein serum concentration increases in patients with systemic tissue injury, inflammation, infection or cancer, which may result in increased plasma protein binding of drugs to alpha-1-acid glycoprotein.

Lipoproteins are complex aggregates of lipids and proteins that primarily responsible for the transport of endogenous fatty acids such as triglycerides, phospholipids, and cholesterol. Lipoproteins play an important role in binding of very lipophilic compounds such as cyclosporine A. The “binding” of drugs to lipoproteins is

not a true specific binding reaction, but is more like the drugs dissolve in the lipids component of lipoproteins.

In vitro methods for plasma protein binding

Several *in vitro* methods have been developed to measure the unbound drug concentration in plasma, including equilibrium dialysis, ultrafiltration, ultracentrifugation, gel filtration, albumin and/or alpha-1-acid glycoprotein columns, microextraction and optical biosensor [55]. Equilibrium dialysis and ultrafiltration are the most commonly used methods to determine plasma protein binding.

Equilibrium dialysis is considered to be the gold standard method for plasma protein binding measurement. Recently, several 96-well equilibrium dialysis apparatuses have been developed as high-throughput screening tools for determining plasma protein binding [55]. There are drawbacks to this technique, including time to reach equilibrium, nonspecific binding, volume shift, Donnan effects and changes in initial equilibrium conditions. In addition, compounds with low water solubility and plasma stability are not suitable to this method.

Ultrafiltration is the simplest and fastest method for determining the free fraction of drug. Similar to equilibrium dialysis, ultrafiltration uses a two chambered device that is separated by a semipermeable filter membrane. Unbound drug can be separated from plasma very quickly by positive pressure or, more commonly, centrifugation (approximately 2,000xg). Ultrafiltration is rapid and technically less challenging than equilibrium dialysis, which makes it more popular at the drug discovery stage to rank-order a number of compounds based on plasma protein binding. The major disadvantage of ultrafiltration is nonspecific binding of free drug to the filter membrane or collection

chamber. This drawback can be partially overcome by mixing control plasma or serum retentate with the filtrate or pre-treatment of the system with Tween 80 or benzalkonium [56].

Ultracentrifugation is an alternative method to the membrane techniques of equilibrium dialysis and ultrafiltration. Ultracentrifugation uses high gravitational force (625,000g) to separate the unbound fraction from the bound compound. Since no semipermeable membrane is involved, ultracentrifugation has fewer nonspecific binding issues, which makes it a good alternative to highly absorptive compounds. However, the equipment used for ultracentrifugation is expensive in contrast to that for equilibrium dialysis and ultrafiltration. Restricted by the equipment, ultracentrifugation can only process relatively small number of samples at one time, which makes this technique a low-throughput application.

In vivo Preclinical Pharmacokinetics

After a series of *in vitro* ADME screening, a few remaining candidates will be processed for further *in vivo* pharmacokinetic studies. The *in vitro* characterization of ADME profiles offers an experimental basis to predict the *in vivo* pharmacokinetic profiles of candidate compounds. These *in vitro* predictions will be justified during *in vivo* pharmacokinetic evaluation. Generally speaking, the primary goal of *in vivo* preclinical pharmacokinetic studies is the identification of drug candidates suitable for clinical testing [57]. One of the major roles of *in vivo* preclinical pharmacokinetic studies is to characterize the primary pharmacokinetic parameters and understand the underlying mechanisms that govern the ADME properties of drugs.

Pharmacokinetic Parameters

Area under the curve (AUC)

The area under the plasma drug concentration-time curve (AUC) reflects the actual body exposure to drug after administration. Under linear pharmacokinetic conditions, AUC is directly proportional to the dose and inversely proportional to the clearance of the drug. AUC is required to calculate values of other pharmacokinetic parameters, such as clearance and bioavailability. It is also a useful parameter to evaluate bioequivalence, when comparing different formulations of a drug or generic drugs.

Clearance (CL)

Clearance is defined as 'the volume of fluid which is totally cleared of the drug in a unit time'. Based on the definition, clearance is not an indicator of how much of a drug is eliminated per unit time, but how much apparent volume of reference fluid is cleared of a drug per unit time. Clearance is a key parameter that describes the ability of the body or an organ to eliminate drug from the body [58]. After IV administration, the total systemic clearance can be determined directly from the concentration-time profile as the ratio of dose to area under the plasma concentration-time curve (AUC). Since many different organs may be involved in the elimination of the drug, total systemic clearance equals the sum of individual organ clearances. Therefore, characterization of the magnitude and routes of clearance is one of the major objectives for preliminary animal studies. In addition, information about the relative contributions of renal, biliary and hepatic clearances *in vivo* may help guide the selection of lead compounds that are cleared by multiple routes and organs. Because, for a drug candidate, renal clearance and

biliary excretion are consider to be preferred elimination pathways, which cause less toxicity and fewer drug-drug interaction.

Volume of Distribution (Vd)

The apparent volume of distribution of a drug can be viewed simply as a proportionality factor between the total amount of drug present in the entire body and the drug concentration in the reference body fluid, usually the plasma, at any given time [58]. Vd does not represent a real physiological parameter and can be used to assess the extent of the distribution of a drug. As an independent parameter, the volume of distribution is indicative of the extent of space or volume into which the drug is distributed.

Oral Bioavailability (F)

The concept of bioavailability refers to the rate and extent to which the active ingredient or active moiety is absorbed from a drug product and becomes available in the systemic circulation [59]. From a pharmacokinetic perspective, bioavailability of a given formulation provides an estimate of the relative fraction of the orally administered dose that is absorbed into the systemic circulation. Bioavailability is a function of both drug absorption and first pass effects. For an orally administered drug, before reaching systemic circulation, there are the several sequential barriers to overcome. In addition, the metabolic enzymes and active transporters involved in these barriers are considered to be the major sources of drug loss following oral administration. Therefore, all of these factors significantly affect the bioavailability of a drug.

Absolute bioavailability is the amount of drug from a formulation that reaches the systemic circulation relative to an intravenous (IV) dose, which is assumed to be 100% bioavailable. Absolute bioavailability is determined by comparing the AUC of a drug

after non-intravenous administration to that after intravenous administration. Relative bioavailability refers to availability of a drug product as compared to another dosage form or product of the same drug [59]. Relative bioavailability can be directly determined by comparing the AUCs of a drug when administered via different routes or formulations.

High-throughput In Vivo Pharmacokinetic Screening

Conventional preclinical pharmacokinetic studies involve the administration of a single compound to animals, sample collection at specific time points, sample preparation, and sample analysis for drug concentration quantification, which are extremely labor intensive [57]. The advances in liquid chromatography/mass spectrometry/mass spectrometry (LC/MS/MS)-based quantitative analytical techniques have made it possible to significantly increase the throughput of *in vivo* pharmacokinetic screening. In recent years, several experimental approaches have been developed based on advances in instrumentation and analytical techniques, including cassette dosing, cassette analysis and rapid rat screen.

Cassette Dosing

Cassette dosing, also called ‘cocktail’ or ‘N-in-one’ dosing, was first developed in 1997. It involves the simultaneous administration of a mixture of compounds (typically five to ten compounds belonging to the same structural class) to a single animal [60, 61]. From collected biological samples, concentrations of each analyte are measured in a single run by mass spectrometry. Compared with conventional single compound administration, cassette dosing can reduce the amount of compound and animal usage, which further reduces sampling, sample preparation, and sample analysis, and significantly increases the throughput.

As a screening tool, cassette dosing is not intended to accurately define pharmacokinetic parameters for each compound; rather, it has mostly been applied to rapidly rank order compounds, eliminate compounds exhibiting poor pharmacokinetic properties, and identify those that should be prioritized for further evaluation. Furthermore, cassette dosing provides rapid feedback to medicinal chemists, and guides future synthetic efforts to optimize ADME properties of new chemical entities [62].

Although there have been many successful applications with cassette dosing, this method is not without controversy. A major concern is the risk of drug-drug interactions following the co-administration of multiple chemical entities (62, 63). These interactions may occur as a result of competitive inhibition of metabolic enzymes, transporters, or plasma protein binding and may lead to false-negative as well as false-positive results (63). White and Manitpiskul reviewed the pharmacokinetic theory behind cassette dosing approaches and made recommendations to minimize the risk of drug-drug interactions, included experimentally minimizing the number of compounds in the dosing cocktail (below five) and administering the lowest doses detectable [63].

Lowest dosing of several compounds may cause another challenge for this approach, which is the requirement of high sensitivity and selectivity of analytical methods. To quantify low levels of multiple compounds in a single sample simultaneously, highly sensitive and selective analytical methods are required, which makes method development and validation time-consuming and effort-intensive. In addition, multiple analytes in one biological sample may cause significant analytical interference, including collision cell cross-talk between structurally related compounds with similar fragmentation patterns, in-source fragmentation of metabolites to produce

the parent compounds, and ion suppression as a result of competition between the analyte and co-eluting analytes, residual matrix components, or mobile phase constituents [64, 65]. Once analytic interference occurs, optimization of sample preparation and chromatographic conditions is required to ensure the resolution of interfering compounds.

Cassette Analysis

Unlike cassette dosing, which reduces the animal use, cassette analysis (sample pooling or cocktail analysis) tries to reduce the sample amount by combining equal aliquots of samples collected at a particular time point from different animals after dosing an individual drug. Although cassette analysis requires more animals and resources for the study, it is a good alternative, if significant drug-drug interactions occur when processing cassette dosing [66]. Another concern of this method is that combination of biological samples will dilute concentrations of each compound, which could be a challenge for simultaneous compound analysis by LC/MS/MS.

Hop et al. developed an alternative strategy, pooling the samples collected at each consecutive time point from a single animal dosed with an individual compound to produce a single sample for analysis (67). The concentration of this pooled sample is then multiplied by the time period of collection to give an estimation of the area under the concentration versus time curve. Cheung et al. applied a related approach, in which a single sample with a concentration proportional to AUC was derived by combining plasma aliquots whose volumes were proportional to the time interval on either side of the sample time point (68). In this study, the area under the first moment curve (AUMC), the mean residence time (MRT) and the steady-state volume of distribution (Vss) of a compound were successfully estimated. However, the drawback of this pooling approach

is obvious; other than obtaining an estimated AUC value, pharmacokinetic parameters cannot be determined due to the lack of a plasma concentration-time profile.

All these *in vivo* high-throughput techniques provide crude estimation of ADME properties for the initial selection of candidate compounds, which may be further subjected to a full pharmacokinetic study to obtain more detailed ADME knowledge.

Full pharmacokinetic study

Generally, a full pharmacokinetic study refers to conventional preclinical pharmacokinetic studies, including administration of a single compound to animals, samples collection at specific time points, sample preparation, and sample analysis for drug concentration quantification. The purpose of a full pharmacokinetic study is to reconfirm the results of *in vivo* high-throughput screening and generate statistically accurate PK parameters. In addition, other studies such as identification of *in vivo* metabolites and tissue distribution study could be involved in full pharmacokinetic evaluations.

Anti-infective Agents

Anthelmintics

Parasitic worms (helminths) are the most common infectious agents in humans. They have plagued humans for thousands of years, and historically infected more than half the world's population [69-71]. Typically, helminths cause relatively nonspecific and nonlethal acute symptoms, with pathology that develops over many years. This limits their priority for control compared to more lethal pathogens like tuberculosis, HIV and malaria. However, some developed parasitic infections may cause extensive morbidity, including fetal/neonatal damage, nutritional deficiencies, cutaneous nodules, skin

eruptions or necrosis, and major end-organ damage of the eyes, central nervous system (CNS), lungs, heart, or liver [72-74]. Recently, the burden on childhood development and economic productivity imposed by parasitic helminths has led to renewed interest in controlling neglected helminthic infection by mass drug administration strategies [75]. The goals of this preventive chemotherapy are minimization of morbidity by yearly or twice-yearly administration of anthelmintics to keep worm burdens below the level associated with symptoms and pathology, and reduction in transmission as the local abundance of infective larvae diminishes [76-78]. Obviously, anthelmintics play an important role in this disease control program.

Currently, drugs for combating worm infections are limited. Of the 1,556 new chemical entities marketed between 1975 and 2004, only four drugs were licensed for use as human anthelmintics. They are albendazole, oxamniquine, praziquantel, and ivermectin [79]. All of these drugs were developed for veterinary use before adoption for humans.

Albendazole

Albendazole is a benzimidazole drug first discovered at the SmithKline Animal Health Laboratories in 1972. It is a broad spectrum anthelmintic, effective against roundworms, tapeworms, and flukes of domestic animals and humans [80]. Albendazole is a pro-drug, which required to be oxidized to albendazole sulphoxide-the active drug. Albendazole sulphoxide binds to the colchicine-sensitive site of β-tubulin and inhibits the polymerization or formation of microtubules. The loss of the cytoplasmic microtubules leads to the impaired uptake of glucose and depletes glycogen stores and production of adenosine triphosphate (ATP), which results in immobilization and eventually death of

the parasite [81]. Resistance to albendazole has been attributed to specific amino acid changes in the β-tubulin protein of parasite, leading to reduced binding affinity for β-tubulin.

Albendazole is poorly absorbed from the gastrointestinal tract due to its low aqueous solubility. Albendazole undergoes extensive first-pass metabolism in the liver, and albendazole sulphoxide is the primary metabolite, which is responsible for the effectiveness against systemic tissue infections. The plasma elimination half- life of albendazole sulphoxide is 8-15 hours. Albendazole sulfoxide is 70% bound to plasma protein and is widely distributed throughout the body. Albendazole sulphoxide appear to be principally eliminated in bile, with only a small proportion appearing in the urine [82].

Ivermectin

Ivermectin is a broad-spectrum anti-parasitic drug. When it first appeared in the late-1970s, ivermectin was considered to be a revolutionary drug. It was the world's first endectocide, the forerunner of a completely new class of anti-parasitic agents, and potently active against a wide range of internal and external nematodes and arthropods [83]. Although initially introduced as a veterinary drug, ivermectin proved to be an ideal anti-parasitic drug for humans, since it was first used to treat onchocerciasis in humans in 1988. Ivermectin is highly effective, broad-spectrum, safe and well tolerated. It is used to treat a variety of internal nematode infections, including onchocerciasis, strongyloidiasis, ascariasis, cutaneous larva migrans, filariases, gnathostomiasis and trichuriasis, as well as for oral treatment of ectoparasitic infections, such as pediculosis and scabies [84].

Initially, ivermectin was believed to block neurotransmitters by acting on GABA-gated chloride channels and exhibiting potent disruption at GABA receptors in

invertebrates and mammals. GABA is recognized as the primary inhibitory neurotransmitter in the somatic neuromuscular system of nematodes. Further studies suggested that it was in fact glutamate-gated chloride channels that were the target of ivermectin and related drugs. Ivermectin binds with high affinity to glutamate-gated chloride channels which occur in invertebrate nerve and muscle cells, causing an increase in the permeability of the cell membrane to chloride ions with hyperpolarization of the nerve or muscle cell. Hyperpolarization results in paralysis and death of the parasite [85].

The oral administration is the only approved for ivermectin administration in humans. Ivermectin highly binds to serum albumin. Due to the high lipid solubility of ivermectin, this compound is widely distributed within the body. Ivermectin is extensively metabolized by CYP-3A4, converting the parent drug to at least 10 metabolites, most of them are hydroxylated and demethylated derivatives. Ivermectin and its metabolites were excreted mainly in faeces and only 1% in urine [86].

Oxamniquine

Oxamniquine is a potent single-dose agent for treatment of *Schistosoma mansoni* infection in human. Oxamniquine is known to inhibit nucleic acid synthesis in schistonsomal cells. The mechanism of action is thought to involve prior activation of the drug by sulfotransferase of the parasite. The sulfate ester metabolite alkylates the DNA of the parasite and prevents DNA replication, resulting in cell death [87]. Oxamniquine is generally well tolerated following oral doses. Dizziness, headache and gastrointestinal effects, such as nausea, vomiting, and diarrhea, are common. At the recommended doses, hallucinations and seizures have been reported rarely. There are no data available on

interactions with other drugs, but the ability of oxamniquine to inhibit CYP2D6 may be of clinical importance [88].

Praziquantel

Praziquantel is an anthelmintic effective against flatworms. It was developed in the laboratories for parasitological research of Bayer AG and Merck KGaA in Germany in the mid-1970s. The excellent pharmacological properties, particularly its effectiveness after only one orally administered dose, its lack of toxicity, and substantial reductions in cost, make praziquantel still the only effective, routinely used compound for the treatment and control of Schistosomiasis, a tropical disease caused by blood-dwelling trematodes (flatworms) of the genus *Schistosoma* [89].

Exact knowledge about the mechanisms of action of praziquantel remains elusive. Voltage-gated calcium channels have been identified as potential molecular targets of praziquantel. A recent study suggested that praziquantel inhibits the uptake of adenosine (and uridine) by schistosomes. Therefore, the explanation for the mechanisms of action is that praziquantel may interfere with the parasite's obligate need to acquire adenosine from its host. In addition, the inhibition of adenosine uptake may relate to praziquantel induced Ca^{2+} influx [90].

Praziquantel is absorbed rapidly from the gastrointestinal (GI) tract after its oral administration. In human, praziquantel undergoes extensive first pass hepatic biotransformation into a series of mono- and dihydroxylated inactive metabolites. Praziquantel is rapidly distributed in body tissues due to its high lipid solubility. Approximately 80 to 85% of the drug is bound to plasma proteins [82].

Anti-tuberculosis drugs

Tuberculosis (TB) is a contagious and deadly disease caused by mycobacterium tuberculosis (M.tb), which could spread through the air. Since it was first identified by Robert Koch in 1882, M.tb has been a serious threat to human health [91]. According to the World Health Organization (WHO), at least one third of the entire world's population is infected with M.tb. In 2011, 8.7 million people became ill with TB and 1.4 million died from TB. TB is also a leading killer of people living with human immunodeficiency virus (HIV) causing one quarter of all deaths [92].

M.tb is an obligate aerobic bacillus that divides at an extremely slow rate (approximately every 15-20 hours). M.tb has an unusual structure of the cell wall that consists of peptidoglycans and complex lipids, in particular mycolic acids. Mycolic acids form a waxy coating on the cell surface, which allows M.tb to lie dormant for many years as a latent infection. M.tb is highly aerobic and requires high levels of oxygen. When active, M.tb is primarily a pathogen of the mammalian respiratory system and typically infects the lungs [93]. In approximately 25% of cases, the bacteria enters the blood and infects other parts of the body, such as the pleura, the meninges, the lymphatic system, the genitourinary system and the bones and joints [94].

A 6-9 month chemotherapy regimen using a combination of 4 drugs (rifampicin, isoniazid, ethambutol, and pyrazinamide) with cure rates of approximately 90% in HIV negative patients is the globally accepted standard treatment of drug-susceptible (DS), active tuberculosis [95]. It is difficult for TB patients to adhere to this standard regimen, due to several reasons, including long and intensive treatment with multiple complementary drugs, abated symptoms after a few weeks of treatment, unpleasant side

effects during the treatment, and the cost of medication and tests. Nonadherence of patients is more likely result in treatment failure and development of drug-resistance [96].

There are 10 drugs currently approved by the U.S. Food and Drug Administration for treating TB. Of the approved drugs, isoniazid (INH), rifampin (RIF), ethambutol (EMB), and pyrazinamide (PZA) have been used as first-line anti-TB agents for more than 40 years and form the core of treatment regimens. The mechanism of action of these first-line agents include the obstruction of cell wall formation, inhibition of fatty acid synthase and inhibition of bacterial DNA-dependent RNA synthesis. Ethambutol inhibits the enzyme arabinosyl transferase, resulting in the obstruction of cell wall formation. Isoniazid disrupts cell wall formation by blocking the synthesis of mycolic acid. Pyrazinamide inhibits fatty acid synthase and disrupts membrane potential and energy production. Rifampin inhibits bacterial DNA-dependent RNA polymerase [97]. All these first line drugs have good oral absorption and tissue distribution, except isoniazid, which is limited absorbed after oral administration due to its high aqueous solubility, poor permeability and extensive hepatic metabolism [98]. Other drugs, such as amikacin, capreomycin, ciprofloxacin and cycloserine are considered as secondary options for tuberculosis treatment due to their potency, toxic side effects or unavailability in many developing countries.

Historically, research into new anti-TB drugs was at a standstill, partly due to complacency, as first-line drug treatments had been shown to cure TB, and the fact that there had been little incentive for investment in new anti-TB drug discovery and development, since the vast majority of patients are found in the developing world. Since the late 1990's, renewed interest in this area has resulted in a number of new drug

candidates entering clinical trials. Some of them exhibit novel mechanisms of action. TMC207 is a diarylquinoline that exhibits excellent activity against drug-susceptible, multiple-drug resistant (MDR) and extensively drug resistant (XDR) M.tb strains. TMC207 acts by inhibiting mycobacterium membrane-bound ATP synthase. This unique mechanism of action offers great selectivity as there is little similarity between the mycobacterial and human ATP synthase [99]. PA-824 is a bicyclic nitroimidazofurans analog, without any unfavourable mutagenic features. PA-824 exhibits high *in vitro* activity against M.tb including drug resistant strains by inhibiting cell wall lipid and protein synthesis. This drug is also active against non-replicating bacteria, which indicates an unknown mechanism of action [100].

The increasing MDR and XDR-TB cases, non-compatibility of regimen treating HIV/TB co-infection, and limited new anti-TB drug candidates make a compelling case for the urgent need for new anti-TB drugs and, in particular, a need for drugs that could shorten treatment regimens as well as treat multiple-drug resistant -TB, extensively drug resistant -TB and HIV/TB co-infection.

Anti-viral nucleoside analogue

A virus is a simple infectious agent that consists of a genome, a protein coat, and in some cases an envelope of lipids. Viruses replicate only inside the living cells of other organisms and could infect all types of life forms, from animals and plants to bacteria and archaea [101]. Several common human diseases are caused by viruses, including influenza, chickenpox, and cold sores. Some serious diseases such as ebola, AIDS, avian influenza and SARS are caused by viruses.

Anti-viral strategies are mainly targeting a specific step of the viral life cycle, including attachment to a host cell, release of viral genes and possibly enzymes into the host cell, replication of viral components using host-cell machinery, assembly of viral components into complete viral particles and release of viral particles to infect new host cells. Serveral key factors in these steps of the life cycle have been used as targets to develop ant-viral agents, such as reverse transcriptase, integrase and protease.

Nucleoside analogues represent an important class of anti-viral agents. Since the first anti-viral nucleoside drug, idoxuridine, was discovered in 1959 [102], nucleoside analogs have played an important role in the battle against various cancers and viral infections. More than 20 anti-viral nucleosides and nucleoside analogs are currently available, including anti-HIV drugs such as didanosine, emtricitabine, zalcitabine and zidovudine , and anti-HBV drugs, such as lamivudine, entecavir and telbivudine. The mechanism of action of nucleoside analogs depends on their ability to mimic natural nucleosides once phosphorylated by viral encoded enzyme. The phosphorylated metabolites are incorporated into growing DNA strands; but they act as chain terminators and inhibitors of viral DNA polymerase, which prevent further nucleic acid chain elongation.

In biological systems, DNA and RNA are composed of β-D-nucleosides as proteins are composed of L-amino acids. Therefore, it has been widely accepted that only natural D-nucleosides could effectively interact and inhibit metabolic enzymes and exhibit biological activities, owing to the stereospecificity of enzymes in living systems [103]. This paradigm has proven not to be true with the discovery of lamivudine (3TC) as

a therapeutic agent, which exhibited more potent anti-viral activity compared to the D-counterparts while exhibiting less toxicity [104].

The discovery of 3TC sparked the interest to explore the L-nucleosides as potential anti-viral agents. Since then, a large number of L-nucleoside analogs have been synthesized and evaluated for their anti-viral activities. Several L-nucleoside analogs exhibit favorable features as therapeutic agents, including comparable or greater anti-viral activities than their D-counterparts, more favorable toxicological profiles and better metabolic stability.

In the past several years, L-nucleosides have drawn greater attention and significant progress has been made in developing L-nucleosides to fight against viral infections. Currently, L-nucleoside analogs, such as lamivudine, emtricitabine and telbivudine, have been applied as treatment for HBV or HIV infections; clevudine, elvucitabine, maribavir, troxacitabine, and valtorcitabine are in clinical studies; other L-nucleosides are also under development to treat herpes simplex virus (HSV) or varicella zoster virus (VZV) infections.

Overall, due to the limited drugs available for the treatment, there was an urgent need for development of new anti-infective drugs, especially for new anti-parasitic drugs and anti-tuberculosis drugs. As one of the most important attributes of drugs, pharmacokinetic properties should be evaluated at earliest development stages. Preclinical pharmacokinetic studies of three anti-infective candidate compounds were performed in this study, including preclinical pharmacokinetic and tissue distribution of an anti-parasitic compound and an anti-tuberculosis compound in mice, and the *in vitro*

stability study of an anti-viral compound. The results will be used to direct further evaluations of these compounds.

REFERENCE

1. Lin JH, Lu AY. Role of pharmacokinetics and metabolism in drug discovery and development. Pharmacol Rev. 1997 Dec;49(4):403-49.

2. DiMasi JA, Hansen RW, Grabowski HG. The price of innovation: New estimates of drug development costs. J Health Econ. 2003, 2:151-85.

3. Tonkens R.An overview of the drug development process. Physician Exec. 2005, 31(3):48-52.

4. Pharmaceutical Research and Manufacturers of America. "New Drug Approvals." Washington, DC: PhRMA, 1997-2012.

5. Dickson M, Gagnon JP. Key factors in the rising cost of new drug discovery and development. Nat Rev Drug Discov. 2004 May; 3(5):417-29.

6. Parexel, Parexel's Bio/pharmaceutical R&D statistical sourcebook 2006/2007. Barnett international, Waltham, Mass. 2006.

7. Twombly R. Slow start to phase 0 as researchers debate value. J Natl Cancer Inst. 2006 Jun; 98(12):804-6.

8. Pharmaceutical Research and Manufacturers of America, PhRMA Annual Member Survey, 2011.

9. Mullard A. Economists propose a US$30 billion boost to biomedical R&D. Nat Rev Drug Discov. 2012 Oct; 11(10):735-7.

10. Mullard A. 2012 FDA drug approvals. Nat Rev Drug Discov. 2013 Feb; 12(2):87-90.

11. Connolly C. Price tag for a new drug: $802 million; Findings of tufts university study are disputed by several watchdog groups. Washington post, 1 Dec 2001.

12. A. Singh, et al. Bain & Co. Research Report, 2003.

13. Matthew H. How Much Does Pharmaceutical Innovation Cost? A Look At 100 Companies. 2013 Aug; Pharma & Healthcare, Forbes.

14. Goodall S. Rising to the productivity challenge: a strategic framework for Biopharma. Boston Consulting Group Report. 2004.

15. Boston Consulting Group. A Revolution in R&D: How Genomics and Genetics are Transforming the Biopharmaceutical Industry. PAREXEL's Pharmaceutical R&D Statistical Sourcebook 2002/2003.

16. Rani PU, Naidu MU. Phase 0 - Microdosing strategy in clinical trials. Indian J Pharmacol. 2008 Nov; 40(6):240-2.

17. Gilbaldi M, Perrier D (Eds.), Phamacokinetics (edn 2), Marcel Dekker, Inc, New York 1982

18. Curtis G, Colburn W, Heath G, Lenehan T, Kotschwar T. Faster drug development. Appl Clin Trials 2000.9: 52-55.

19. Derendorf H, Lesko LJ, Chaikin P, Colburn WA, Lee P, Miller R, Powell R, Rhodes G, Stanski D, Venitz J. Pharmacokinetic/pharmacodynamic modeling in drug research and development. 2000 Dec; J Clin Pharmacol 40: 1399-1418.

20. White RE. High-throughput screening in drug metabolism and pharmacokinetic support of drug discovery. Annu Rev Pharmacol Toxicol. 2000; 40:133-57.

21. J. B. Dressman, G. L. Amidon, and D. Fleisher. Absorption potential: estimating the fraction absorbed for orally administered compounds. 1985 May; J. Pharm. Sci. 74:588-589

22. Sanghvi T, Ni N, Yalkowsky SH. A simple modified absorption potential. Pharm Res. 2001 Dec; 18(12):1794-6.

23. Palm K, Stenberg P, Luthman K, Artursson P. Polar molecular surface properties predict the intestinal absorption of drugs in humans. Pharm Res. 1997 May; 14(5):568-71.

24. Palm K, Luthman K, Ungell AL, Strandlund G, Beigi F, Lundahl P, Artursson P. Evaluation of dynamic polar molecular surface area as predictor of drug absorption: comparison with other computational and experimental predictors. J Med Chem. 1998 Dec; 41(27):5382-92.

25. Kelder J, Grootenhuis PDJ, Bayada DM, Delbressinc LPC, Ploemen JP. Polar molecular surface as a dominating determinant for oral absorption and brain penetration of drugs. Pharm Res 1999 Oct; 16:1514-1519.

26. Lipinski CA. Drug-like properties and the causes of poor solubility and poor permeability. J Pharmacol Toxicol Methods. 2000 Jul-Aug; 44(1):235-49.

27. Lipinski CA, Lombardo F, Dominy BW, Feeney PJ. Experimental and computational approaches to estimate solubility and permeability in drug discovery and development settings. Adv Drug Deliv Rev. 2001 Mar;46(1-3):3-26.

28. Veber DF, Johnson SR, Cheng HY, Smith BR, Ward KW, Kopple KD. Molecular properties that influence the oral bioavailability of drug candidates. J Med Chem. 2002 Jun; 45(12):2615-23.

29. Oprea TI. Property distribution of drug-related chemical databases. J Comput Aided Mol Des 2000;14: 251-264.

30. Hidalgo IJ. Assessing the absorption of new pharmaceuticals. Curr Top Med Chem. 2001Nov; 1:385-401.

31. Bohets H, Annaert P, Mannens G, Van Beijsterveldt L, Anciaux K, Verboven P, Meuldermans W, Lavrijsen K. Strategies for absorption screening in drug discovery and development. Curr Top Med Chem. 2001Nov; 1:367-83.

32. Matsson P, Bergström CAS, Nagahara N, Tavelin S, Norinder U, Artursson P. Exploring the role of different drug transport routes in permeability screening. J Med Chem. 2005 Jan; 48:604-13.

33. Artursson P. Cell cultures as models for drug absorption across the intestinal mucosa. Crit Rev Ther Drug Carrier Syst. 1991; 8(4):305-30.

34. van de Kerkhof EG, de Graaf IA, Ungell AL, Groothuis GM. Induction of metabolism and transport in human intestine: validation of precision-cut slices as a tool to study induction of drug metabolism in human intestine *in vitro*. Drug Metab Dispos. 2008 Mar; 36(3):604-13.

35. Press B, Di Grandi D. Permeability for intestinal absorption: Caco-2 assay and related issues. Curr Drug Metab. 2008 Nov; 9(9):893-900.

36. Kansy M, Senner F, Gubernator K. Physicochemical high throughput screening: parallel artificial membrane permeation assay in the description of passive absorption processes. J Med Chem. 1998 Mar; 41(7):1007-10.

37. Fortuna A, Alves G, Soares-da-Silva P, Falcão A. Optimization of a parallel artificial membrane permeability assay for the fast and simultaneous prediction of human

intestinal absorption and plasma protein binding of drug candidates: Application to dibenz[b,f]azepine-5-carboxamide derivatives. J Pharm Sci. 2012 Feb;101(2):530-40.

38. Akamatsu M, Fujikawa M, Nakao K, Shimizu R. In silico prediction of human oral absorption based on QSAR analyses of PAMPA permeability. Chem Biodivers. 2009 Nov; 6(11):1845-66.

39. Tam KY, Avdeef A, Tsinman O, Sun N. The permeation of amphoteric drugs through artificial membranes--an in combo absorption model based on paracellular and transmembrane permeability. J Med Chem. 2010 Jan 14;53(1):392-401.

40. Di L, Kerns EH, Fan K, McConnell OJ, Carter GT. High throughput artificial membrane permeability assay for blood-brain barrier. Eur J Med Chem. 2003 Mar; 38(3):223-32.

41. Parallel artificial membrane permeability assay: a new membrane for the fast prediction of passive human skin permeability. Ottaviani G, Martel S, Carrupt PA. J Med Chem. 2006 Jun; 49(13):3948-54.

42. Sinkó B, Garrigues TM, Balogh GT, Nagy ZK, Tsinman O, Avdeef A, Takács-Novák K. Skin-PAMPA: a new method for fast prediction of skin penetration. Eur J Pharm Sci. 2012 Apr; 45(5):698-707.

43. Balimane PV, Chong S, Morrison RA. Current methodologies used for evaluation of intestinal permeability and absorption. J Pharmacol Toxicol Methods. 2000 Jul-Aug; 44(1):301-12.

44. Ruan LP, Chen S, Yu BY, Zhu DN, Cordell GA, Qiu SX. Prediction of human absorption of natural compounds by the non-everted rat intestinal sac model. Eur J Med Chem. 2006 May; 41(5):605-10.

45. Youdim KA, Avdeef A, Abbott NJ. *In vitro* trans-monolayer permeability calculations: often forgotten assumptions. Drug Discov Today. 2003 Nov; 8(21):997-1003.

46. Hidalgo IJ. Assessing the absorption of new pharmaceuticals. Curr Top Med Chem. 2001 Nov; 1(5):385-401.

47. Gombar VK, Silver IS, Zhao Z. Role of ADME characteristics in drug discovery and their in silico evaluation: in silico screening of chemicals for their metabolic stability. Curr Top Med Chem. 2003; 3(11):1205-25.

48. Chiu SH. The use of *in vitro* metabolism studies in the understanding of new drugs. J Pharmacol Toxicol Methods. 1993 Apr; 29(2):77-83.

49. Singh SS. Preclinical pharmacokinetics: an approach towards safer and efficacious drugs. Curr Drug Metab. 2006 Feb; 7(2):165-82.

50. Dearden JC. In silico prediction of ADMET properties: how far have we come? Expert Opin Drug Metab Toxicol. 2007 Oct; 3(5):635-9.

51. van de Waterbeemd H, Gifford E. ADMET in silico modelling: towards prediction paradise? Nat Rev Drug Discov. 2003 Mar; 2(3):192-204.

52. Wan H, Rehngren M. High-throughput screening of protein binding by equilibrium dialysis combined with liquid chromatography and mass spectrometry. J Chromatogr A. 2006 Jan; 1102(1-2):125-34.

53. Sinha VK, De Buck SS, Fenu LA, Smit JW, Nijsen M, Gilissen RA, Van Peer A, Lavrijsen K, Mackie CE. Predicting oral clearance in humans: how close can we get with allometry? Clin Pharmacokinet. 2008; 47(1):35-45.

54. Sudlow G, Birkett DJ, Wade DN. The characterization of two specific drug binding sites on human serum albumin. Mol Pharmacol. 1975 Nov; 11(6):824-32.

55. Howard ML, Hill JJ, Galluppi GR, McLean MA. Plasma protein binding in drug discovery and development. Comb Chem High Throughput Screen. 2010 Feb; 13(2):170-87.

56. Banker MJ, Clark TH. Plasma/serum protein binding determinations. Curr Drug Metab. 2008 Nov; 9(9):854-9.

57. Peter LB Danny RH. Pharmacokinetics in drug development: regulatory and development paradigms. 2005 AAPS PRESS

58. younggil Kwon. Handbook of essential pharmacokinetics, pharmacodynamics,and drug metabolism for industrial scientists. 2001 Springer-Verlag New York, Inc.

59. A. Wallance Hayes. Principles and methods of toxicology. 2008 Informa Healthcare USA Inc. New York.

60. Berman J, Halm K, Adkison K, Shaffer J. Simultaneous pharmacokinetic screening of a mixture of compounds in the dog using API LC/MS/MS analysis for increased throughput. J Med Chem 1997; 40:827-9.

61. Olah TV, McLoughlin DA, Gilbert JD. The simultaneous determination of mixtures of drug candidates by liquid chromatography/atmospheric pressure chemical ionization mass spectrometry as an *in vivo* drug screening procedure. Rapid Commun Mass Spectrom. 1997;11(1):17-23.

62. Frick LW, Adkison KK, Wells-Knecht KJ, Woollard P, Higton DM. Cassette dosing: rapid *in vivo* assessment of pharmacokinetics. Pharm Sci Technol Today 1998; 1:12-8.

63. White RE, Manitpisitkul P. Pharmacokinetic theory of cassette dosing in drug discovery screening. Drug Metab Dispos 2001; 29:957-66.

64. A. Peter Snyder. Biochemical and biotechnological applications of electrospray ionization mass spectrometry. 1996 American Chemical Society.

65. Wagner DS, Pirhalla JL, Bowers GD. Metabolite structure analysis by high-resolution MS: supporting drug-development studies. Bioanalysis. 2013 Feb;5(4):463-79.

66. Kuo BS, Van Noord T, Feng MR, Wright DS. Sample pooling to expedite bioanalysis and pharmacokinetic research. J Pharm Biomed Anal. 1998 Jan; 16(5):837-46.

67. Hop CE, Wang Z, Chen Q, Kwei G. Plasma-pooling methods to increase throughput for *in vivo* pharmacokinetic screening. J Pharm Sci 1998; 87:901-3.

68. Cheung BW, Cartier LL, Russlie HQ, Sawchuk RJ. The application of sample pooling methods for determining AUC, AUMC and mean residence times in pharmacokinetic studies. Fundam Clin Pharmacol. 2005 Jun; 19(3):347-54.

69. Cox, F.E.G. History of human parasitology. Clin. Microbiol. Rev. 2002. 15:595-612.

70. Hotez, P.J., Ottesen, E., Fenwick, A., and Molyneux, D. The neglected tropical diseases: the ancient afflictions of stigma and poverty and the prospects for their control and elimination. Adv. Exp. Med. Biol. 2006. 582:23-33.

71. Olds GR. Deworming the world. Trans Am Clin Climatol Assoc. 2013. 124:265-7472.

72. Montoya JG, Boothroyd JC, Kovacs JA. Toxoplasma gondii. In: Mandell GL, Bennett JE, Dolin R, eds. Mandell, Douglas, and Bennett's Principles and Practice of Infectious Diseases. 7th ed. Philadelphia, PA: Churchill Livingstone Elsevier; 2010:3495-3527.

73. Maguire JH. Intestinal nematodes (roundworms). In: Mandell GL, Bennett JE, Dolin R, eds. Mandell, Douglas, and Bennett's Principles and Practice of Infectious Diseases. 7th ed. Philadelphia, PA: Churchill Livingstone Elsevier; 2010:3577-3587.

74. Parasites-Cysticercosis. CDC. Updated November 2, 2010. www.cdc.gov/parasites/cysticercosis/health_professionals/index.html. Accessed February 16, 2012.

75. Smits HL. Prospects for the control of neglected tropical diseases by mass drug administration. Expert Rev Anti-Infect Ther 2009; 7:37-56.

76. World Health Organization. Preventive chemotherapy in human helminthiasis. Coordinated use of anthelminthic drugs in control interventions: a manual for health professionals and programme managers. WHO Press, Geneva; 2006. p. 62.

77. Hanson C, Weaver A, Zoerhoff KL, Kabore A, Linehan M, Doherty A, Engels D, Savioli L, Ottesen EA. Integrated implementation of programs targeting neglected tropical diseases through preventive chemotherapy: proving the feasibility at national scale. Am J Trop Med Hyg 2011; 84:5-14.

78. Gabrielli AF, Montresor A, Chitsulo L, Engels D, Savioli L. Preventive chemotherapy in human helminthiasis: theoretical and operational aspects. Trans R Soc Trop Med Hyg. 2011 Dec;105(12):683-93.

79. Chirac, P., and Torreele, E. Global framework on essential health R&D. Lancet. 2006. 367:1560-1.

80. Theodorides VJ, Gyurik RJ, Kingsbury WD, Parish RC. Anthelmintic Activity of Albendazole Against Liver Flukes, Tapeworms, Lung and Gastrointestinal Roundworms. Experientia. 1976; 32 (8): 702-703.

81. Lacey, E. The role of the cytoskeletal protein tubulin in the mode of action and mechanism of drug resistance to benzimidazoles. Int. J. Parasitol. 1988; 18, 855-936

82. Sotelo J, Jung H. Pharmacokinetic optimisation of the treatment of neurocysticercosis. Clin Pharmacokinet. 1998 Jun; 34(6):503-15.

83. Burg R.W., Miller B.M., Baker E.E., Birnbaum J., Currie S.A., Hartman R., Kong Y.L., Monaghan R.L., Olson G., Putter I., Tunac J.B., Wallick H., Stapley E.O., Oiwa R., Ōmura S. Avermectins, new family of potent anthelmintic agents: producing organisms and fermentation. Antimicrob. Agents Chemother. 1979; 15 (3), 361-367.

84. Ottesen E., Campbell W. Ivermectin in human medicine. J. Antimicrob. Chemother. 1994; 34, 195-203.

85. Omura, S. Mode of action of avermectin. In Macrolide antibiotics; Chemistry, Biology & Practice (2nd Edition) (ed. Omura, S.). Academic Press, San Diego, 2002. pp. 571-575.

86. González Canga A, Sahagún Prieto AM, Diez Liébana MJ, Fernández Martínez N, Sierra Vega M, García Vieitez JJ. The pharmacokinetics and interactions of ivermectin in humans--a mini-review. AAPS J. 2008;10(1):42-6.

87. Pica-Mattoccia L, Carlini D, Guidi A, Cimica V, Vigorosi F, Cioli D. The *schistosome* enzyme that activates oxamniquine has the characteristics of a sulfotransferase. Mem Inst Oswaldo Cruz. 2006 Sep;101 Suppl 1:307-12.

88. Masimirembwa CM, Hasler JA, Johansson I. Inhibitory effects of antiparasitic drugs on cytochrome P450 2D6. Eur J Clin Pharmacol. 1995; 48(1):35-8.

89. Doenhoff MJ, Cioli D, Utzinger J. Praziquantel: mechanisms of action, resistance and new derivatives for schistosomiasis. Curr Opin Infect Dis. 2008 Dec;21(6):659-67.

90. Angelucci F, Basso A, Bellelli A, Brunori M, Pica Mattoccia L, Valle C. The anti-schistosomal drug praziquantel is an adenosine antagonist. Parasitology. 2007 Aug;134(Pt 9):1215-21.

91. Alex Sakula. Robert Koch: Centenary of the Discovery of the Tubercle Bacillus, 1882. Can Vet J. 1983. 24(4): 127-31.

92. World Health Organization. Tuberculosis, Fact sheet Number 104. WHO, Geneva, Switzerland (2013).

93. Ismael Kassim, Ray CG (editors). Sherris Medical Microbiology (4th ed.). 2004 McGraw Hill.

94. Rivers EC, Mancera RL. New anti-tuberculosis drugs in clinical trials with novel mechanisms of action. Drug Discov Today. 2008 Dec;13(23-24):1090-8.

95. Cohn DL, Iseman MD. Treatment and prevention of multidrug-resistant tuberculosis. Res Microbiol. 1993.144(2):150-3.

96. Wang YT, Gan SH, Chee CB. Nonadherence to TB treatment: who cares? Singapore Med J. 2012 Dec; 53(12):782-3.

97. Yew WW. Development of new antituberculosis drugs. 2006. Nova Science Publishers, Inc.

98. Bhandari R, Kaur IP. Pharmacokinetics, tissue distribution and relative bioavailability of isoniazid-solid lipid nanoparticles. Int J Pharm. 2013 Jan 30;441(1-2):202-12.

99. Andries K, Verhasselt P, Guillemont J, Göhlmann HW, Neefs JM, Winkler H, Van Gestel J, Timmerman P, Zhu M, Lee E, Williams P, de Chaffoy D, Huitric E, Hoffner S, Cambau E, Truffot-Pernot C, Lounis N, Jarlier V. A diarylquinoline drug active on the ATP synthase of Mycobacterium tuberculosis. Science. 2005 Jan 14;307(5707):223-7.

100. Stover CK, Warrener P, VanDevanter DR, Sherman DR, Arain TM, Langhorne MH, Anderson SW, Towell JA, Yuan Y, McMurray DN, Kreiswirth BN, Barry CE, Baker WR.

A small-molecule nitroimidazopyran drug candidate for the treatment of tuberculosis. Nature. 2000 Jun 22;405(6789):962-6.

101. Koonin EV, Senkevich TG, Dolja VV. The ancient Virus World and evolution of cells. Biol Direct. 2006 Sep 19;1:29.

102. Prusoff, W.H. Synthesis and biological activities of iododeoxyuridine, an analog of thymidine. Biochim Biophys Acta. 1959. 32(1): 295–6.

103. Focher F, Spadari S, Maga G. Antivirals at the mirror: the lack of stereospecificity of some viral and human enzymes offers novel opportunities in antiviral drug development. Curr Drug Targets Infect Disord. 2003. 3(1):41-53.

104. Furman, P. A., Wilson , J. E., Reardon , J. E., Painter, G. R. The effect of absolute configuration on the anti-HIV and anti-HBV activity of nucleoside analogs. Antiviral Chem. Chemother. 1995. 6:345–355.

Table 2.1 Typical ranges for parameters related to drug-likeness (Modified from Mark W. and Terry W. Management of chemical and biological samples for screening applications. Wiley-VCH Verlag & Co. KGaA, Boschstr. Weinheim, Germany. 2012)

Parameter	**Minimum**	**Maximum**
Solubility (in water)	100 ug/mL	/
LogP	-2	5
Molecular weight	100	500
Hydrogen bond acceptors	0	10
Hydrogen bond donors	0	5
Rotatable bonds	0	8
Rings	0	4
Polar surface are	0	120
Molar refractivity	40	130
Heavy atoms	20	70
Net charge	-2	+2

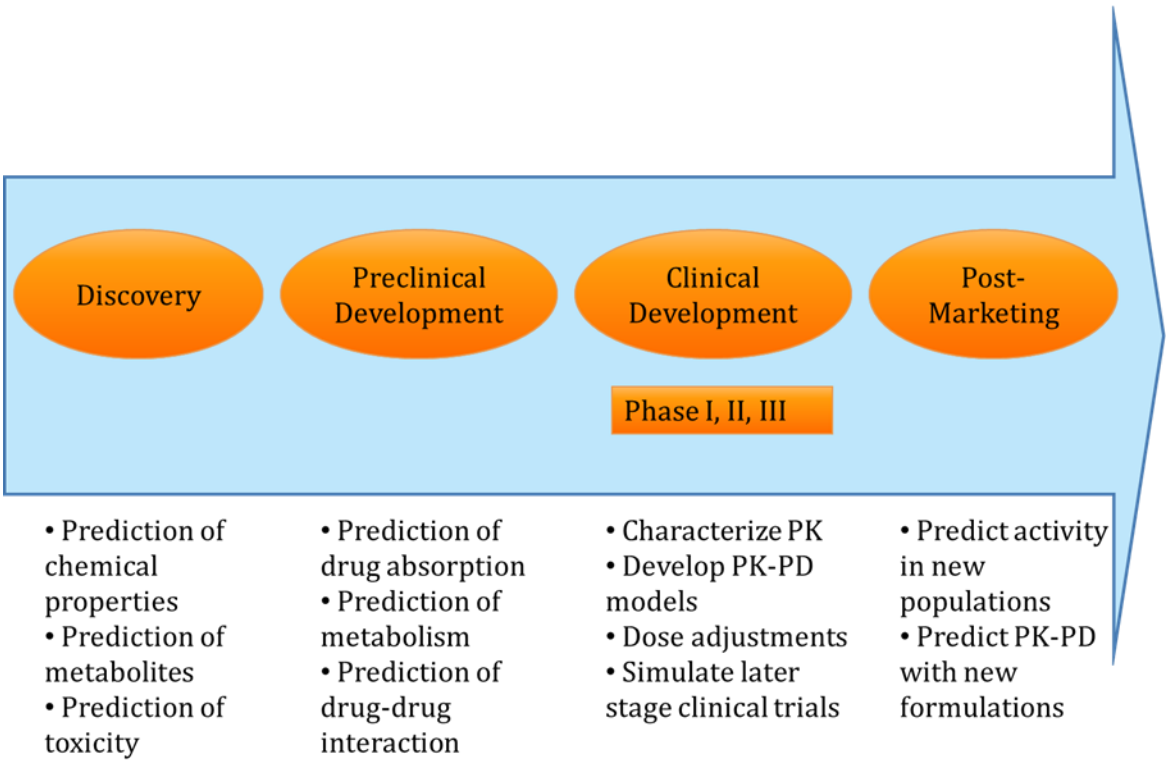

Figure 2.1 Applications of PK concepts during preclinical and clinical drug product development. Figure modified from Peter LB Pharmacokinetic-Pharmacodynamic Modeling and Simulation (second edition) Springer New York Dordrecht Heidelberg London 2011

CHAPTER 3

PRECLINICAL PHARMACOKINETICS AND TISSUE DISTRIBUTION OF (1-DECYL) TRIPHENYLPHOSPHONIUM BROMIDE (dTPP) IN MICE*

*Li, Dawei; James L. Franklin; Catherine A. White. To be submitted to AAPS Journal

ABSTRACT

(1-Decyl) triphenylphosphonium bromide (dTPP) is a potential broad-spectrum, anthelmintic drug. The purpose of this study is to evaluate the preclinical pharmacokinetic profile and tissue distribution of dTPP in mice. An HPLC method for the quantification of dTPP in mouse plasma, brain, liver, kidney, heart, lung, spleen and intestine was developed and validated. Intra-day and inter-day assay precision (<15%) and accuracy (<15%) were observed over a linear range of 0.1-150 ug/mL in plasma or 0.25-150 ug/g in tissues (r2>0.99). The recoveries of dTPP ranged from 93.8-98.9%. Pharmacokinetic parameters were determined in mice after IV and oral dosing. After IV administration, dTPP extensively distributed in tissues, especially in heart and kidney, and was retained in tissues (tissue t½ 2-10 hrs). After oral administration, dTPP extensively distributed in the GI tract, indicating it may be effective in treating infections of GI tract, while, it would be ineffective in treating systemic infections due to the low bioavailability (F=4.8%). After subcutaneous injection, dTPP also extensively distributed in tissues, and maintained steady levels for up to 12 hr, which may make this a good route of administration for treating systemic infections.

Key words: Anthelmintics, HPLC assay, pharmacokinetics, tissue distribution

INTRODUCTION

Parasitic worms (helminths) are the most common infectious agents in humans. They have plagued humans for thousands of years, and historically infected more than half the world's population [1-3]. Generally, parasitic worms are categorized into three groups: nematodes, trematodes and cestodes. The nematodes (hookworm, whipworm, and roundworm), include the major intestinal worms (also known as soil-transmitted helminths) and the filarial worms that cause lymphatic filariasis (LF) and onchocerciasis. The trematodes are also known as flatworms, including the schistosomes that cause schistosomiasis. The cestodes are also known as tapeworms, including pork tapeworm that causes cysticercosis [4, 5]. To date, it is estimated that more than two billion people harbour parasitic worm infections worldwide. Infections are widely distributed in developing regions of sub-Saharan Africa, East Asia, and the South America [6, 7]. In addition, some studies suggest human helminth infections have both direct and indirect effects on malaria and HIV/AIDS. In sub-Saharan Africa and elsewhere, helminthiases are frequently reported to co-infect with malaria and HIV/AIDS, which causes increased susceptibility to infection with these pathogens, and an exacerbated progression of these two lethal diseases (8-10).

The prevalence of parasitic worm infections and associated high medical, educational, and economic burden makes it urgent to launch a global assault on parasitic worms. However, the drugs currently available for combating worm infections are limited. Of the 1,556 new chemical entities marketed between 1975 and 2004, only four drugs- albendazole, oxamniquine, praziquantel, and ivermectin- were licensed for use as human anthelmintics [11]. All of these drugs were initially developed for treating

veterinary parasites [12], and have been used for three decades or more. The limited arsenal of available anthelmintics, coupled with very little development of new drugs specifically targeted for human helminthiasis, makes the situation of anthelmintic resistance even worse [13]. Consequently, there is a desperate need for new anthelmintics to treat human infections.

(1-Decyl)triphenylphosphonium bromide (dTPP, Fig.1a) is an analog of MitoQ (Fig.1b), MitoQ is a mitochondria-targeted antioxidant consisting of a quinone moiety linked to a triphenylphosphonium moiety by a 10-carbon alkyl chain [14-16]. dTPP also contains the triphenylphosphonium cation, which facilitates uptake into mitochondria and this uptake is driven by the membrane potential across the plasma membrane (30-60 mV) and by the mitochondrial membrane potential (150-180 mV) [17, 18]. The hydrophobicity of the carbon chain increases the rate of uptake of MitoQ across biological membranes [18-20]. Due to the similar chemical structure as MitoQ, without the reductive quinone component, dTPP has been used as a negative control compound in several studies investigating the antioxidant activity of MitoQ [21-23]. The anthelmintic activity of dTPP was initially discovered in a study determining the effects of the mitochondria-targeted antioxidant MitoQ on *Caenorhabditis elegans* (C. elegans, a free living soil nematode) longevity. As a negative control in this study, dTPP was applied to *C. elegans* cultures, and paralysis and/or death of nematodes was observed. Further *in vitro* studies suggest that dTPP kills several different types of parasitic worms, such as, *C. elegans*, *H. contortus*, *Brugia malayi*, and *Dirofilaria immitis*, at uM concentration with an IC50 range from 1 to 100uM. The mechanism of action is not yet well understood, but it is highly related to the mitochondria-targeting property of dTPP, which may trigger the

release of calcium from intracellular stores. Other studies suggested that long-term treatment of dTPP causes no adverse effects in rodents [21- 24]. All of this evidence indicates that dTPP is a potential, broad-spectrum anthelmintic, with low toxicity and a novel mechanism of action. In addition, the special structure of dTPP and associated membrane permeability make it interesting to investigate the *in vivo* pharmacokinetics profile and tissue distribution of this compound. Therefore, the purpose of this study is to investigate the pharmacokinetics and tissue distribution of dTPP in mice, and test our hypothesis that dTPP will be extensively distributed in tissues due to its good membrane permeability and mitochondria targeting ability. To achieve the objective of this study, an accurate, sensitive and reproducible HPLC method for the quantification of dTPP in mouse plasma, brain, heart, intestine, kidney, liver, lung, muscle, and spleen was developed and validated

EXPERIMENTAL

Chemicals and Reagents

(1-Decyl)triphenylphosphonium bromide (dTPP) was purchased from Santa Cruz Biotech. (Dallas, TX, USA.). HPLC grade Acetonitrile (ACN) was purchased from Fisher Scientific Inc. (Pittsburgh, PA, USA). Diazepam was used as the internal standard (IS), and was purchased from Sigma Aldrich (St. Louis, MO, USA). Formic Acid was obtained from J.T Baker Inc. (Philipsburg, NJ, USA). Heparin was manufactured by Baxter Healthcare Corporation (Deerfield, IL, USA). Water used throughout the study was purified with a Milli-Q water purification system from Millipore (Millipore, Bedford, MA, USA). Other reagents were analytical grade.

Preparation of Stocks and Standard Solutions

Stock solutions of dTPP and the internal standard at a concentration of 10 mg/mL were prepared in acetonitrile, respectively. Standard solutions of dTPP were prepared by mixing and diluting the appropriate amounts from the stock solutions. The final concentration of the standard solutions were 1000, 500, 100, 50, 10, 5, 2.5 and 1.0 ug/mL. Quality control solutions with concentrations of high (600 ug/mL), medium (60 ug/mL) and low (6 ug/mL) were prepared with acetonitrile from 10 mg/ml stock. An internal standard solution was prepared by diluting the stock solution with acetonitrile to 1000 μg /mL. Stock solutions were stored in brown glass bottles at -80°C when not in use and replaced on a bi-weekly basis. Fresh standard solutions were prepared each day of analysis and validation.

Preparation of standards, quality control samples

Blank plasma, brain, heart, intestine, kidney, liver, lung, muscle and spleen tissue were collected from untreated euthanized mice. The tissues were homogenized with an equivalent volume of deionized water (w/v) with poyltron PT 1200 handheld homogenizers (Kinematica AG, Switzerland). Calibration standards of plasma were constructed by adding 10 μL of the working standard solution and the internal standard working solution to 100 μL of blank plasma. Calibration standards of tissues were constructed by adding 10 μL of the working standard solution and the internal standard working solution to 200 μL of the tissue homogenates. The calibration curve of plasma was in the range of 0.1-100 ug/mL, calibration curves of other biological matrices were in the range of 0.25-100 μg/mL, and the internal standard concentration in each sample was 100 μg/mL. Quality-control samples (QCs) were prepared with blank plasma and tissues

at low (0.6 ug/mL), medium (6 ug/mL) and high (60 ug/mL) concentrations. The calibration standards and QCs were extracted on each day of the analysis with the procedure described below.

Sample Preparation

To each standard, blank and QC samples, 3 volumes of the acetonitrile were added. After mixing on a vortex shaker for 10 min, the samples were centrifuged at 13000 rpm for 10 min. The clear supernatants were collected and 30 uL of the solution was injected for HPLC analysis.

Chromatographic System

HPLC analysis was performed on an Agilent 1100 series system (Santa Clara, CA, USA) equipped with a variable wavelength UV detector, an on-line degasser, a quaternary gradient pump, an autosampler and a column oven. A Phenomenex Luna C18 column (250 x 4.6 mm, 5u particle size), protected by a Phenomenex C18 guard column (Torrance, CA, USA) was used to achieve chromatographic separation.

Chromatographic Conditions

The column temperature was set at 35°C. The mobile phase was comprised of solution A (water with 0.1% formic acid) and solution B (acetonitrile with 0.1% formic acid). The composition of the initial mobile phase was 50:50 (v/v) of solutions A/B, and was changed linearly to 20:80 (v/v) till 5 min, then kept the composition until 8 min. From 8 min to 9 min, the mobile phase was changed to the initial composition, and kept for 3 min before the next injection. The mobile phase flow rate was 1.0 ml/min and the UV detection wavelength was set at 260 nm. HPLC run time for each sample was 12 min.

Under the chromatographic conditions described, dTPP and the internal standard eluted at 5.3 and 6.9 min, respectively.

Method validation

The method was validated according to the FDA guidance for bioanalytical method validation [25].

Linearity

The linearity of the HPLC method for the determination of dTPP was evaluated by a calibration curve in the range of 0.1-100 μg/mL for plasma and 0.25-100 μg/g for tissues. Calibration curves were constructed by plotting peak area ratio (y-axis) of the analyte to the IS versus the nominal concentrations (x-axis) with a weighting (1/y) least-squares linear regression. The calibration curve required a coefficient of determination (R^2) of 0.99 or better, which was considered appropriate for a validated method.

Precision and accuracy

To evaluate the intra-day precision and accuracy, QC samples (n = 5) at low (0.6 ug/mL), medium (6 ug/mL), and high (60 ug/mL) concentrations were processed and injected in one batch. To determine inter-day precision and accuracy, three batches of QC samples were processed by the same procedure on three consecutive days. Each day, a freshly prepared calibration curve was constructed when the QC samples were extracted. The precision was reported as the relative standard deviation (RSD %) which was calculated as the ratio of standard deviations of replicates to the mean concentrations. The accuracy was expressed as the relative error (RE %) which is the % bias of theoretical versus calculated concentrations. For a validated method, the precision of all the measurements should ≤15%, and the accuracy should be within the limits of ±15%.

Recovery and LLOQ

Absolute recoveries were assessed by comparing the peak area of the analyte extracted from QC samples to those of pure compound in the mobile phase at the same concentration. Five repetitions were carried out on QC samples spiked with LLOQ, low, medium and high concentration of dTPP. The lower limit of quantification (LLOQ) was defined as the lowest concentration on the calibration plot with a precision of <20% and an accuracy (RE %) within ± 20%.

Stability

Autosampler stability (25°C, 8 h), bench-top stability (25°C, 4 h) and freeze-thaw stability (3 freeze-thaw cycles, -80°C, 72 h) in plasma and tissues homogenate were tested for the analyte at both low (0.6 ug/mL) and high (60 ug/mL) concentrations (n = 5). The bench-top stability of spiked biological samples stored at room temperature was evaluated for 4h. The freeze-thaw stability was investigated by comparing the samples following three freeze-thaw cycles, against freshly spiked samples. The autosampler stability was evaluated by comparing the extracted plasma or tissue samples that were injected immediately, with the samples that were re-injected after storage in the autosampler for up to 8h.

Animal experiment

Black Swiss mice (weighing 18-22g) were purchased from Charles River Laboratories International, Inc. (Wilmington, MA, USA). All experimental protocols were approved by the University of Georgia Animal Care and Use Committee, and conducted in accordance with guidelines established by the Animal Welfare Act and the National Institutes of Health Guide for the Care and Use of Laboratory Animals. Animals

were maintained on Purina Lab Rodent Chow 5001 and water ad libitum. They were maintained at a constant temperature of 70-75° F with light/dark cycle from 6:00 to 18:00 at an AAALAC (Association for Assessment and Accreditation of Laboratory Animal Care) approved facility on campus. The mice were acclimated (5 mice/cage) for at least a week before they were utilized in the experiments.

Preliminary studies were performed to determine the dosage for pharmacokinetic study of dTPP in mice. The dosages were optimized at 20mg/kg, 100mg/kg and 100mg/kg for IV, oral and subcutaneous injection by testing the dose concentration, dose volume and no adverse effects. Mice were randomly separated into three groups, and were fasted for 12 h before receiving dTPP and provided feed 4 h after drug administration. Mice in group one received an IV bolus dose of dTPP (20 mg/kg) via tail vein injection. Three mice were euthanized at each time point. Blood and tissue samples were collected at 3, 7, 15, 30, 45, 60, 90, 120, 240, 480, 720, 1080, 1440 and 2160 min after administration. Mice in group two received an oral dose of dTPP (100 mg/kg) via gavage. Three mice were euthanized at each time point. Blood and tissue samples were collected at 5, 15, 30, 45, 60, 120, 240, 360, 480 and 720 min after administration. Mice in group three received a subcutaneous injection of dTPP at 100 mg/kg. Three mice were euthanized at a series of time points. Blood and tissue samples were collected at 30, 120, 240, 480 and 720 min after the injection. All blood samples were collected by cardiac puncture. Blood samples were transferred into heparinized microcentrifuge tubes immediately. Plasma was separated by centrifuging blood samples at 6000 rpm for 10 min at 4°C. Portal vein perfusion was performed with 5 mL of saline before collecting tissues. The intestinal contents were removed and the fluid was collected after

centrifuging at 20,000xg at 4°C for 30 min [26]. Brain, heart, kidney, intestine, liver, lung, muscle and spleen tissues were homogenized with an equal amount of water. All samples were stored at -80°C until analysis. All samples were processed and analyzed by a validated HPLC assay to determine the concentrations of dTPP present in the samples. The concentration-time profiles of dTPP in all matrices were plotted.

Pharmacokinetic analysis

The plasma data was analyzed using WinNonlin 5.2. (Pharsight, Mountain View, CA, USA). Plasma data after IV administration were fitted to a two-compartment intravenous bolus model with first-order elimination. Plasma data after oral administration were subjected to one compartmental analysis with first order absorption and elimination. A 1/y weighting scheme was used to analyze both IV and oral data. The following pharmacokinetic parameters were generated; absorption rate constant (Ka), volume of distribution (Vd), elimination half-life (t1/2), peak concentration (Cmax), time to reach peak concentration (Tmax), area under the concentration-time curve (AUC), and total body clearance (CL). Oral bioavailability was calculated by the equation:

$$F = (AUC_{PO}/AUC_{IV}) \text{ X } (Dose_{IV}/Dose_{PO})$$

where, F = bioavailability, AUC_{PO} = area under the concentration-time curve after oral administration, AUC_{IV} = area under the concentration-time curve after intravenous administration, $Dose_{IV}$ = IV dosage and $Dose_{PO}$ = oral dosage.

The tissue data were subjected to non-compartmental analysis using WinNonlin 5.2. Pharmacokinetic parameters such as half-life and area under curve were generated. Relative exposure (RE) of each tissue was calculated by the equation:

$$RE = AUC_{tissue} / AUC_{plasma}$$

where, AUC_{tissue} = area under the concentration-time curve of tissue, AUC_{plasma} = area under the concentration-time curve of plasma. The tissue distribution coefficient of dTPP in tissues after subcutaneous injection was calculated by using dTPP concentrations in tissues divided by dTPP concentration in plasma at the same time point.

RESULTS AND DISCUSSION

Chromatographic results

Since dTPP contains the triphenylphosphonium cation, ion pair chromatography was initially tested for the separation. Different ion pair reagents, pH and gradient conditions were investigated, however, the separation was not acceptable. Considering dTPP also contains carbon alkyl chain, which may be retained by a C18 column, we tested reverse phase C18 column. At low pH levels, good peak shape and separation were observed. The complexity of the biological matrices limited the use of available techniques for the extraction of dTPP due to the wide variety of endogenous substances. It was necessary to perform appropriate sample preparation to eliminate the interference of endogenous substances with peaks of interest. The method was ultimately optimized as the condition described above. Chromatograms were generated by applying optimized sample preparation and HPLC conditions; Fig. 3.2 shows the chromatograms of blank and spiked plasma (a), brain (b), heart (c), intestine (d), kidney (e), liver (f), lung (g), muscle (h) and spleen (i), respectively. By comparing the blank and spiked chromatograms, no interfering peaks from endogenous components were observed where dTPP and the internal standard (IS) were eluted, which indicates good specificity and selectivity for this assay. Under these chromatographic conditions, dTPP and IS were well separated, and eluted at 5.3 min and 6.9 min, respectively.

Method validation

Linearity and range

The linearity of the calibration curves for dTPP was determined using least square regression analysis. The peak area ratio of dTPP is linear in the range of 0.1-100 ug/mL or ug/mg. The coefficient of determination (R^2) of dTPP calibration curves in plasma, brain, heart, intestine, kidney, liver, lung, muscle and spleen are all greater than 0.999 (Table 3.1). The coefficient of variations of slopes for all calibration curves are less than 5%, which indicates a high precision of the present assay.

Precision and accuracy

The intra- and inter-day precision and accuracy of the assay were calculated from 3QC standard and LLOQ samples. Precision is reported as RSD and accuracy is reported RE. RSD and RE values for dTPP in plasma and tissue homogenates are shown in Table 3.2. The intra-assay RSD and RE for the analyte range from 0.44 to 6.69% and ±0.04 to ±10.82%; the inter-assay RSD and RE from 0.26 to 7.50% and ±0.09 to ±7.90%, which met the FDA requirements of less than 15% for QCs and less than 20% for LLOQs.

Recovery

The absolute recoveries of dTPP from plasma and tissues are summarized in Table 3.3. At the concentration range of 0.1-60 ug/mL in plasma or 0.25-60 ug/g in tissue homogenates, the absolute recoveries of dTPP from mouse plasma, brain, heart, intestine, kidney, liver, lung muscle and spleen are greater than 93%. The coefficient of variations of the recoveries are less than 15% for each concentration. The good recovery of dTPP from these biological matrixes is mainly due to the simplified sample preparation.

Stability

When performing method validation, a stability study is an important part that affects the recovery of the analyte from biological samples and the reproducibility of the assay. Stability of dTPP in plasma and tissues was investigated under a variety of storage and processing conditions, including bench-top stability (25°C, 4 h) freeze-thaw stability (3 freeze-thaw cycles, -80°C, 72 h) and autosampler stability (25°C, 8 h). As shown in Table 3.4, the RSD % and RE % of all samples are less than 15%, which indicates dTPP in mouse plasma and tissue homogenates were stable in terms of autosampler, bench-top and freeze-thaw stability.

Pharmacokinetic study of dTPP in mice

The mean plasma and tissues concentration-time profiles after intravenous injection of 20 mg/kg of dTPP are shown in Fig. 3.3. The plasma data after IV administration was fitted to a two-compartment model with first order elimination (Fig. 3.5). Pharmacokinetic parameters for dTPP are displayed in Table 3.5. The pharmacokinetic parameters generated from WINNONLIN non-compartmental analysis for tissues are shown in Table 3.6.

After IV injection, the plasma concentrations of dTPP declined quickly in a bi-exponential fashion, and were not detectable after 2 hr. The elimination half-life (t1/2), systemic clearance (CL), and volume of distribution (Vd) of dTPP are 48.6 ± 10.1 min, 116.0 ± 3.4 mL/min/kg and 6.1 ± 0.3 L/kg, respectively. The CL is considered to be high since the hepatic blood flow of mouse is 70-90 mL/min/kg [27, 28], which suggests that this compound is cleared rapidly from the body. In addition, the CL of dTPP is greater than the hepatic blood flow, which indicates that renal clearance or biliary excretion is

involved in the elimination of dTPP. The Vd of the compound is much higher than the total body water of mouse (0.43 L/kg) [29], indicating that dTPP is extensively distributed in total body fluid. The distribution half-life of dTPP is 2.7 ± 0.1 min. The short distribution half-life indicates fast tissue uptake, which mainly due to the lipophilicity and membrane permeability of dTPP.

As shown in concentration-time profiles of all tissues (Fig. 3.3), dTPP reached peak concentrations at 3-7 min, and then declined in a biexponential fashion. The terminal half-life of dTPP in tissues range from 1.4 to 9.8 hr, which is longer than t1/2 in plasma (48.6 min). The longer half-life of the compound in tissues suggests that dTPP may be sequestered in tissues (especially in heart, with a t1/2 of 9.8 hr), which may be due, in part, to the mitochondria-targeting property of dTPP. The AUCs of all tissues are larger than the plasma AUC, yielding a RE that range from 1.5 to 267.8, which suggests the extensive distribution of dTPP in these tissues. Brain has the lowest RE value (1.5) in all tissues examined, which indicates that dTPP can cross the blood brain barrier and distribute into the brain. The ability of dTPP to cross the blood brain barrier is of particular interest, considering the difficulties of delivering drugs to the brain and the number of CNS parasitic worms. Previous study of Mito Q also showed the substantial accumulation of MitoQ within mouse heart and liver, with significantly less in the brain [24].

The mean plasma and tissues concentration-time profiles after oral administration of 100 mg/kg of dTPP are shown in Fig. 3.4. The plasma data was analyzed using a one-compartment model analysis (Fig. 3.6). The pharmacokinetic parameters generated from WINNONLIN for plasma and tissues are shown in Table 3.5 and Table 3.7, respectively.

After oral administration, dTPP reached peak concentrations in plasma at approximately 30 min, and then declined quickly in a mono-exponential fashion. Since the distribution half-life is approximately 3 min, this phase was masked by the absorption phase. After 2 hr, the dTPP concentration was lower than the LLOQ. The t1/2, CL and Vd estimated from oral data are consistent with those obtained from the IV data, which indicates that the oral administration route did not significantly alter the intrinsic pharmacokinetic behavior of dTPP. The oral bioavailability of dTPP is 4.8%, which is similar to the previous reported low bioavailability of MitoQ [14, 30-32]. dTPP and MitoQ have similar hydrophobicities (log P = 3.7 and 3.4, respectively in octan-1-ol:PBS) and are soluble in water [20, 21, 24]. The solubility would not be considered as factor to limit the absorption and bioavailability of these compounds. Other studies suggested the low bioavailability of MitoQ is mainly due to the intracellular metabolism and the efflux transporting by P-glycoprotein (P-gp) and breast cancer resistance protein (BCRP) [33, 34], which may result in significant first pass effects. *In vitro* Caco2 cell study also showed the low P_{appAB} and high intracellular accumulation of MitoQ, which suggests MitoQ was trapped within the cells possibly due to its superior ability to bind within the mitochondrial membrane [35]. This may also explain the low bioavailability of dTPP, considering the similar chemical structure and cellular up-take behavior of dTPP and MitoQ [36].

High concentrations of dTPP were detected in the intestinal fluid and the intestine after oral administration, and dTPP concentration in intestinal fluid and intestine declined slowly. The concentrations of dTPP in the intestine and the intestine fluid are higher than the IC50 obtained from the *in vitro* efficacy studies. It should be effective to treat

parasitic worms in the GI tract. The high concentration and long t1/2 in intestinal fluid and intestine yields extremely high AUC and RE value in these tissues. In this study, only 10-15cm of small intestine was collected for sample analysis, which may have limitation to represent the distribution of dTPP in the whole GI tract. In the other tissues examined, dTPP concentrations were too low to be detected. The limited tissue distribution of dTPP after oral administration is mainly due to the low oral bioavailability of this compound, which may limit its use in the treatment of systemic parasitic infections.

The mean plasma and tissues concentration after subcutaneous injection of 100 mg/kg of dTPP are shown in Fig. 3.7. The tissue distribution coefficient of dTPP in different tissues was calculated by using the concentration of tissue divided by the concentration of plasma at the same time point, and the result are shown in Fig. 3.8.

After subcutaneous injection, dTPP concentration in plasma and tissues reached a relatively stable concentration at 2-4 hr, and maintained this concentration up to 12 hr. All tissues, except brain, have higher dTPP concentrations than plasma, yielding tissue distribution coefficients of these tissues greater than 1. Kidney has the highest tissue distribution coefficient; heart, intestine, lung and spleen have intermediate tissue distribution coefficients; liver, muscle have the relatively low tissue distribution coefficients; and the brain has the lowest tissue distribution coefficient. The tissue distribution coefficient followed the same rank order as the RE for the tissues following IV administration (Table 3.6). The highest distribution of dTPP in the kidney after IV and subcutaneous injection may due to the renal elimination pathway of dTPP, in which dTPP is distributed in the kidney before excreted into unrein. Efflux transporters present in the blood brain barrier may contribute to the lowest distribution of dTPP in the brain,

considering Mito Q is the substrate of P-gp and BCRP. The tissue distribution coefficient indicates that dTPP is extensively distributed in these tissues after subcutaneous injection, which confirms the membrane permeability of dTPP, and suggests that subcutaneous injection is a good option to treat systemic infections.

The studies presented here improve our understanding of the preclinical pharmacokinetics of dTPP and confirm that dTPP is extensively distributed in tissues such as, brain, heart, intestine, kidney, liver, lung, muscle, and spleen after administration. Our results are consistent with the previous reports about the tissue distribution of MitoQ and other TPP containing compounds [17, 37]. Unlike previous studies that roughly described the pharmacokinetics and tissue distribution of TPP containing compounds, our studies provides the detail pharmacokinetic profile of dTPP with estimated pharmacokinetic parameters in mice.

After IV and oral administration, dTPP is cleared rapidly from the plasma, which may limit its use in clinical treatment for systemic parasitic infections. To obtain more stable plasma and tissue concentration, for the first time, dTPP plasma concentration and tissue distribution after subcutaneous injection were evaluated in this study. The extensive tissue distribution and the maintenance of steady dTPP concentrations in plasma and tissues make subcutaneous injection an alternative route of administration to treat systemic infections. At 100mg/kg dosage of subcutaneous injection, no adverse effects were observed in mice, which indicates that there is still room to increase the dosage to reach the therapeutic concentrations in plasma and tissues. The pharmacokinetic parameters also indicate that dTPP is cleared by multiple elimination pathways, which is also observed in the elimination of MitoQ [36, 38]. Since no detail

information about the elimination of these TPP containing compounds are available now, it would be necessary to investigate the elimination pathways and evaluate their contribution to the total clearance of dTPP. The metabolism study of dTPP is of particular interest, because metabolism is closely related to the hepatic clearance and first pass effect.

CONCLUSIONS

A rapid and sensitive HPLC method was developed to determine dTPP concentrations in mouse plasma, brain, heart, intestine, kidney, liver, lung, muscle and spleen. This method showed high sensitivity, reliability, and specificity, with a total run time of 12.0 min per sample. This method was successfully applied to a pharmacokinetic and tissue distribution study of dTPP in mice. The pharmacokinetic characteristics suggested that dTPP is rapidly cleared from plasma and extensively distributed in tissues such as, brain, heart, intestine, kidney, liver, lung, muscle, and spleen. The extensive tissue distribution and accumulation of dTPP is an ideal property to treat parasitic worm infections. Oral administration of dTPP could be used to treat GI tract parasitic infection, IV and subcutaneous injections could be used to treat systemic infections.

REFERENCES

1. Cox, F.E.G. History of human parasitology. Clin. Microbiol. Rev. 2002. 15:595-612.

2. Hotez, P.J., Ottesen, E., Fenwick, A., and Molyneux, D. The neglected tropical diseases: the ancient afflictions of stigma and poverty and the prospects for their control and elimination. Adv. Exp. Med. Biol. 2006. 582:23-33.

3. Olds GR. Deworming the world. Trans Am Clin Climatol Assoc. 2013. 124:265-74

4. Bethony J, Brooker S, Albonico M, Geiger SM, Loukas A, Diemert D, Hotez PJ. Soil-transmitted helminth infections: ascariasis, trichuriasis, and hookworm. Lancet 2006. 367: 1521-32.

5. Hotez PJ, Brindley PJ, Bethony JM, King CH, Pearce EJ, Jacobson J. Helminth infections: the great neglected tropical diseases. J Clin Invest. 2008. 118(4):1311-21.

6. World Health Organization. Soil-transmitted helminth infections, Fact sheet N°366. WHO, Geneva, Switzerland (2013).

7. Tchuem Tchuenté LA. Control of soil-transmitted helminths in sub-Saharan Africa: Diagnosis, drug efficacy concerns and challenges. Acta Trop. 2011. 120: S4-S11.

8. Hotez PJ, Molyneux DH, Fenwick A, Ottesen E, Ehrlich Sachs S, Sachs JD. Incorporating a rapid-impact package for neglected tropical diseases with programs for HIV/AIDS, tuberculosis, and malaria. PLoS Med. 2006. 3(5):e102.

9. Druilhe, P., Tall, A., and Sokhna, C. Worms can worsen malaria: towards a new means to roll back malaria? Trends Parasitol. 2005. 21:359-362.

10. Borkow, G., and Bentwich, Z. HIV and helminth co-infection. Parasite Immunol. 2006. 28:605-12.

11. Chirac, P., and Torreele, E. Global framework on essential health R&D. Lancet. 2006. 367:1560-1.

12. Geary TG, Woo K, McCarthy JS, Mackenzie CD, Horton J, Prichard RK, de Silva NR, Olliaro PL, Lazdins-Helds JK, Engels DA, Bundy DA. Unresolved issues in anthelmintic pharmacology for helminthiases of humans. Int J Parasitol 2010. 40: 1-13.

13. Prichard RK, Basáñez MG, Boatin BA, McCarthy JS, García HH, Yang GJ, Sripa B, Lustigman S. A research agenda for helminth diseases of humans: intervention for control and elimination. PLoS Negl Trop Dis 2012. 6:e1549.

14. Murphy, M.P. & R.A. Smith. Targeting antioxidants to mitochondria by conjugation to lipophilic cations. Annu. Rev. Pharmacol. Toxicol. 2007. 47:629-56.

15. Chacko BK, Srivastava A, Johnson MS, Benavides GA, Chang MJ, Ye Y, Jhala N, Murphy MP, Kalyanaraman B, Darley-Usmar VM. Mitochondria-targeted ubiquinone (MitoQ) decreases ethanol-dependent micro and macro hepatosteatosis. Hepatology. 2011. 54(1):153-63.

16. Lowes DA, Webster NR, Murphy MP, Galley HF. Antioxidants that protect mitochondria reduce interleukin-6 and oxidative stress, improve mitochondrial function, and reduce biochemical markers of organ dysfunction in a rat model of acute sepsis. Br J Anaesth. 2013. 110(3):472-80.

17. Smith RA, Porteous CM, Gane AM, Murphy MP. Delivery of bioactive molecules to mitochondria *in vivo*. Proc Natl Acad Sci. 2003. 100(9):5407-12.

18. Ross MF, Kelso GF, Blaikie FH, James AM, Cochemé HM, Filipovska A, Da Ros T, Hurd TR, Smith RA, Murphy MP. Lipophilic triphenylphosphonium cations as tools in mitochondrial bioenergetics and free radical biology. Biochemistry (Mosc). 2005. 70(2):222-30.

19. James AM, Cochemé HM, Murphy MP.oxidative damage and ageing. Mitochondria-targeted redox probes as tools in the study of oxidative damage and ageing. Mech Ageing Dev. 2005. 126(9):982-6.

20. James AM, Sharpley MS, Manas AR, Frerman FE, Hirst J, Smith RA, Murphy MP.

Interaction of the mitochondria-targeted antioxidant MitoQ with phospholipid bilayers and ubiquinone oxidoreductases. J Biol Chem. 2007. 282(20):14708-18.

21. Graham D, Huynh NN, Hamilton CA, Beattie E, Smith RA, Cochemé HM, Murphy MP, Dominiczak AF. Mitochondria-targeted antioxidant MitoQ10 improves endothelial function and attenuates cardiac hypertrophy. Hypertension. 2009. 54(2):322-8.

22. Mitchell T, Rotaru D, Saba H, Smith RA, Murphy MP, MacMillan-Crow LA. The mitochondria-targeted antioxidant mitoquinone protects against cold storage injury of renal tubular cells and rat kidneys. J Pharmacol Exp Ther. 2011. 336(3):682-92.

23. Ojano-Dirain CP, Antonelli PJ. Prevention of gentamicin-induced apoptosis with the mitochondria-targeted antioxidant mitoquinone. Laryngoscope. 2012. 122(11):2543-8.

24. Rodriguez-Cuenca S, Cochemé HM, Logan A, Abakumova I, Prime TA, Rose C, Vidal-Puig A, Smith AC, Rubinsztein DC, Fearnley IM, Jones BA, Pope S, Heales SJ, Lam BY, Neogi SG, McFarlane I, James AM, Smith RA, Murphy MP. Consequences of long-term oral administration of the mitochondria-targeted antioxidant MitoQ to wild-type mice. Free Radic Biol Med. 2010. 48(1):161-72.

25. U. S. Department of Health and Human Services, Food and Drug Administration, Guidance for Industry, Bioanalytical Method Validation, May 2001, http://www.fda.gov/CDER/GUIDANCE/4252fnl.pdf.

26. Hamilton DL, Roe WE. Electrolyte levels and net fluid and electrolyte movements in the gastrointestinal tract of weanling swine. Can J Comp Med. 1977. 41(3):241-50.

27. Pang KS, Rowland M. Hepatic clearance of drugs. I. Theoretical considerations of a "well-stirred" model and a "parallel tube" model. Influence of hepatic blood flow, plasma

and blood cell binding, and the hepatocellular enzymatic activity on hepatic drug clearance. J Pharmacokinet Biopharm. 1977. 5(6):625-53.

28. R Brown, M Delp, S Lindstedt, L Rhomberg, R Beliles. Toxicology and industrial health, Vol. 13, No. 4, (1997) 407

29. B Künnecke, P Verry, A Bénardeau, M Kienlin. Obesity Research 12 2004, 1604-15.

30. Li Y, Zhang H, Fawcett JP and Tucker IG. Effect of cyclosporin A on the pharmacokinetics of mitoquinone (MitoQ10), a mitochondria-targeted antioxidant, in rat. AJPS 2010. 5 (3):106-113.

31. Snow BJ, Rolfe FL, Lockhart MM, Frampton CM, O'Sullivan JD, Fung V, Smith RA, Murphy MP, Taylor KM. A double-blind, placebo-controlled study to assess the mitochondria-targeted antioxidant MitoQ as a disease-modifying therapy in Parkinson's disease. Mov Disord 2010. 25:1670-4.

32. Smith RA, Murphy MP. Animal and human studies with the mitochondria-targeted antioxidant MitoQ. Ann N Y Acad Sci. 2010. 1201:96-103.

33. Li Y, Fawcett JP, Zhang H, Tucker IG. Transport and metabolism of MitoQ10, a mitochondria-targeted antioxidant, in Caco-2 cell monolayers. J Pharm Pharmacol. 2007. 59(4):503-11.

34. Porteous CM, Menon DK, Aigbirhio FI, Smith RA, Murphy MP. P-glycoprotein (Mdr1a/1b) and breast cancer resistance protein (Bcrp) decrease the uptake of hydrophobic alkyl triphenylphosphonium cations by the brain. Biochim Biophys Acta. 2013. 1830(6):3458-65.

35. Li Y, Fawcett JP, Zhang H, Tucker IG. Transport and metabolism of some cationic ubiquinone antioxidants (MitoQn) in Caco-2 cell monolayers. Eur J Drug Metab Pharmacokinet. 2008 Oct-Dec;33(4):199-204.

36. Ross MF, Prime TA, Abakumova I, James AM, Porteous CM, Smith RA, Murphy MP. Rapid and extensive uptake and activation of hydrophobic triphenylphosphonium cations within cells. Biochem J. 2008. 411(3):633-45.

37. Porteous CM, Logan A, Evans C, Ledgerwood EC, Menon DK, Aigbirhio F, Smith RAJ, Murphy MP. Rapid uptake of lipophilic triphenylphosphonium cations by mitochondria *in vivo* following intravenous injection: implications for mitochondria-specific therapies and probes. Biochim Biophys Acta 1800(9):1009-1017, 2010.

38. Li Y, Zhang H, Fawcett JP, Tucker IG. Quantitation and metabolism of mitoquinone, a mitochondria-targeted antioxidant, in rat by liquid chromatography/tandem mass spectrometry. Rapid Commun Mass Spectrom. 2007;21(13):1958-64.

Table 3.1. Linear regression equations generated from validation data for each matrix; slope (mean± s.d.), intercept (mean± s.d.), coefficient of determination (mean± s.d.).

Matrix	Slope	Intercept	R^2
Plasma	88.3 ± 0.4	0.03 ± 0.01	0.9997 ± 0.0002
Brain	172.9 ± 0.9	-0.02 ± 0.004	0.9996 ± 0.0004
Heart	172.8 ± 2.4	-0.02 ± 0.02	0.9995 ± 0.0002
Intestine	171.5 ± 3.6	0.03 ± 0.007	0.9992 ± 0.0005
Kidney	171.5 ± 2.3	-0.005 ± 0.02	0.9996 ± 0.0003
Liver	172.1 ± 0.6	-0.09 ± 0.07	0.9993 ± 0.0004
Lung	172.7 ± 1.2	-0.03 ± 0.02	0.9997 ± 0.0001
Muscle	173.6 ± 2.5	0.04 ± 0.01	0.9994 ± 0.0003
Spleen	173.8 ± 2.2	-0.02 ± 0.006	0.9997 ± 0.002

Table 3.2. Intra-day (n=5) and Inter-day (n=15) precision (RSD %) and accuracy (RE %) of the HPLC assay used to quantitate dTPP in mouse plasma, brain, heart, kidney, intestine, liver, lung, muscle, and spleen.

Plasma:

dTPP Conc. (ug/mL)	Intra-day (n=5)			Inter-day (n=15)		
	Conc. observed (ug/mL)	RSD (%)	RE (%)	Conc. observed (ug/mL)	RSD (%)	RE (%)
0.1	0.10 ± 0.004	4.50	4.71	0.11 ± 0.003	2.72	7.90
0.6	0.63 ± 0.01	1.53	5.07	0.59 ± 0.01	1.27	-0.97
6	6.18 ± 0.05	0.77	3.01	6.01 ± 0.07	1.21	0.09
60	60.60 ± 0.26	0.44	1.01	59.90 ± 2.45	0.68	-0.17

Brian:

dTPP Conc. (ug/g)	Intra-day (n=5)			Inter-day (n=15)		
	Conc. observed (ug/g)	RSD (%)	RE (%)	Conc. observed (ug/g)	RSD (%)	RE (%)
0.25	0.27 ± 0.02	5.62	1.64	0.26 ± 0.02	7.50	3.14
0.6	0.58 ± 0.03	5.76	0.04	0.60 ± 0.04	6.12	0.55
6	6.00 ± 0.35	5.86	-3.42	6.05 ± 0.36	5.87	0.86
60	60.99 ± 1.79	2.94	8.09	61.23 ± 2.68	4.37	2.05

Heart:

dTPP Conc. (ug/g)	Intra-day (n=5)			Inter-day (n=15)		
	Conc. observed (ug/g)	RSD (%)	RE (%)	Conc. observed (ug/g)	RSD (%)	RE (%)
0.25	0.25 ± 0.01	3.97	1.34	0.26 ± 0.01	5.78	2.12
0.6	0.61 ± 0.02	4.46	1.41	0.61 ± 0.03	4.45	1.15
6	6.03 ± 0.18	2.94	0.57	6.01 ± 0.22	3.59	0.09
60	61.45 ± 0.73	1.19	2.42	61.61 ± 2.02	3.28	2.68

Intestine:

dTPP Conc. (ug/g)	Intra-day (n=5)			Inter-day (n=15)		
	Conc. observed (ug/g)	RSD (%)	RE (%)	Conc. observed (ug/g)	RSD (%)	RE (%)
0.25	0.26 ± 0.01	5.02	5.95	0.25 ± 0.02	6.04	-0.50
0.6	0.60 ± 0.02	3.39	0.41	0.59 ± 0.04	6.40	-2.11
6	6.22 ± 0.27	4.36	3.61	5.82 ± 0.30	5.08	-3.04
60	59.21 ± 3.18	5.37	-1.31	60.46 ± 2.45	4.05	0.76

Kidney:

dTPP Conc. (ug/g)	Intra-day (n=5)			Inter-day (n=15)		
	Conc. observed (ug/g)	RSD (%)	RE (%)	Conc. observed (ug/g)	RSD (%)	RE (%)
0.25	0.26 ± 0.01	4.80	4.36	0.26 ± 0.01	4.95	4.46
0.6	0.63 ± 0.02	3.50	4.53	0.61 ± 0.03	5.50	1.66
6	6.07 ± 0.25	4.07	1.16	6.06 ± 0.30	4.98	0.96
60	59.35 ± 2.84	4.79	-1.08	59.28 ± 2.62	4.42	-1.19

Liver:

dTPP Conc. (ug/g)	Intra-day (n=5)			Inter-day (n=15)		
	Conc. observed (ug/g)	RSD (%)	RE (%)	Conc. observed (ug/g)	RSD (%)	RE (%)
0.25	0.25 ± 0.01	3.97	1.34	0.26 ± 0.01	5.78	2.12
0.6	0.61 ± 0.02	4.46	1.41	0.61 ± 0.03	4.45	1.15
6	6.03±0.18	2.94	0.57	6.01 ± 0.22	3.59	0.09
60	61.45±0.73	1.19	2.42	61.61 ± 2.02	3.28	2.68

Lung:

dTPP Conc. (ug/g)	Intra-day (n=5)			Inter-day (n=15)		
	Conc. observed (ug/g)	RSD (%)	RE (%)	Conc. observed (ug/g)	RSD (%)	RE (%)
0.25	0.28 ± 0.02	5.99	10.82	0.26 ± 0.02	6.97	5.43
0.6	0.62 ± 0.02	3.06	3.93	0.60 ± 0.03	4.86	0.74
6	6.29 ± 0.22	3.47	4.85	6.11 ± 0.33	5.32	1.81
60	64.26 ± 2.27	3.54	7.10	61.31 ± 3.32	5.41	2.18

Muscle:

dTPP Conc. (ug/g)	Intra-day (n=5)			Inter-day (n=15)		
	Conc. observed (ug/g)	RSD (%)	RE (%)	Conc. observed (ug/g)	RSD (%)	RE (%)
0.25	0.25 ± 0.02	6.42	-0.50	0.26 ± 0.02	6.50	4.37
0.6	0.59 ± 0.02	2.90	-3.22	0.61 ± 0.04	5.91	1.56
6	5.89 ± 0.25	4.20	-1.81	5.87 ± 0.29	4.97	-2.24
60	58.15 ± 2.33	4.01	-3.08	59.40 ± 2.40	4.05	-1.01

Spleen:

dTPP Conc. (ug/g)	Intra-day (n=5)			Inter-day (n=15)		
	Conc. observed (ug/g)	RSD (%)	RE (%)	Conc. observed (ug/g)	RSD (%)	RE (%)
0.25	0.28 ± 0.02	6.69	10.12	0.27 ± 0.02	6.61	7.04
0.6	0.63 ± 0.02	3.28	5.47	0.62 ± 0.03	4.73	3.20
6	6.15 ± 0.32	5.15	2.55	6.06 ± 0.31	5.19	1.03
60	62.60 ± 2.26	3.61	4.33	60.94 ± 2.48	4.07	2.48

Table 3.3. Absolute recoveries of dTPP from mouse plasma, brain, heart, kidney, intestine, liver, lung, muscle, and spleen (mean ± s.d., n=15).

Conc. (ug/ml or ug/g)	Plasma*	Brain	Heart	Intestine	Kidney	Liver	Lung	Muscle	Spleen
0.25	95.2 ± 0.01	96.8 ± 0.63	98.2 ± 0.26	98.5 ± 0.32	96.1 ± 0.75	95.7 ± 1.35	97.3 ± 0.77	94.3 ± 1.32	98.0 ± 0.57
0.6	94.1 ± 0.01	98.6 ± 0.25	98.1 ± 0.81	96.2 ± 0.59	93.8 ± 0.18	97.3 ± 0.82	98.7 ± 0.26	96.3 ± 0.85	96.9 ± 1.26
6	95.6 ± 0.004	97.0 ± 0.58	94.1 ± 0.38	94.6 ± 0.96	98.4 ± 0.82	98.9 ± 0.58	97.8 ± 0.93	95.7 ± 1.18	98.7 ± 0.61
60	96.2 ± 0.02	97.5 ± 0.31	97.0 ± 0.74	98.1 ± 0.67	97.0 ± 1.06	96.6 ± 1.02	95.6 ± 1.62	97.2 ± 1.33	94.1 ± 1.18

*Spiked concentration in plasma were 0.1, 0.6, 6 and 60 ug/mL

Table 3.4. Autosampler stability (n = 5), bench-top stability (n = 5) and freeze-thaw stability (n =5) of dTPP at 0.6 and 60.0 ug/mL or g concentrations in mouse plasma, brain, heart, kidney, intestine, liver, lung, muscle, and spleen.

Plasma:

Stability	Spiked conc. (ug/mL)	Conc.observe (ug/mL)	RSD %	RE %
Three freeze-thaw cycles	0.6	0.59 ± 0.01	2.31	-2.20
	60	57.9 ± 3.33	5.76	-3.43
Bench-top (4h)	0.6	0.63 ± 0.03	4.59	4.24
	60	58.8 ± 2.02	3.43	-1.90
Auto-sampler (8h)	0.6	0.59 ± 0.01	1.26	-0.97
	60	59.9 ± 0.45	0.68	-0.17

Brain:

Stability	Spiked conc. (ug/g)	Conc.observe (ug/g)	RSD %	RE %
Three freeze-thaw cycles	0.6	0.59 ± 0.03	4.46	-3.77
	60	57.7 ± 2.57	5.07	-1.94
Bench-top (4h)	0.6	0.60 ± 0.03	3.43	-2.3
	60	58.6 ± 2.10	4.98	-0.81
Auto-sampler (8h)	0.6	0.61 ± 0.02	3.31	-1.9
	60	58.9 ± 1.95	4.21	1.06

Heart:

Stability	Spiked conc. (ug/g)	Conc.observe (ug/g)	RSD %	RE %
Three freeze-thaw cycles	0.6	0.57 ± 0.03	4.96	-4.52
	60	58.1 ± 1.00	1.73	-3.21
Bench-top (4h)	0.6	0.59 ± 0.02	4.17	-2.09
	60	58.1 ± 1.85	3.18	-3.25
Auto-sampler (8h)	0.6	0.60 ± 0.02	2.74	-0.52
	60	58.4 ± 1.10	1.84	-2.6

Intestine:

Stability	Spiked conc. (ug/g)	Conc.observe (ug/g)	RSD %	RE %
Three freeze-thaw cycles	0.6	0.59 ± 0.03	5.78	-1.9
	60	59.3 ± 2.43	4.1	-1.17
Bench-top (4h)	0.6	0.60 ± 0.02	3.39	0.41
	60	59.2 ± 3.18	5.37	-1.31
Auto-sampler (8h)	0.6	0.61 ± 0.04	7.01	2.15
	60	58.2 ± 4.01	6.99	-3.07

Kidney:

Stability	Spiked conc. (ug/g)	Conc.observe (ug/g)	RSD %	RE %
Three freeze-thaw cycles	0.6	0.55 ± 0.01	2.24	-7.6
	60	59.4 ± 1.45	2.45	-1.04
Bench-top (4h)	0.6	0.58 ± 0.02	3.13	-4.04
	60	57.5 ± 2.06	3.58	-4.23
Auto-sampler (8h)	0.6	0.56 ± 0.02	3.78	-6.04
	60	54.2 ± 2.53	4.68	-9.73

Liver:

Stability	Spiked conc. (ug/g)	Conc.observe (ug/g)	RSD %	RE %
Three freeze-thaw cycles	0.6	0.59 ± 0.01	2.39	-1.80
	60	59.1 ± 1.09	1.84	-1.53
Bench-top (4h)	0.6	0.59 ± 0.03	4.89	-1.97
	60	60.3 ± 1.07	1.77	0.45
Auto-sampler (8h)	0.6	0.61 ± 0.03	4.72	1.37
	60	61.5 ± 2.21	3.59	2.49

Lung:

Stability	Spiked conc. (ug/g)	Conc.observe (ug/g)	RSD %	RE %
Three freeze-thaw cycles	0.6	0.54 ± 0.04	7.42	-9.51
	60	56.4 ± 3.08	5.47	-6.04
Bench-top (4h)	0.6	0.56 ± 0.04	6.82	-6.39
	60	56.5 ± 3.74	6.62	-5.78
Auto-sampler (8h)	0.6	0.57 ± 0.02	4.08	-5.34
	60	57.8 ± 0.86	1.49	-3.64

Muscle:

Stability	Spiked conc. (ug/g)	Conc.observe (ug/g)	RSD %	RE %
Three freeze-thaw cycles	0.6	0.59 ± 0.04	7.43	-1.35
	60	58.2 ± 4.07	6.99	-3.07
Bench-top (4h)	0.6	0.59 ± 0.03	4.92	-1.58
	60	56.7 ± 3.13	5.52	-5.56
Auto-sampler (8h)	0.6	0.59 ± 0.04	6.39	-2.11
	60	60.5 ± 2.45	4.05	0.76

Spleen:

Stability	Spiked conc. (ug/g)	Conc.observe (ug/g)	RSD %	RE %
Three freeze-thaw cycles	0.6	0.57 ± 0.03	5.79	-4.97
	60	58.5 ± 3.81	6.52	-2.52
Bench-top (4h)	0.6	0.59 ± 0.03	4.98	-0.81
	60	58.6 ± 2.01	3.43	-2.30
Auto-sampler (8h)	0.6	0.61 ± 0.04	6.99	1.40
	60	59.4 ± 4.06	6.84	-0.97

Table 3.5. Plasma pharmacokinetic parameter estimates for dTPP at 20 mg/kg IV bolus dosing and 100 mg/kg oral dosing (mean± s.d.).

	IV	Oral
Cmax (ug/mL)	32.9 ± 1.4	0.4 ± 0.01
Tmax (min)	-	33.8 ± 1.8
AUC0→∞ (min ug/mL)	172.4 ± 5.0	41.6 ± 2.4
Distribution Half-life (min)	2.7 ± 0.1	-
Elimination Half-life (min)	48.6 ± 10.1	47.8 ± 7.6
Clearance (mL/min/kg)	116.0 ± 3.4	116.1 ± 6.7
Ka (min -1)	-	0.05 ± 0.009
Vd (L/kg)	6.1 ± 0.3	8.0 ± 0.9
Bioavailability (%)	-	4.8 ± 0.2

Table 3.6: Tissue pharmacokinetic parameters and relative exposure (RE) of dTPP at 20 mg/kg IV bolus dosing.

	Half-life (hr)	AUC (min•ug/g)	Cmax (ug/g)	Tmax (min)	RE*
Brain	2.2	257.9	3.1	7	1.5
Heart	9.8	28144.9	72.1	3	163.3
Intestine	1.4	2385.0	28.7	7	13.8
Kidney	4.6	46175.4	109.1	15	267.8
Liver	2.1	1284.9	59.6	3	7.5
Lung	2.6	4161.3	171.3	3	24.1
Spleen	5.1	5968.3	27.0	7	34.6

*Relative Exposure = $AUC_{tissue}/AUC_{plasma}$

Table 3.7: Tissue pharmacokinetic parameters and relative exposure (RE) of dTPP at 100 mg/kg oral dosing.

	Half-life (min)	**AUC (min•ug/g)**	**Cmax (ug/g)**	**Tmax (min)**	**RE***
Intestine	10.8	43761.6	367.0	30	1041.9
GI Tract	11.6	92591.2	1877.9	5	2204.6

*Relative Exposure = $AUC_{tissue}/AUC_{plasma}$

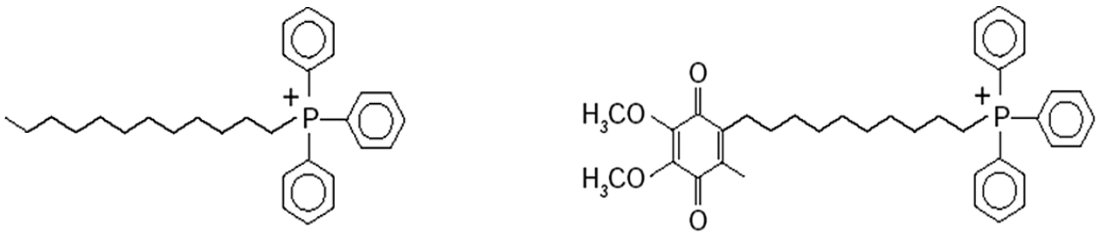

a: dTPP b: MitoQ

Figure 3.1. Chemical structure of dTPP and Mito-Q

a)

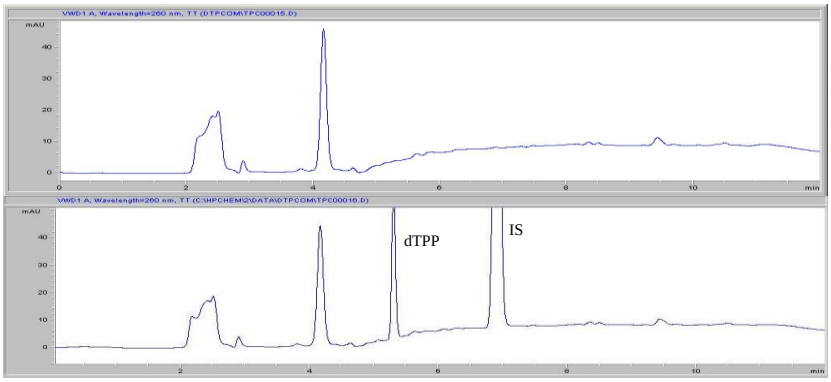

b)

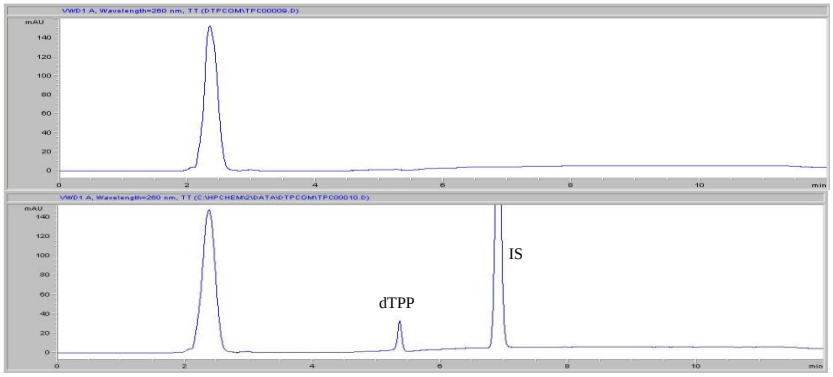

c)

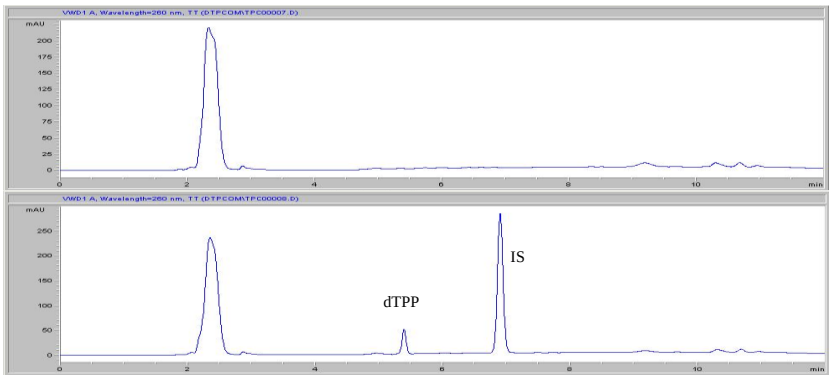

d)

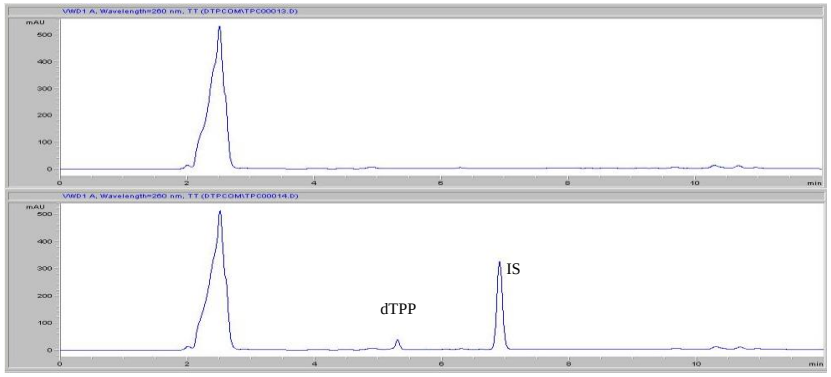

e)

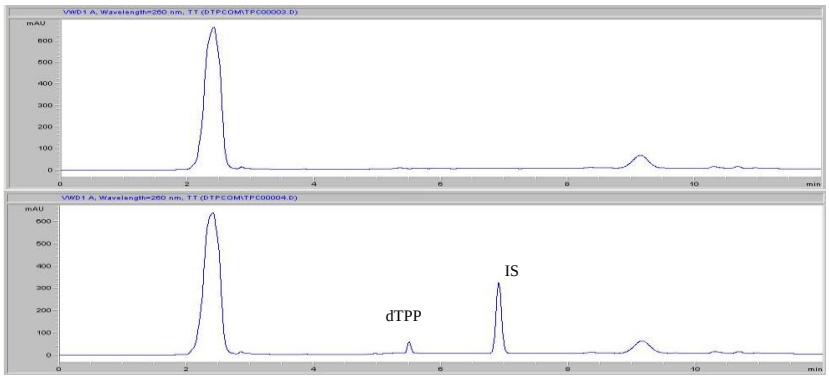

f)

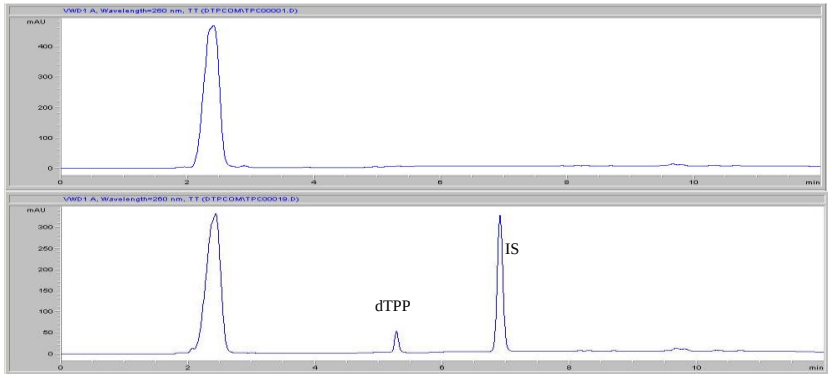

g)

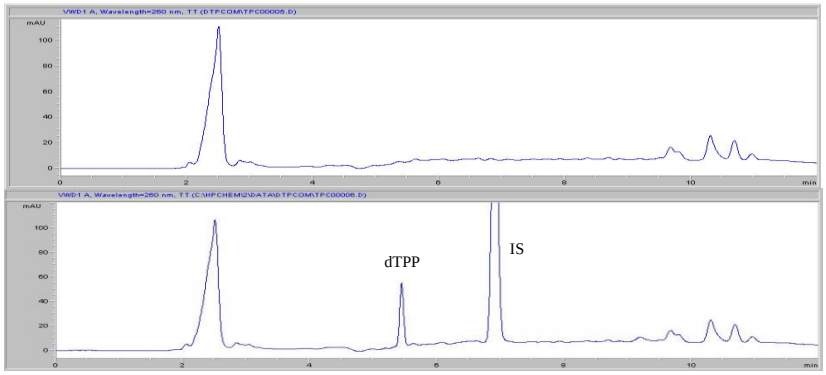

h)

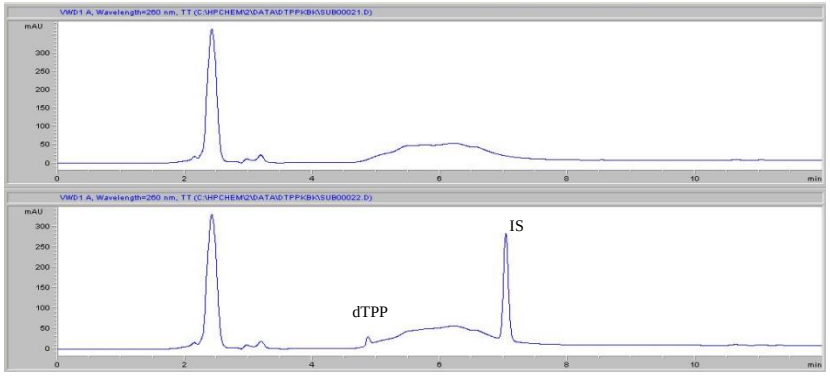

i)

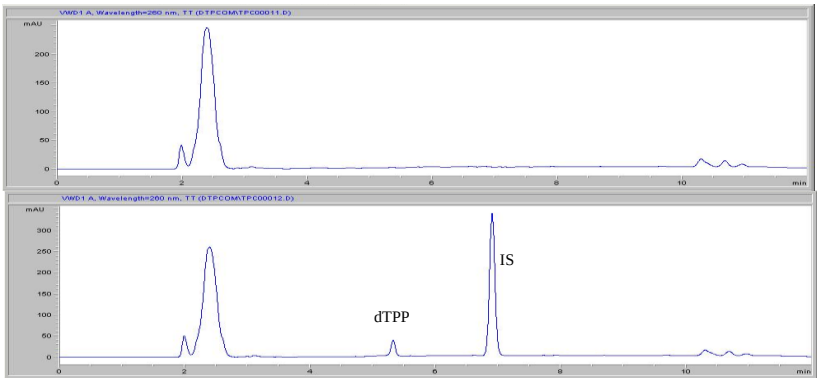

Figure 3.2. Representative HPLC chromatograms of blank (top) and spiked* (bottom) plasma or tissue homogenates: (a) plasma, (b) brain, (c) heart, (d) intestine, (e) kidney, (f) liver, (g) lung, (h) muscle, and (i) spleen.

*plasma or tissue homogenates were spiked with 2 ug/mL dTPP and 100 ug/mL IS

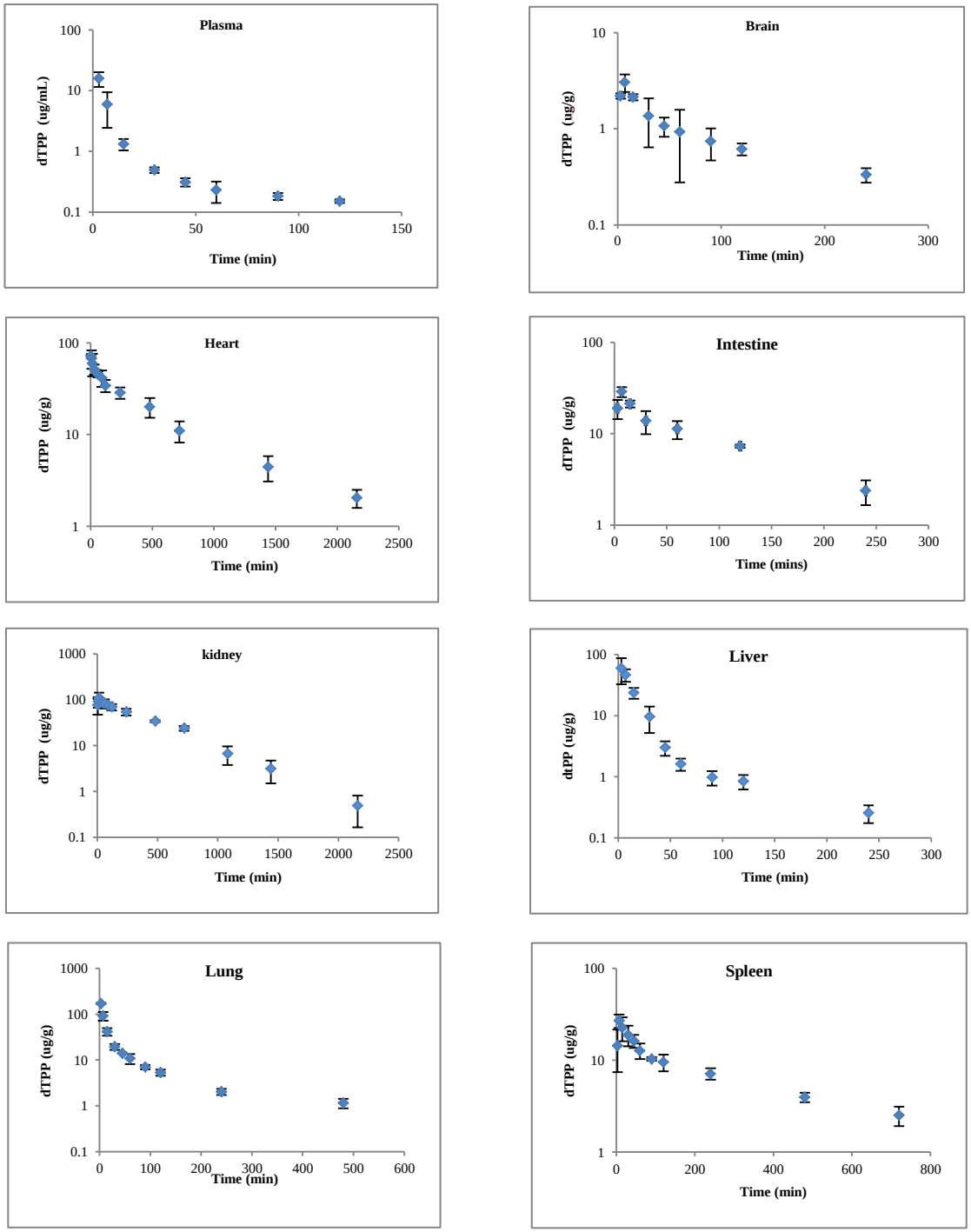

Figure 3.3. Concentration vs. time profiles of dTPP in plasma, brain, heart, intestine, kidney, liver, lung, and spleen after 20 mg/kg of IV bolus

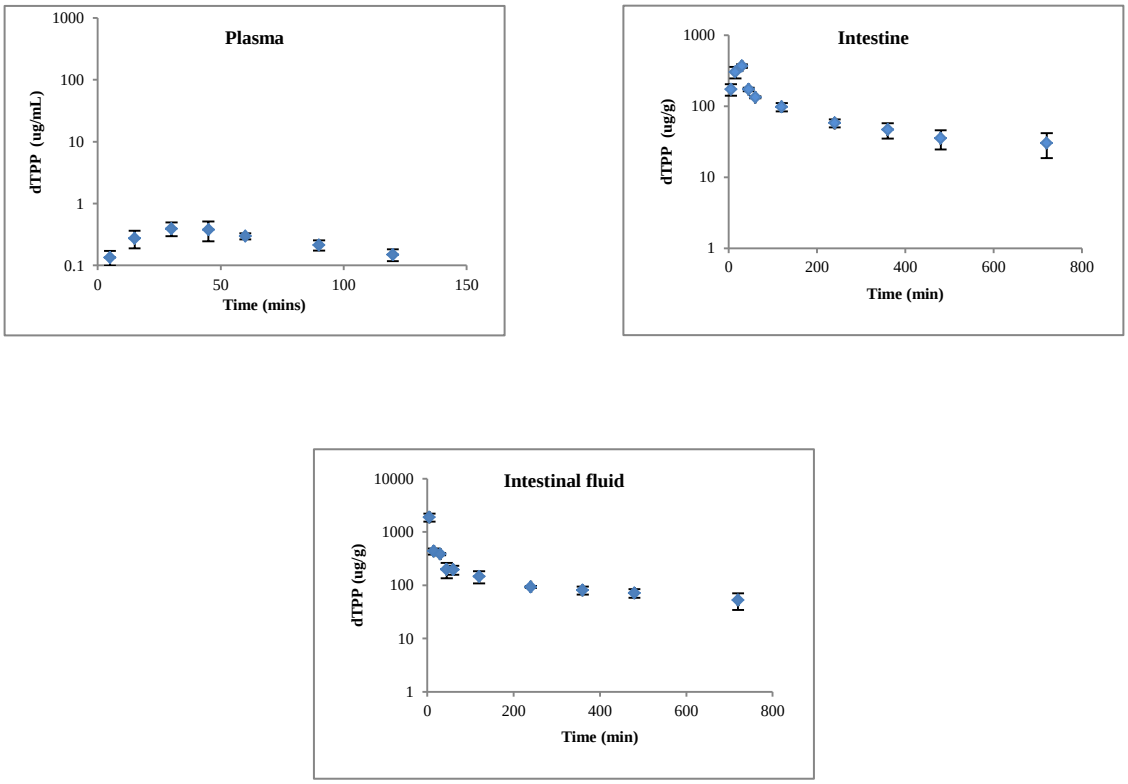

Figure 3.4. Concentration vs. time profiles of dTPP in plasma, intestine, and intestinal fluid after 100 mg/kg of oral administration.

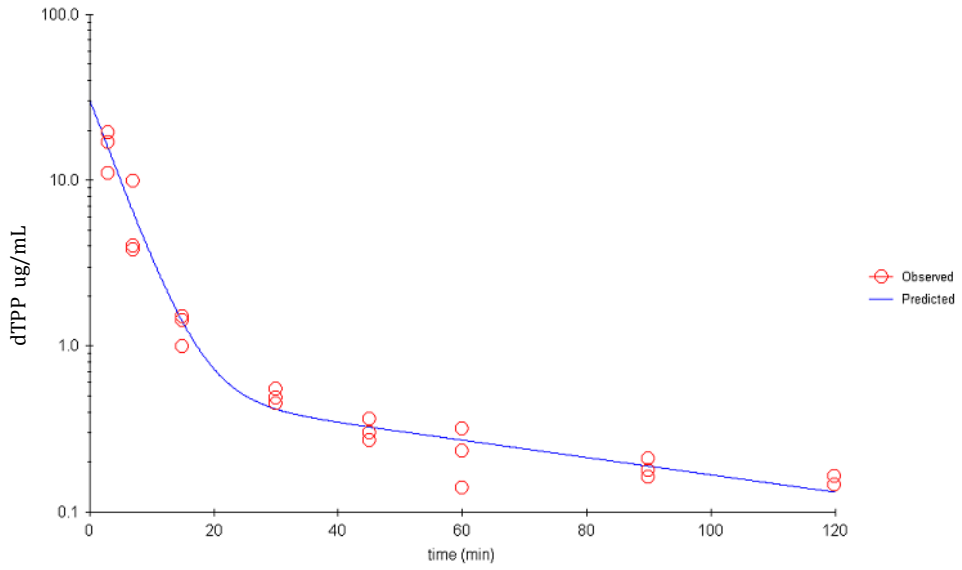

Figure 3.5. Individual plasma concentration after IV administration of dTPP was fitted to a two compartment model.

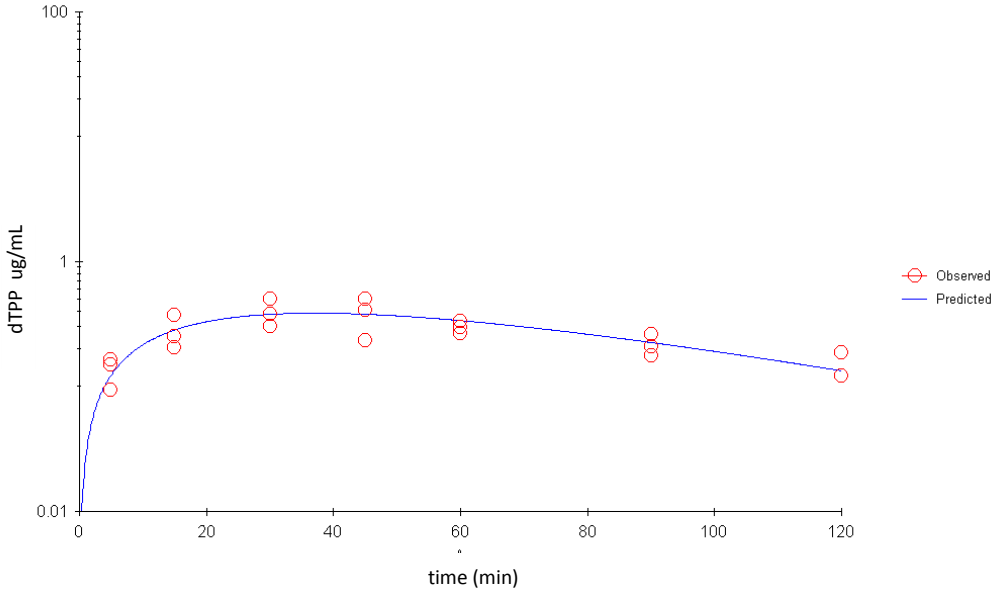

Figure 3.6. Individual plasma concentration after oral administration of dTPP was fitted to a one compartment model.

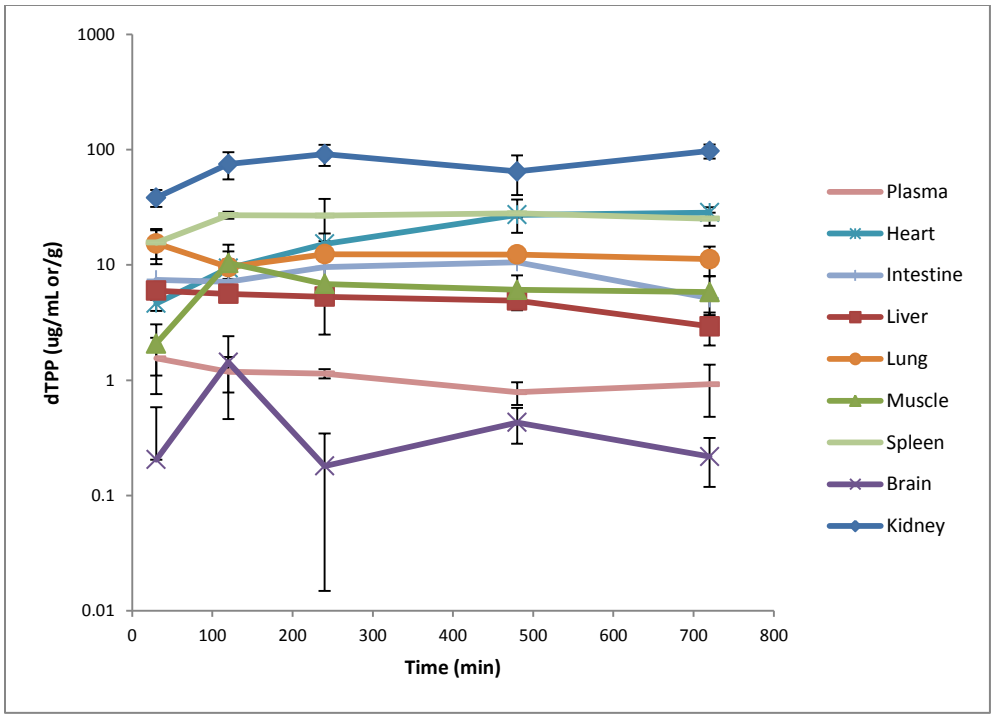

Fig 3.7. dTPP concentration in plasma, brain, heart, kidney, intestine, liver, lung, muscle, and spleen at 30, 120, 240, 480, and 720 min after 100 mg/kg of subcutaneous injection.

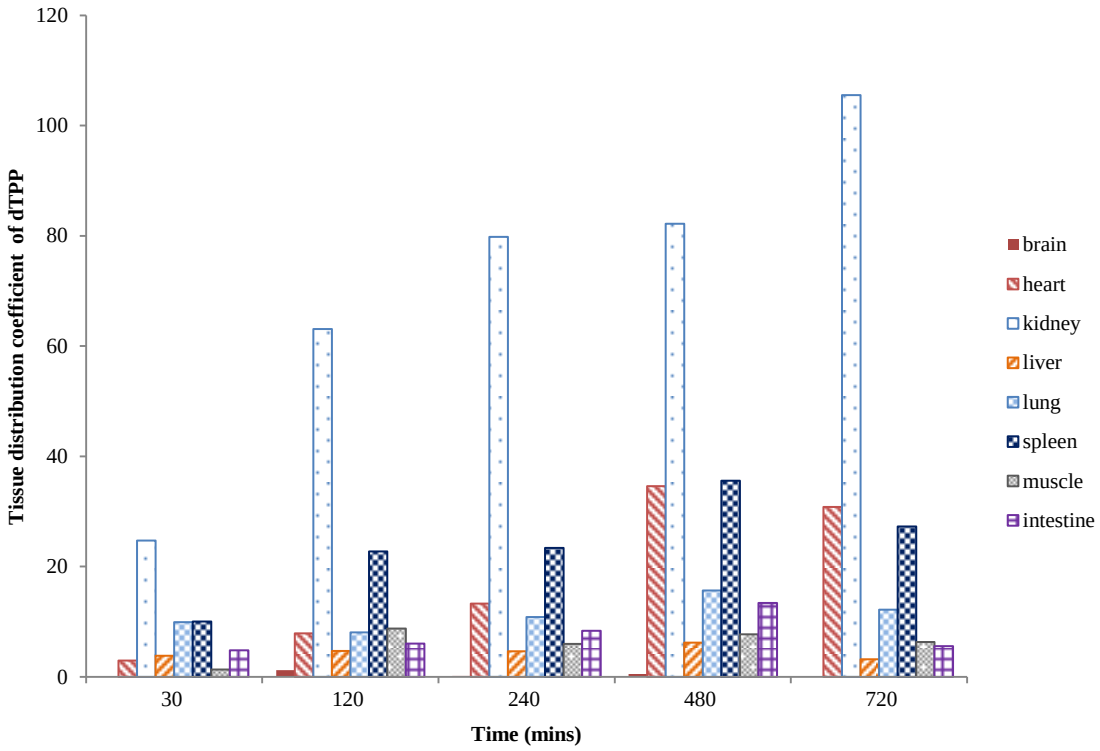

Fig 3.8. Tissue distribution coefficient of dTPP in brain, heart, kidney, intestine, liver, lung, muscle, and spleen at 30, 120, 240, 480, and 720 min after 100 mg/kg of subcutaneous injection.

CHAPTER 4

PRECLINICAL PHARMACOKINETICS AND TISSUE DISTRIBUTION OF OH49, A POTENTIAL ANTI-TUBERCULOSIS COMPOUND*

* Li, Dawei; Catherine A. White. To be submitted to AAPS Journal

ABSTRACT

2-(Hydroxymethyl)phenylboronic acid cyclic monoester (OH49) is an analog of aryl boronic acid, and shows anti-tuberculosis *in vitro*. The purpose of this study was to investigate the preclinical pharmacokinetic profile and tissue distribution of OH49 in mice. In this study, an HPLC method for the quantification of OH49 in mouse plasma, brain, heart, liver, kidney, lung, and spleen was developed and validated. The pharmacokinetics and tissue distribution of OH49 was studied in male CD-1mice following IV and oral administration. After IV administration, OH49 was cleared rapidly from the body with the systemic clearance of 45 mL/min/kg. OH 49 also showed extensive tissue distribution in brain, heart, liver, kidney, lung, and spleen whit the relative exposure value ranging from 1.3 to 2.2. After oral administration, the pharmacokinetics and tissue distribution of OH49 showed a similar pattern with IV data. The bioavailability of OH49 was 28.3%. The pharmacokinetic characteristics suggested that OH49 has rapid oral absorption, low bioavailability, rapid clearance, short elimination half-life, and wide tissue distribution.

Key words: Aryl boronic acid analog, anti- tuberculosis, HPLC assay, pharmacokinetics, tissue distribution

INTRODUCTION

Tuberculosis (TB), is a common, but lethal, infectious disease caused by *mycobacterium tuberculosis* (M.tb) [1]. Since it was first identified by Robert Koch in 1882, M.tb has been a serious threat to human health [2]. Today, at least one third of the entire world's population is infected with M.tb. In 2011, 8.7 million people became ill with TB and 1.4 million died. TB is also a leading killer of people living with human immunodeficiency virus (HIV) causing one quarter of all deaths [3]. A 6-9 month chemotherapy regimen using a combination of 4 drugs (rifampicin, isoniazid, ethambutol, and pyrazinamide) with cure rates of approximately 90% in HIV negative patients is the globally accepted standard treatment of drug-susceptible (DS), active tuberculosis [4]. The concept of TB drug combinations was empirically reached in the 1960s [5, 6], and, in fact, these four first-line drugs and most of the drugs in the second-line treatment are at least 40 years old [7, 8, 9]. The long and intensive treatment with multiple complementary drugs results in poor patient compliance and irrational prescribing practices, which increase the risk of drug-resistant strains of M.tb. Recently, multiple-drug resistant TB (MDR-TB, strains that are resistant to isoniazid and rifampin) and extensively drug resistant TB (XDR-TB, strains that are resistant to isoniazid and rifampin, as well as any fluoroquinolone and at least one of three injectable second-line drugs, such as amikacin, kanamycin, or capreomycin) are on the rise. This makes the disease management of TB more difficult [10, 11]. Now, only eleven new or repurposed tuberculosis drugs are in clinical investigation, 1 in phase I, 7 in phase II, and 3 in phase III trials [12]. Consequently, there is an urgent need for new TB drugs and, in particular, a need for drugs that could shorten treatment regimens as well as treat MDR-TB, XDR-

TB and HIV-TB co-infection. Considering the attrition rate and the length of drug development in general, the need for an even larger assortment of new TB drug candidates is equally urgent [13].

Boronic acids are boron-containing compounds of increasing interest due to their new applications in organic synthesis, catalysis, supramolecular chemistry, biology and medicine [14, 15]. Recently, great attention has been paid to the derivatives of aryl boronic acids for their therapeutic applications. Some boron-based compounds have been discovered and showed excellent antifungal activity [16, 17], anti-inflammatory activity [18], antibiotic activity [19, 20], and antiprotozoal activity [21, 22, 23]. Two-(Hydroxymethyl)phenylboronic acid cyclic monoester (OH49) (Fig. 1) is an aryl boronic acid analog. *In vitro* study has shown the anti-tuberculosis activity of OH49 with minimum inhibitory concentration (MIC) of 12.5 ng/uL. The physicochemical properties of OH49 fully satisfied the Lipinski's rule of five, with molecular weight = 133.9, hydrogen bond acceptors =2, hydrogen bond donors = 1and logP = 2.09. In addition, OH49 has no rotatable bonds and very low polar surface area (29.46 $Å^2$). Therefore, OH49 most likely has good oral absorption, bioavailability and extensive tissue distribution. The purpose of this study was to investigate the tissue distribution and pharmacokinetic profile of this potential anti-tuberculosis agent. In this study, an accurate, sensitive and reproducible HPLC method for the quantification of OH49 in mouse plasma, brain, heart, kidney, liver, lung, and spleen was developed and validated. The pharmacokinetic and tissue distribution study of OH49 was performed in mice following the administration of a 150 mg/kg i.v. or 200 mg/kg oral dose.

MATERIALS AND METHODS

Chemicals and reagents

Two-(Hydroxymethyl)phenylboronic acid cyclic monoester (OH49) was purchased from Sigma-Aldrich (St. Louis, MO, USA). HPLC grade acetonitrile (ACN) was purchased from Fisher Scientific Inc. (Pittsburgh, PA, USA). Diazepam was used as the internal standard (IS), and was purchased from Sigma Aldrich (St. Louis, MO, USA). Potassium hydroxide (KOH), phosphoric acid (H_3PO_4) and monopotassium phosphate (KH_2PO_4) were obtained from J.T Baker Inc. (Philipsburg, NJ, USA). Heparin was manufactured by Baxter Healthcare Corporation (Deerfield, IL, USA). Water used throughout the study was purified with a Milli-Q water purification system from Millipore (Millipore, Bedford, MA, USA). Other reagents were analytical grade.

Preparation of stocks and standard solutions

Stock solutions of OH49 and the internal standard at a concentration of 10 mg/mL were prepared in acetonitrile, respectively. Standard solutions of OH49 were prepared by mixing and diluting the appropriate amounts from the stock solutions. The final concentration of the standard solutions were 1000, 500, 100, 50, 10, 5, and 2.5 ug/mL. Quality control solutions with concentrations of high (600 ug/mL), medium (60 ug/mL) and low (6 ug/mL) of OH49 were prepared with acetonitrile from 10 mg/ml stock. An internal standard solution of diazepam was prepared by diluting the stock solution with acetonitrile to 1000 μg /mL. Stock solutions were stored in brown glass bottles at -80°C when not in use and replaced on a bi-weekly basis. Fresh standard solutions were prepared each day of analysis and validation.

Preparation of standards and quality control samples

Blank plasma, brain, heart, kidney, liver, lung and spleen tissue were collected from untreated euthanized mice. The tissues were homogenized with an equivalent volume of deionized water (w/v) by POLYTRON® PT 1200 Handheld Homogenizers (KINEMATICA AG, Switzerland). Calibration standards of plasma were constructed by adding 10 μL of the working standard solution and the internal standard working solution to 100 μL of blank plasma. Calibration standards of tissues were constructed by adding 10 μL of the working standard solution and the internal standard working solution to 200 μL of the biological matrices. The calibration curves of all matrices were in the range of 0.25-100 μg/mL, with an internal standard concentration in each sample of 100 μg/mL. Quality-control samples (QCs) were prepared with blank plasma and tissues at low (0.6 ug/mL), medium (6 ug/mL) and high (60 ug/mL) concentrations. The calibration standards and QCs were extracted on each day of the analysis with the procedure described below.

Sample Preparation

To each standard, blank and QC samples, 3 volumes of the acetonitrile were added. After mixing vigorously on a vortex shaker for 10 min, the samples were centrifuged at 13000 rpm for 10 min. The clear supernatants were collected, and 40 uL of the solution was injected for HPLC analysis.

Chromatographic System

HPLC analysis was performed on an Agilent 1100 series system (Santa Clara, CA, USA) equipped with a variable wavelength UV detector, an on-line degasser, a quaternary gradient pump, an autosampler and a column oven. A Phenomenex Gemini

C18 column (250 x 4.6 mm, 5u particle size), protected by a Phenomenex C18 guard column (Torrance, CA, USA) was used to achieve chromatographic separation.

Chromatographic Conditions

The column temperature was held at room temperature. The mobile phase was comprised of solution A (20 mM KH_2PO_4, pH 7.0) and solution B (acetonitrile). The composition of the initial mobile phase was 65:35 (v/v) of solutions A/B and was kept until 5 min. From 5 to 7 min the mobile phase was changed linearly to 20:80 (v/v), and was then kept until 9 min. From 9 to 10 min, the mobile phase was changed to the initial composition, and kept for 3 min before the next injection. The mobile phase flow rate was 1.0 ml/min and the UV detection wavelength was set at 265nm. HPLC run time for each sample was 13 min. Under the chromatographic conditions described, OH49 and the internal standard eluted at 7.2 min and 11.5 min, respectively.

Method validation

The method was validated according to the FDA guidance for bioanalytical method validation.

Linearity

The linearity of the HPLC method for the determination of OH49 was evaluated by a calibration curve in the range of 0.25-100 μg/mL or μg/g. Calibration curves were constructed by plotting the peak area ratio (y-axis) of the analyte to the IS versus the nominal concentrations (x-axis) with a weighting (1/y) least-squares linear regression. The calibration curve required a coefficient of determination (R^2) of 0.99 or better, which was considered appropriate for a validated method.

Precision and accuracy

To evaluate the intra-day precision and accuracy, QC samples (n = 5) at low (0.6 ug/mL), medium (6 ug/mL), and high (60 ug/mL) concentrations were processed and injected in one batch. For the assay of the inter-day precision and the accuracy, three batches of QC samples were processed and injected by the same procedure on three consecutive days. Each day, a freshly prepared calibration curve was constructed when the QC samples were extracted. The precision was reported as the relative standard deviation (RSD %), which was calculated by the ratio of standard deviations of replicates to the mean concentrations. The accuracy was expressed as the relative error (RE %) which is the % bias of theoretical versus calculated concentrations. For a validated method, the precision of all the measurements should be ≤15%, and the accuracy should be within the limits of ±15%.

Recovery and LLOQ

Absolute recoveries were assessed by comparing the peak area of the analyte extracted from QC samples to those of pure compound in the mobile phase at the same concentration. Five repetitions were carried out on QC samples spiked with LLOQ, low, medium and high concentration of OH49. The lower limit of quantification (LLOQ) was defined as the lowest concentration on the calibration plot with a precision of <20% and an accuracy (RE %) within ± 20% [24].

Stability

Autosampler stability (25°C, 8 h), bench-top stability (25°C, 4 h) and freeze-thaw stability (3 freeze-thaw cycles, -80°C, 72 h) in plasma and tissues homogenates were tested for the analyte at both low (0.6 ug/mL) and high (60 ug/mL) concentrations (n =

5). The bench-top stability of spiked biological samples stored at room temperature was evaluated for 4 h. The freeze-thaw stability was investigated by comparing the samples following three freeze-thaw cycles, against freshly spiked samples. The autosampler stability was evaluated by comparing the extracted plasma or tissue samples that were injected immediately, with the samples that were re-injected after storage in the autosampler for up to 8 h.

Animal experiment

Male CD-1 mice (weighing 18-22g) were purchased from Charles River Laboratories International, Inc. (Wilmington, MA, USA). All experimental protocols were approved by the University of Georgia Animal Care and Use Committee, and conducted in accordance with guidelines established by the Animal Welfare Act and the National Institutes of Health Guide for the Care and Use of Laboratory Animals. Animals were maintained on Purina Lab Rodent Chow 5001 and water *ad libitum* and maintained at light/dark cycle from 6:00 to 18:00 at an AAALAC (Association for Assessment and Accreditation of Laboratory Animal Care) approved facility on campus. The mice were acclimated (5 mice/cage) for at least a week before they were utilized in the experiments.

According to preliminary studies, the dosages for pharmacokinetic studies were optimized at 150 mg/kg and 200 mg/kg for IV and oral administration. The mice were fasted 12 h before receiving OH49 and provided feed 4 h after drug administration. The mice received an IV bolus dose of OH49 (150 mg/kg) via tail vein injection. Three mice were euthanized at each time point, blood samples were collected at 5, 15, 30, 45, 60, 120 and 180 min after administration and transferred into heparinized microcentrifuge tubes. Plasma was collected after centrifuging blood samples at 6000 rpm for 10 min at 4°C.

Portal vein perfusion was performed with 5 mL of saline before collecting tissues. Brain, heart, kidney, liver, lung and spleen were also collected and homogenized with an equal volume of water. The mice received an oral dose of OH49 (200 mg/kg) via gavage. Three mice were euthanized at each time point, blood samples were collected at 2, 5, 7, 15, 30, 45, 60, 120 and 180 min after administration and transferred into heparinized microcentrifuge tubes. Plasma was collected after centrifuging blood samples at 6000 rpm for 10min at 4°C. Portal vein perfusion was performed with 5 mL of saline before collecting tissues. Brain, heart, kidney, liver, lung and spleen tissues were also collected and homogenized with an equal amount of water. All samples were stored at -80°C until analysis. All samples were processed and analyzed by a validated HPLC assay to determine the concentrations of OH49 present in the samples. The concentration-time profiles of OH49 in all matrices were plotted.

Pharmacokinetic analysis

The plasma data was subjected to compartmental analysis by using WinNonlin 5.2. (Pharsight, Mountain View, CA, USA). The IV data were fitted to a one-compartment model with first-order elimination. Plasma data after oral administration were subjected to one compartmental analysis with first order absorption and elimination. A 1/y2 weighting scheme was used to analyze the IV and oral data. The following pharmacokinetic parameters were determined: absorption rate constant (ka), volume of distribution (Vd), elimination half-life (t1/2), peak concentration (Cmax), time to reach peak concentration (Tmax), area under the concentration-time curve (AUC), and total body clearance (CL). Oral bioavailability was calculated by the equation:

$$F = (AUC_{PO}/AUC_{IV}) \times (Dose_{IV}/Dose_{PO})$$

where, F = bioavailability, AUC_{PO} = area under the concentration-time curve after oral administration, AUC_{IV} = area under the concentration-time curve after intravenous administration, Dose $_{IV}$ = IV dose and Dose $_{PO}$ = oral dose.

The tissue data were subjected to non-compartmental analysis using WinNonlin 5.2. Half-life and area under curve were generated. Relative exposure (RE) of each tissue was calculated by the equation:

$$RE = AUC_{tissue} / AUC_{plasma}$$

where, AUC_{tissue} = area under the concentration-time curve of tissue and AUC_{plasma} = area under the concentration-time curve of plasma.

Stability in mice plasma

The plasma stability of OH49 was investigated using a modified method described previously [25, 26]. Briefly, 1.0 mL of CD-1 mice plasma (Bioreclamation LLC, Westbury, NY, USA) was pre-incubated for 30 min at 37 °C followed by the addition of 10 µL of a 5.0 mg/mL stock solution of OH49. Aliquots (50 µL) were withdrawn at 0, 2, 4, 8, 12, 24, 36, 48 and 72 hr and immediately quenched with three volumes of ice cooled acetonitrile to precipitate the proteins. After mixing vigorously on a vortex shaker for 10 min, the samples were centrifuged at 13000 rpm for 10 min. The clear supernatants were collected for HPLC injection.

RESULTS AND DISCUSSION

Chromatographic results

Chromatograms were generated using optimized sample preparation and HPLC conditions described above. Fig. 4.2 shows the chromatograms of blank and spiked plasma (a), brain (b), heart (c), kidney (d), liver (e), lung (f) and spleen (g), respectively.

In these chromatograms, no endogenous components are found to interfere with the OH49 and diazepam (internal standard) peaks, which indicates good specificity and selectively for this assay. Under these chromatographic conditions, OH49 and diazepam are well separated, and eluted at 7.2 min and 11.4 min, respectively.

Method validation

Linearity and range

The linearity of the calibration curves for OH49 was calculated and constructed by least square regression method. The peak area ratio of OH49 is linear in the range of 0.25-100 ug/mL or ug/g. The coefficient of determination (R^2) of the OH49 calibration curves in plasma, brain, liver, kidney, lung, heart, and spleen were all greater than 0.99 (Table 4.1). The coefficients of variation for slopes of calibration curves were <15%, which indicated high precision of the assay.

Precision and accuracy

The intra- and inter-day precision and accuracy of the assay were calculated from 3 QC standard and LLOQ samples. Precision was reported as the percent relative standard deviation (RSD) and accuracy was reported as relative error (RE). RSD and RE values for OH49 in plasma and tissue homogenates are shown in Table 4.2. The intra-assay RSD and RE for the analyte range from 0.6 to 9.5% and ±0.34 to ±11.0%. The inter-assay RSD and RE from 2.8 to 9.6% and ±0.14 to ±7.0%, which met the FDA requirements of less than 15% for QCs and less than 20% for LLOQs.

Recovery

The absolute recoveries of OH49 from plasma and tissues are summarized in Table 4.3. At the concentration range of 0.25-60 ug/mL or ug/g, the absolute recoveries

of OH49 from mouse plasma and tissues ranged from 91-96%. The coefficient of variations of the recoveries are less than 15% for each concentration.

Stability

Stability studies are very important for validated methods in biological samples. To ensure good reproducibility of the assay, the stability of OH49 in plasma and tissues was investigated under a variety of storage and processing conditions. As shown in Table 4.4, the RSD % and RE % of all samples are less than 15%, which indicate OH49 in mouse plasma and tissue homogenates are stable in terms of autosampler, bench-top and freeze-thaw stability.

Pharmacokinetic study of OH49 in mice

The mean plasma and tissues concentration-time profile of OH49 in mice following intravenous injection of 150 mg/kg and oral gavage of 200 mg/kg are shown in Fig. 4.3 and Fig. 4.4, respectively. After oral administration, the plasma concentration of OH49 increased quickly and reached peak concentration at approximately 7 min. The plasma concentrations of OH49 declined in a mono-exponential fashion for both routes of administration. The concentrations of OH49 in tissues declined in a similar pattern as in plasma after both IV and oral administration. The peak concentrations of OH49 in plasma and tissues are higher than MIC (12.5 ug/mL). OH49 concentrations in plasma and tissues are higher than minimum inhibitory concentration (MIC) for 30-60 min after administration.

The fitted individual plasma concentration-time curve of OH49 using one compartment model analysis are shown in Fig. 4.5 (IV administration) and Fig. 4.6 (oral administration), respectively. The pharmacokinetic parameters generated from

WINNONLIN are shown in Table 4.5. After IV administration, the t1/2 of OH49 is 19.8 ± 0.6 min, indicating the rapid elimination of OH49. Clearance of OH49 is 45.0 ± 3.0 mL/min/kg, which suggests that this compound is cleared rapidly from the body. The hepatic blood flow of mouse is about 74 mL/min/kg [27]. Vd of OH49 is 1.3 ± 0.1 L/kg, which is much higher than the total body water of mouse (0.43 L/kg) [28], suggesting that OH49 is extensively distributed and has significant tissue binding in mice.

The t1/2, CL and Vd of OH49 obtained from oral data are consistent with those from IV data, which indicates that the oral administration route did not alter the intrinsic pharmacokinetic behavior of OH49. The bioavailability of OH49 is 28.3%. Considering the high CL of this compound, the low bioavailability may be due, in part, to first pass metabolism.

The pharmacokinetic parameters for tissues generated from WINNONLIN non-compartmental analysis are shown in Table 4.6 and Table 4.7. The terminal half-life of OH49 in tissues after IV and oral administration ranged from 22.0 to 32.1 min and 25.0 to 34.7 min, which are higher than the terminal half-life of OH49 in plasma. After IV administration, all tissues (except spleen) have higher Cmax than plasma and OH49 concentrations in tissues are higher than those in plasma at all time points. OH49 concentration in spleen exceeds OH49 plasma concentration after 30 min of IV administration. The AUCs of all tissues are larger than plasma AUC, yielding REs range from 1.3 to 2.2 (IV data) and 1.4 to 3.1 (oral data). The REs of all tissues are greater than 1, which suggests extensive distribution of OH49 in these tissues. RE values of brain are 1.6 (IV) and 1.4 (oral), which indicates that OH49 can cross the blood brain barrier easily and distribute into brain. The small molecular size (MW 133.9) and lipophilicity (logP

2.09) of OH49 may contribute to the rapid tissue uptake. The primary target of M.tb infection is the respiratory system and typically the lungs. In addition, in approximately 25% of cases the bacteria enter the blood and infect other parts of the body, such as the pleura, the meninges, the lymphatic system, the genitourinary system and the bones and joints [29]. Therefore, extensive tissue distribution of OH49 is a desired characteristic for treating systemic infection of M.tb.

Our studies provide pharmacokinetic information of OH49 in mice and confirm that OH49 is rapidly absorbed and widely distributed into tissues after administration. Based upon Lipinski's rule of five, the low bioavailability of OH49 is unexpected. Considering the limitation of Lipinski's rule of five which assumes drug absorption follows Fick's first law of diffusion and no other factors, such as, transporters and metabolism, are involved in this process, the low bioavailability of OH49 is acceptable and it may due to the involvement of efflux transporters and first pass metabolism. To better understand the absorption of OH49, it is necessary to perform *in vitro* Caco-2 cells permeability study and metabolic stability study in the future. The species difference of metabolism of OH49 could also be investigated to help the extrapolation of current data to the pharmacokinetics of OH49 in human. Since small animals have relatively high metabolism rate, higher oral bioavailability and longer half-life of OH49 could be expected in human. In addition, modification of the structure of OH49 could improve the pharmacokinetics of this compound. Previous studies showed that minor structure changes in benzoxaborole derivatives result in significant increase of oral bioavailability and elimination half-life [30, 31]. Other published benzoxaborole derivatives with good pharmacokinetic profiles can be used as a reference for the structure modification of

OH49 [31- 33]. Formulations and routes of administration could also be considered to obtain better efficacy of OH49 *in vivo*.

In-vitro stability in mice plasma

OH49 is an analog of aryl boronic acid, and contains cyclic monoester structure. Therefore, OH49 could be a substrate of esterase. Esterases are widely distributed in tissues, especially in the intestine, liver and plasma, which play a major role in drug metabolism and pro-drug activation [34- 36]. To investigate the effect of plasma esterase activity on OH49, an *in vitro* stability study of OH49 was performed in mouse plasma. The concentration-time profile of OH49 incubated in plasma up to 72 hr is shown in Fig. 4.7. The concentration of OH49 declined slowly, which indicates that OH49 is stable in plasma *in vitro*, and esterase is not a significant factor that contributes to the rapid clearance of OH49 in mice. It would be necessary to further investigate the clearance pathways of OH49, and determine the contribution of each pathway to the total clearance.

CONCLUSIONS

A rapid and sensitive HPLC method was developed to determine OH49 concentrations in mouse plasma, brain, heart, kidney, liver, lung and spleen. This method showed high sensitivity, reliability, and specificity, with a total run time of 13.0 min per sample. This method was successfully applied to a pharmacokinetic and tissue distribution study of OH49 in mice. The pharmacokinetic characteristics suggested that OH49 has rapid oral absorption, low bioavailability, short elimination half-life, rapid clearance from the body and wide tissue distribution. The *in vitro* study showed that OH49 was stable in mouse plasma, which is mainly due to the stable oxaborole ring and the high hydrolytic resistance of the boron-carbon bond [37].

REFERENCES

1. Kumar V, Abbas AK, Fausto N, Mitchell RN. Robbins Basic Pathology (8th ed.). 2007. Saunders Elsevier. pp. 516-22.

2. Alex Sakula. Robert Koch: Centenary of the Discovery of the Tubercle Bacillus, 1882. Can Vet J. 1983. 24(4): 127-31.

3. World Health Organization. Tuberculosis, Fact sheet Number 104. WHO, Geneva, Switzerland (2013).

4. World Health Organization. Treatment of tuberculosis: guidelines. 4th ed. (WHO/HTM/TB/2009.420).Geneva, Switzerland: WHO, 2009.

5. Cohn DL, Iseman MD. Treatment and prevention of multidrug-resistant tuberculosis. Res Microbiol. 1993.144(2):150-3.

6. Snell NJ. The treatment of tuberculosis: current status and future prospects. Expert Opin Investig Drugs. 1998. 7(4):545-52.

7. Hans LR. Fourth-generation fluoroquinolones in tuberculosis. 2009. Lancet 373 (9670): 1148-9.

8. Sensi P, Margalith P, Timbal MT. Rifomycin, a new antibiotic—preliminary report. 1959. Farmaco Ed Sci 14: 146-7.

9. Yendapally R, Lee RE. Design, synthesis, and evaluation of novel ethambutol analogues. 2008. Bioorg Med Chem Lett. 18 (5): 1607-11.

10. Sacchettini JC, Rubin EJ, Freundlich JS. Drugs versus bugs: in pursuit of the persistent predator Mycobacterium tuberculosis. Nat Rev Microbiol. 2008. 6:41-52.

11. Moraski GC, Markley LD, Hipskind PA, Boshoff H, Cho S, Franzblau SG, Miller MJ. Advent of Imidazo[1,2-a]pyridine-3-carboxamides with Potent Multi- and Extended Drug Resistant Antituberculosis Activity. ACS Med Chem Lett. 2011. 2(6):466-70.

12. Lienhardt C, Raviglione M, Spigelman M, Hafner R, Jaramillo E, Hoelscher M, Zumla A, Gheuens J. New drugs for the treatment of tuberculosis: needs, challenges, promise, and prospects for the future. J Infect Dis. 2012. 205 Suppl 2:S241-9.

13. Kaneko T, Cooper C, Mdluli K. Challenges and opportunities in developing novel drugs for TB. Future Med Chem. 2011. 13(11):1373-400.

14. D.G. Hall (Ed.), Boronic Acids: Preparation and Applications in Organic Synthesis and Medicine, Wiley-VCH, Weinheim, Germany, 2005

15. Philipp M, Bender ML. Inhibition of serine proteases by arylboronic acids. Proc. Natl Acad. Sci. 1971. 68(2), 478-80.

16. Baker SJ, Zhang YK, Akama T, Lau A, Zhou H, Hernandez V, Mao W, Alley MR, Sanders V, Plattner JJ. Discovery of a new boron-containing antifungal agent, 5-fluoro-1,3-dihydro-1-hydroxy-2,1- benzoxaborole (AN2690), for the potential treatment of onychomycosis. J Med Chem. 2006. 49(15):4447-50.

17. Rock FL, Mao W, Yaremchuk A, Tukalo M, Crépin T, Zhou H, Zhang YK, Hernandez V, Akama T, Baker SJ, Plattner JJ, Shapiro L, Martinis SA, Benkovic SJ, Cusack S, Alley MR. An antifungal agent inhibits an aminoacyl-tRNA synthetase by trapping tRNA in the editing site. Science. 2007. 316(5832):1759-61.

18. Akama T, Baker SJ, Zhang Y-K, Hernandez V, Zhou H, Sanders V, Freund Y, Kimura R, Maples KR, Plattner JJ. Discovery and structure-activity study of a novel benzoxaborole anti-inflammatory agent (AN2828) for the potential topical treatment of psoriasis and atopic dermatitis. Bioorg Med Chem Lett. 2009. 19: 2129-32.

19. Bouchillon SK, Hackel M, Hoban DJ, Hawser SP, Scanarella-Oman NE. GSK2251052, a novel boron-containing protein synthesis inhibitor, with comparative *in*

vitro activity against Pseudonomas aeruginosa from a global population. 2011. Presented at the 51st Interscience Conference on Antimicrobial Agents and Chemotherapy (ICAAC) Meeting, Chicago, IL. Abstract E-129.

20. Xia Y, Cao K, Zhou Y, Alley MRK, Rock F, Mohan M, Meewan M, Baker SJ, Lux S, Ding CZ, Jia G, Kully M, Plattner JJ. Synthesis and SAR of novel benzoxaboroles as a new class of blactamase inhibitors. Bioorg Med Chem Lett. 2011 21:2533-6.

21. Jacobs RT, Plattner JJ, Keenan M. Boron-based drugs as antiprotozoals. Curr Opin Infect Dis 2011. 24:586-92.

22. Jacobs RT, Plattner JJ, Nare B, Wring SA, Chen D, Freund Y, Gaukel EG, Orr MD, Perales JB, Jenks M, Noe1 RA, Sligar JM, Zhang YK, Bacchi CJ, Yarlett N, Don R. Benzoxaboroles: A new class of potential drugs for human African trypanosomiasis. Future Med Chem 2011. 3:1259-78.

23. Zhang YK, Plattner JJ, Freund YR, Easom EE, Zhou Y, Gut J, Rosenthal PJ, Waterson D, Gamo F-J, Angulo-Barturen I, Ge M, Li Z, Li L, Jian Y, Cui H, Wang H, Yang J. Synthesis and structure-activity relationships of novel benzoxaboroles as a new class of antimalarial agents. Bioorg Med Chem Lett. 2011. 21:644-51.

24. U. S. Department of Health and Human Services, Food and Drug Administration, Guidance for Industry, Bioanalytical Method Validation, May 2001, http://www.fda.gov/CDER/GUIDANCE/4252fnl.pdf.

25. Simões MF, Valente E, Gómez MJ, Anes E and Constantino L. Lipophilic pyrazinoic acid amide and ester prodrugs stability, activation and activity against M. tuberculosis. Eur J Pharm Sci. 2009. 37(3-4):257-63.

26. McDonnell ME, Vera MD, Blass BE, Pelletier JC, King RC, Fernandez Metzler C, Smith GR, Wrobel J, Chen S, Wall BA and Reitz AB. Riluzole prodrugs for melanoma and ALS: Design, synthesis, and *in vitro* metabolic profiling. Bioorg Med Chem. 2012. 20(18):5642-8.

27. R Brown, M Delp, S Lindstedt, L Rhomberg, R Beliles. Toxicology and industrial health, Vol. 13, No. 4, (1997) 407.

28. B Künnecke, P Verry, A Bénardeau, M Kienlin. Obesity Research 12 (2004), 1604-15.

29. Ismael Kassim, Ray CG (editors). Sherris Medical Microbiology (4th ed.). 2004 McGraw Hill.

30. Nare B, Wring S, Bacchi C et al. Discovery of novel orally bioavailable oxaborole 6-carboxamides that demonstrate cure in a murine model of late-stage central nervous system African trypanosomiasis. Antimicrob. Agents Chemother. 2010. 54(10), 4379-88.

31. Akama T, Virtucio C, Dong C, Kimura R, Zhang YK, Nieman JA, Sharma R, Lu X, Sales M, Singh R, Wu A, Fan XQ, Liu L, Plattner JJ, Jarnagin K, Freund YR. Structure-activity relationships of 6-(aminomethylphenoxy)-benzoxaborole derivatives as anti-inflammatory agent. Bioorg Med Chem Lett. 2013. 23(6):1680-3.

32. Jacobs RT, Nare B, Wring SA, Orr MD, Chen D, Sligar JM, Jenks MX, Noe RA, Bowling TS, Mercer LT, Rewerts C, Gaukel E, Owens J, Parham R, Randolph R, Beaudet B, Bacchi CJ, Yarlett N, Plattner JJ, Freund Y, Ding C, Akama T, Zhang YK, Brun R, Kaiser M, Scandale I, Don R. SCYX-7158, an orally-active benzoxaborole for the treatment of stage 2 human African trypanosomiasis. PLoS Negl Trop Dis. 2011. 5(6):e1151.

33. Bowers GD, Tenero D, Patel P, Huynh P, Sigafoos J, O'Mara K, Young GC, Dumont E, Cunningham E, Kurtinecz M, Stump P, Conde JJ, Chism JP, Reese MJ, Yueh YL, Tomayko JF. Disposition and metabolism of GSK2251052 in humans: a novel boron-containing antibiotic. Drug Metab Dispos. 2013 May;41(5):1070-81.

34. Li B, Sedlacek M, Manoharan I, Boopathy R, Duysen EG, Masson P, Lockridge O. Butyrylcholinesterase, paraoxonase, and albumin esterase, but not carboxylesterase, are present in human plasma. Biochem Pharmacol. 2005. 25;70(11):1673-84.

35. Ettmayer, G. L. Amidon, B. Clement, and B. Testa. Lessons learned from marketed and investigational prodrugs. J. Med. Chem. 2004. 47:2393-2404

36. Liederer BM, Borchardt RT. Enzymes involved in the bioconversion of ester-based prodrugs. J Pharm Sci. 2006. 95(6):1177-95.

37. R. R. Haynes , H. R. Snyder. Arylboronic Acids. VIII. Reactions of Boronophthalide. J. Org. Chem., 1964. 29 (11): 3229-33.

Table 4.1. Linear regression equations generated from validation data for each matrix; slope (mean± s.d.), coefficient of determination (mean± s.d.).

Matrix	Slope	R^2
Plasma	103.1 ± 11.2	0.9981 ± 0.0016
Brain	78.8 ± 6.6	0.9991 ± 0.0006
Heart	83.2 ± 2.8	0.999 ± 0.0009
Kidney	80.5 ± 4.1	0.9991 ± 0.0007
Liver	78.3 ± 2.1	0.9995 ± 0.0002
Lung	93.6 ± 3.7	0.9985 ± 0.0007
Spleen	94.6 ± 1.4	0.9985 ± 0.001

Table 4.2. Intra-day (n=5) and Inter-day (n=15) precision (RSD %) and accuracy (RE %) of the HPLC assay used to quantitate OH49 in mouse plasma, brain, heart, kidney, liver, lung, and spleen.

Plasma:

OH49 Conc. (ug/mL)	Intra-day (n=5)			Inter-day (n=15)		
	Conc. observed (ug/mL)	RSD (%)	RE (%)	Conc. observed (ug/mL)	RSD (%)	RE (%)
0.25	0.26 ± 0.01	5.5	2.7	0.26 ± 0.02	7.1	2.9
0.6	0.61 ± 0.03	4.9	1.2	0.59 ± 0.03	5.1	-1.2
6	5.7 ± 0.4	7.1	-5.0	5.6 ± 0.3	4.8	-6.1
60	56.7 ± 1.5	2.7	-5.6	59.6 ± 2.7	4.6	-0.6

Brian:

OH49 Conc. (ug/g)	Intra-day (n=5)			Inter-day (n=15)		
	Conc. observed (ug/g)	RSD (%)	RE (%)	Conc. observed (ug/g)	RSD (%)	RE (%)
0.25	0.22 ± 0.01	6.2	-11.0	0.25 ± 0.02	9.6	-0.4
0.6	0.56 ± 0.01	2.6	-6.3	0.59 ± 0.03	4.5	-7.0
6	6.3 ± 0.2	2.5	5.6	5.6 ± 0.5	9.4	-5.9
60	61.1 ± 1.0	1.7	1.9	58.8 ± 4.2	7.2	-2.1

Heart:

OH49 Conc. (ug/g)	Intra-day (n=5)			Inter-day (n=15)		
	Conc. observed (ug/g)	RSD (%)	RE (%)	Conc. observed (ug/g)	RSD (%)	RE (%)
0.25	0.23 ± 0.02	8.1	-7.1	0.25 ± 0.02	9.7	0.14
0.6	0.58 ± 0.06	9.5	-2.9	0.59 ± 0.05	8.9	-1.6
6	5.5 ± 0.2	4.3	-7.9	5.7 ± 0.3	5.9	-5.6
60	58.7 ± 1.0	1.7	-2.2	60.2 ± 2.5	4.1	0.4

Kidney:

OH49 Conc. (ug/g)	Intra-day (n=5)			Inter-day (n=15)		
	Conc. observed (ug/g)	RSD (%)	RE (%)	Conc. observed (ug/g)	RSD (%)	RE (%)
0.25	0.25 ± 0.01	5.1	0.34	0.26 ± 0.02	8.2	3.0
0.6	0.61 ± 0.04	6.0	1.8	0.63 ± 0.04	6.4	4.3
6	5.5 ± 0.1	2.2	-8.2	5.6 ± 0.3	5.2	-7.4
60	58.3 ± 0.9	1.6	-2.8	59.8 ± 3.3	5.6	-0.3

Liver:

OH49 Conc. (ug/g)	Intra-day (n=5)			Inter-day (n=15)		
	Conc. observed (ug/g)	RSD (%)	RE (%)	Conc. observed (ug/g)	RSD (%)	RE (%)
0.25	0.25 ± 0.01	5.0	0.21	0.26 ± 0.02	7.9	4.9
0.6	0.58 ± 0.03	6.1	-3.2	0.58 ± 0.04	6.8	-2.6
6	5.6 ± 0.05	1.0	-6.8	5.7 ± 0.2	2.8	-5.6
60	57.3 ± 0.3	0.6	-4.4	59.3 ± 2.4	4.0	-1.2

Lung:

OH49 Conc. (ug/g)	Intra-day (n=5)			Inter-day (n=15)		
	Conc. observed (ug/g)	RSD (%)	RE (%)	Conc. observed (ug/g)	RSD (%)	RE (%)
0.25	0.27 ± 0.01	3.9	6.4	0.25 ± 0.02	9.5	0.8
0.6	0.60 ± 0.01	2.0	0.9	0.62 ± 0.04	6.0	3.2
6	5.5 ± 0.08	1.5	-8.6	5.8 ± 0.4	7.2	-3.4
60	61.3 ± 1.7	2.7	2.1	58.9 ± 2.4	4.1	-1.8

Spleen:

OH49 Conc. (ug/g)	Intra-day (n=5)			Inter-day (n=15)		
	Conc. observed (ug/g)	RSD (%)	RE (%)	Conc. observed (ug/g)	RSD (%)	RE (%)
0.25	0.26 ± 0.02	8.2	5.1	0.26 ± 0.02	8.3	4.3
0.6	0.61 ± 0.02	4.5	2.1	0.62 ± 0.03	4.5	2.5
6	5.9 ± 0.04	0.7	-2.5	6.1 ± 0.3	5.1	1.1
60	58.1 ± 4.6	8.0	-3.1	59.4 ± 3.1	5.3	-1.0

Table 4.3. Absolute recoveries of OH49 from mouse plasma, brain, liver, kidney, lung, heart, and spleen (mean± s.d., n=15).

Conc. (ug/ml or ug/g)	Plasma	Brain	Heart	Kidney	Liver	Lung	Spleen
0.25	92.0 ± 2.5	91.5 ± 3.2	93.0 ± 1.3	92.1 ± 3.8	93.5 ± 6.7	95.0 ± 3.2	93.5 ± 0.6
0.6	92.9 ± 1.8	92.2 ± 1.8	94.5 ± 1.8	95.6 ± 2.5	92.9 ± 2.6	92.6 ± 4.6	92.0 ± 5.0
6	93.0 ± 0.7	91.1 ± 2.0	95.5 ± 2.0	93.2 ± 3.5	93.0 ± 1.0	93.9 ± 3.4	94.7 ± 2.9
60	96.1 ± 1.3	95.8 ± 1.6	95.8 ± 1.7	94.3 ± 1.4	96.1 ± 0.1	92.3 ± 3.4	93.9 ± 0.2

Table 4.4. Autosampler stability (n = 5), bench-top stability (n = 5) and freeze-thaw stability (n =5) of OH49 at 0.6 and 60.0 ug/mL or g concentrations in mouse plasma, brain, heart, kidney, liver, lung, and spleen.

Plasma:

Stability	Spiked conc. (ug/mL)	Conc.observe (ug/mL)	RSD %	RE %
Three freeze-thaw cycles	0.6	0.56 ± 0.02	2.9	-6.8
	60	58.0 ± 1.0	1.7	-3.3
Bench-top (4h)	0.6	0.54 ± 0.02	3.8	-9.9
	60	55.3 ± 1.4	2.6	-7.8
Auto-sampler (8h)	0.6	0.56 ± 0.03	6.1	-7.2
	60	59.4 ± 0.3	0.56	-1.0

Brain:

Stability	Spiked conc. (ug/g)	Conc.observe (ug/g)	RSD %	RE %
Three freeze-thaw cycles	0.6	0.55 ± 0.03	6.1	-7.6
	60	59.0 ± 0.6	1.1	-1.7
Bench-top (4h)	0.6	0.56 ± 0.03	5.9	-7.0
	60	60.2 ± 5.3	8.9	0.3
Auto-sampler (8h)	0.6	0.56 ± 0.04	7.1	-6.7
	60	58.1 ± 1.0	1.8	-3.2

Heart:

Stability	Spiked conc. (ug/g)	Conc.observe (ug/g)	RSD %	RE %
Three freeze-thaw cycles	0.6	0.56 ± 0.04	7.3	-6.5
	60	56.0 ± 2.1	3.8	-6.7
Bench-top (4h)	0.6	0.56 ± 0.05	9.2	-7.1
	60	59.8 ± 3.7	6.2	-0.3
Auto-sampler (8h)	0.6	0.55 ± 0.02	3.6	-8.1
	60	60.1 ± 0.6	0.9	0.1

Kidney:

Stability	Spiked conc. (ug/g)	Conc.observe (ug/g)	RSD %	RE %
Three freeze-thaw cycles	0.6	0.57 ± 0.01	2.3	-5.6
	60	56.0 ± 0.1	1.8	-6.6
Bench-top (4h)	0.6	0.57 ± 0.04	7.5	-5.1
	60	59.0 ± 1.4	2.3	-1.7
Auto-sampler (8h)	0.6	0.58 ± 0.03	5.9	-2.7
	60	57.6 ± 1.3	2.3	-4.0

Liver:

Stability	Spiked conc. (ug/g)	Conc.observe (ug/g)	RSD %	RE %
Three freeze-thaw cycles	0.6	0.54 ± 0.02	4.2	-9.5
	60	54.9 ± 1.5	2.7	-8.5
Bench-top (4h)	0.6	0.56 ± 0.05	8.1	-6.0
	60	58.2 ± 3.7	6.4	-3.0
Auto-sampler (8h)	0.6	0.54 ± 0.03	5.3	-10.5
	60	61.2 ± 2.9	4.7	3.0

Lung:

Stability	Spiked conc. (ug/g)	Conc.observe (ug/g)	RSD %	RE %
Three freeze-thaw cycles	0.6	0.56 ± 0.03	4.7	-6.1
	60	59.1 ± 2.2	3.8	-1.4
Bench-top (4h)	0.6	0.62 ± 0.03	5.2	3.9
	60	62.3 ± 1.6	2.6	3.9
Auto-sampler (8h)	0.6	0.58 ± 0.03	4.6	-3.8
	60	58.9 ± 1.3	2.2	-1.9

Spleen:

Stability	Spiked conc. (ug/g)	Conc.observe (ug/g)	RSD %	RE %
Three freeze-thaw cycles	0.6	0.56 ± 0.02	2.9	-6.2
	60	57.9 ± 0.7	1.2	-3.5
Bench-top (4h)	0.6	0.58 ± 0.04	6.7	-3.4
	60	64.3 ± 4.0	6.2	7.2
Auto-sampler (8h)	0.6	0.56 ± 0.03	4.8	-6.4
	60	57.5 ± 1.95	1.4	-4.2

Table 4.5. Plasma pharmacokinetic parameter estimates for OH49 at 150 mg/kg IV bolus dosing and 200 mg/kg oral dosing (mean± s.d.).

	IV	**Oral**
Cmax (ug/mL)	116.5 ± 10.0	33.8 ± 5.4
Tmax (min)	-	7.4 ± 2.7
AUC0→∞ (min ug/mL)	3334.5 ± 225.7	1258.8 ± 188.4
Elimination Half-life (min)	19.8 ± 0.6	19.9 ± 1.5
Clearance (mL/min/kg)	45.0 ± 3.0	44.3 ± 6.7
Ka (min -1)	-	0.32 ± 0.16
Vd (L/kg)	1.3 ± 0.1	1.2 ± 0.3
Bioavailability (%)	-	28.3 ± 0.62

Table 4.6: Tissue pharmacokinetic parameters and relative exposure (RE) of OH49 at 150 mg/kg IV bolus dosing.

	Half-life (min)	AUC (min•ug/g)	Cmax (ug/g)	Tmax (min)	RE*
Brain	22.0	5347.4	154.0	5	1.6
Heart	25.9	7262.9	194.3	5	2.2
Kidney	23.9	6499.5	167.7	5	1.9
Liver	22.9	6721.9	185.6	5	2.0
Lung	25.6	4683.6	143.8	5	1.4
Spleen	32.1	4280.7	96.4	5	1. 3

*Relative Exposure = $AUC_{tissue}/AUC_{plasma}$

Table 4.7: Tissue pharmacokinetic parameters and relative exposure (RE) of OH49 at 200 mg/kg oral dosing.

	Half-life (min)	**AUC (min•ug/g)**	**Cmax (ug/g)**	**Tmax (min)**	**RE***
Brain	29.9	1774.2	75.3	7	1.4
Heart	34.7	2262.5	84.2	7	1.8
Kidney	29.0	2695.5	113.5	7	2.1
Liver	25.0	3916.6	159.7	7	3.1
Lung	30.0	1619.4	52.6	7	1.3
Spleen	31.2	2717.3	86.2	7	2.2

*Relative Exposure = $AUC_{tissue}/AUC_{plasma}$

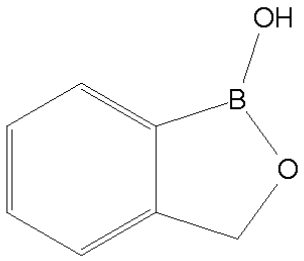

Figure 4.1. Chemical structure of OH49

(a)

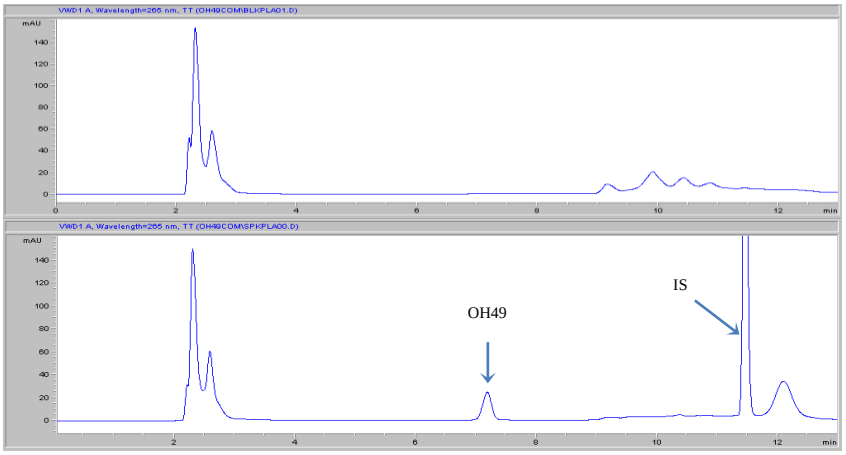
VWD1 A, Wavelength=265 nm, TT (OH49COM\BLKPLA01.D)
mAU
min
VWD1 A, Wavelength=265 nm, TT (OH49COM\SPKPLA00.D)
OH49
IS

(b)

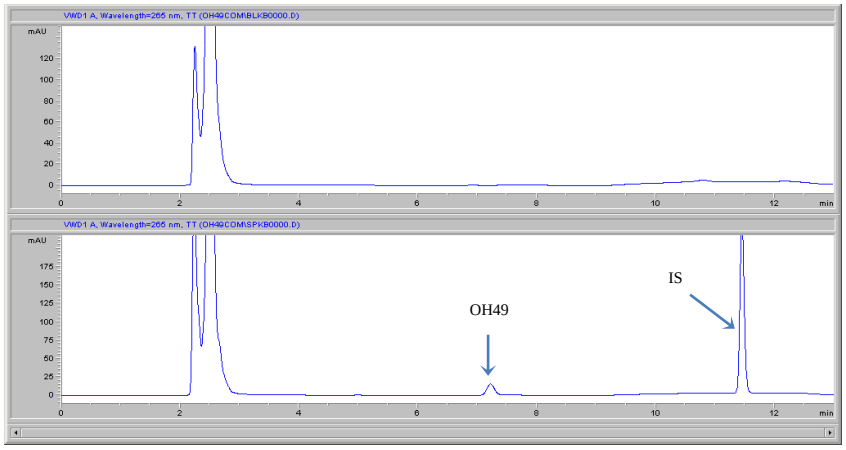
VWD1 A, Wavelength=265 nm, TT (OH49COM\BLKB0000.D)
mAU
min
VWD1 A, Wavelength=265 nm, TT (OH49COM\SPKB0000.D)
OH49
IS

(c)

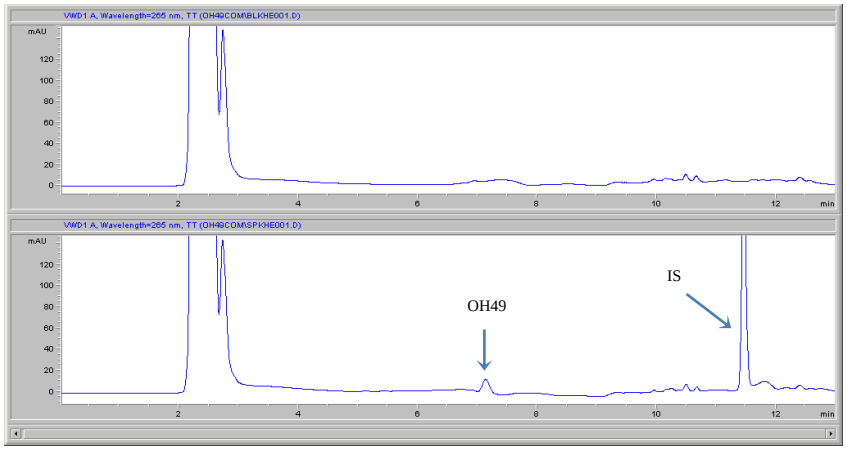
VWD1 A, Wavelength=265 nm, TT (OH49COM\BLKHE001.D)
mAU
min
VWD1 A, Wavelength=265 nm, TT (OH49COM\SPKHE001.D)
OH49
IS

(d)

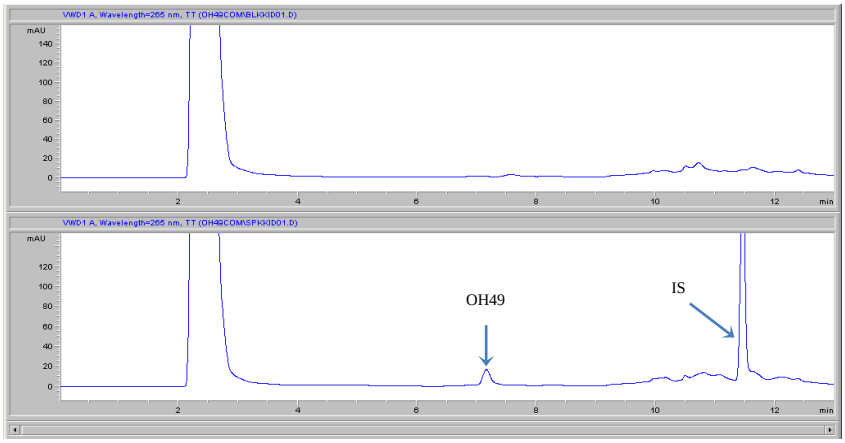

(e)

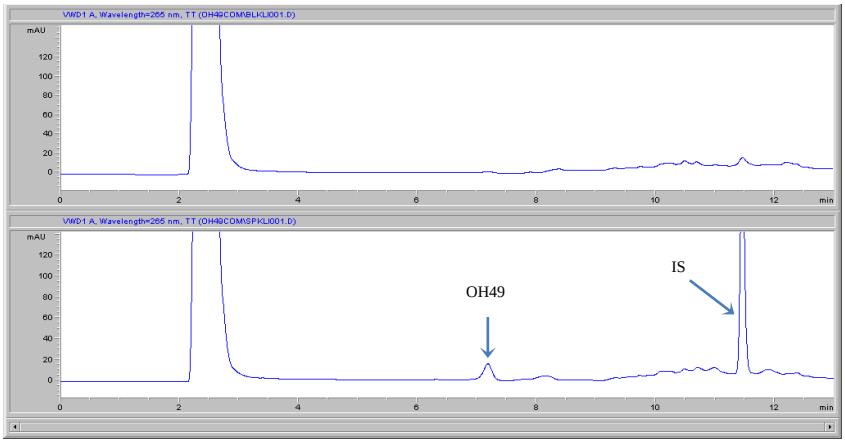

(f)

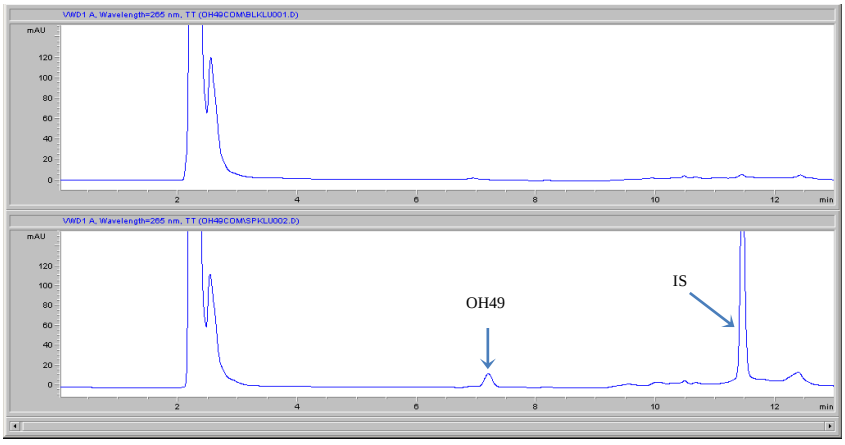

(g)

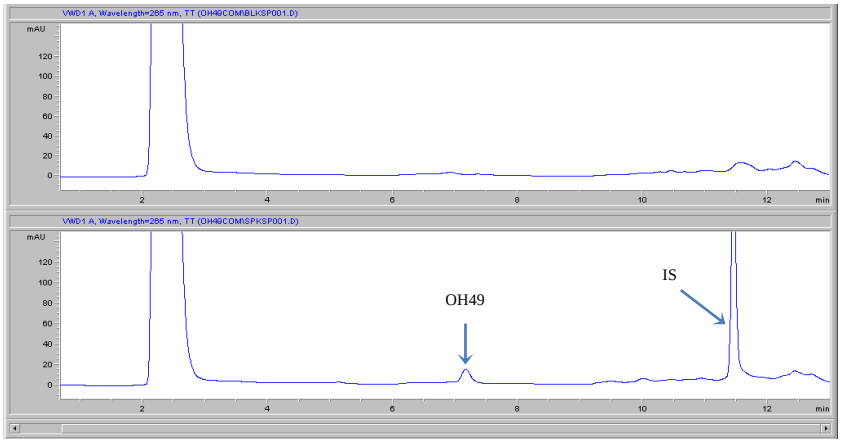

Figure 4.2. Representative HPLC chromatograms of blank (top) and spiked* (bottom) plasma or tissue homogenates: (a) plasma, (b) brain, (c) heart, (d) kidney, (e) liver, (f) lung, and (g) spleen.

*plasma or tissue homogenates were spiked with 2 ug/mL OH49 and 100 ug/mL IS

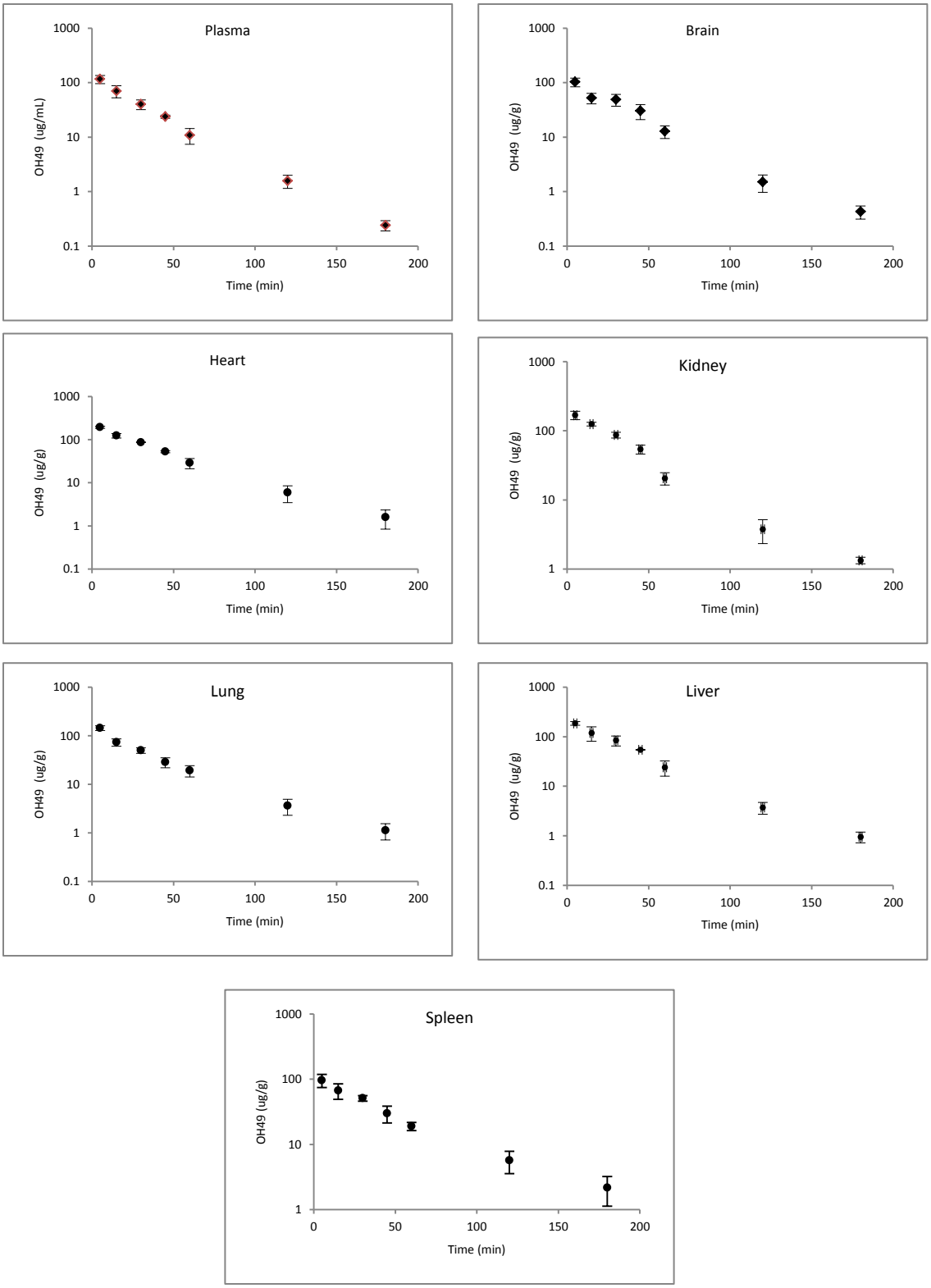

Figure 4.3. Concentration vs. time profiles of OH49 in plasma, brain, heart, kidney, liver, and spleen after 150 mg/mL of IV bolus

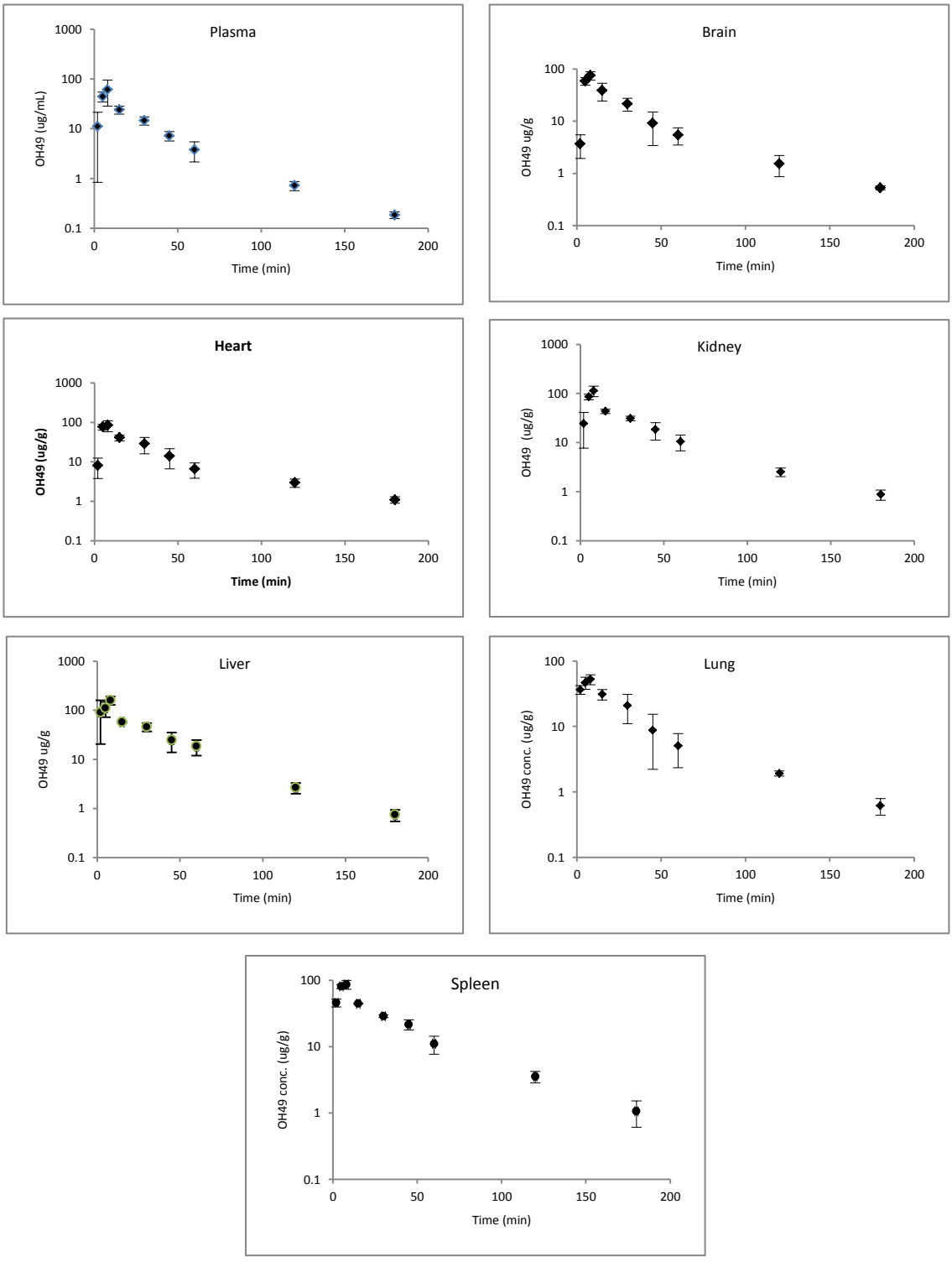

Figure 4.4. Concentration vs. time profiles of OH49 in plasma, brain, heart, kidney, liver, and spleen after 200 mg/mL of oral dose

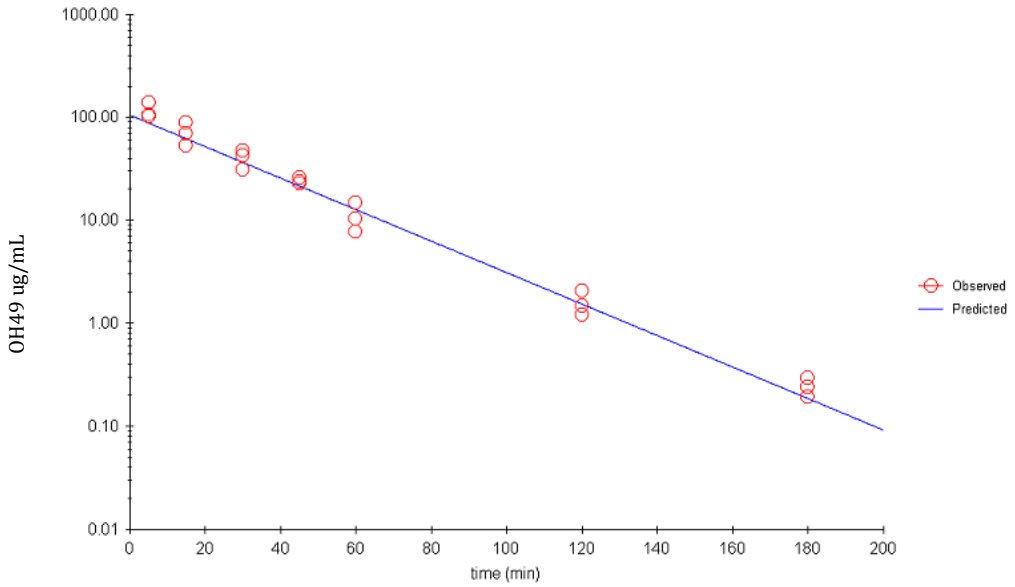

Figure 4.5. Individual plasma concentration after IV administration of OH49 was fitted to one compartment model.

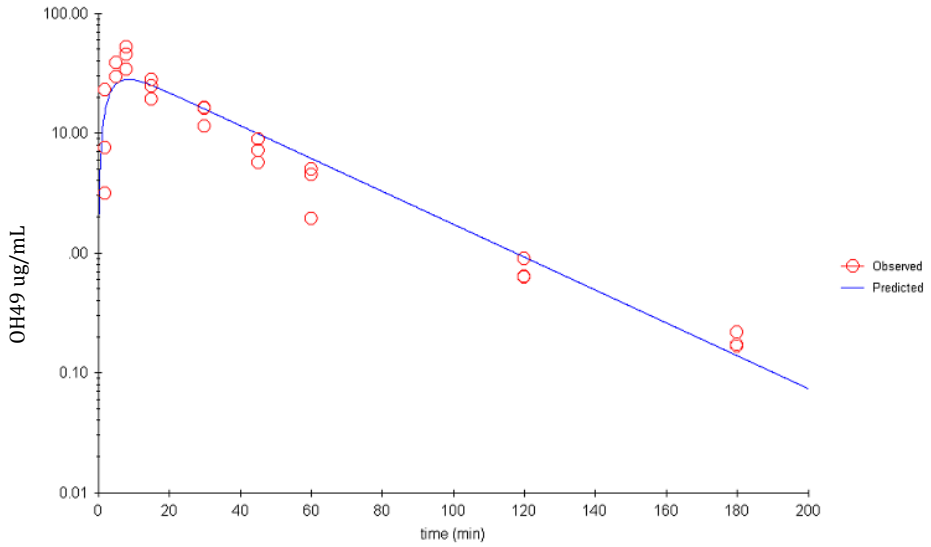

Figure 4.6. Individual plasma concentration after oral administration of OH49 was fitted to one compartment model.

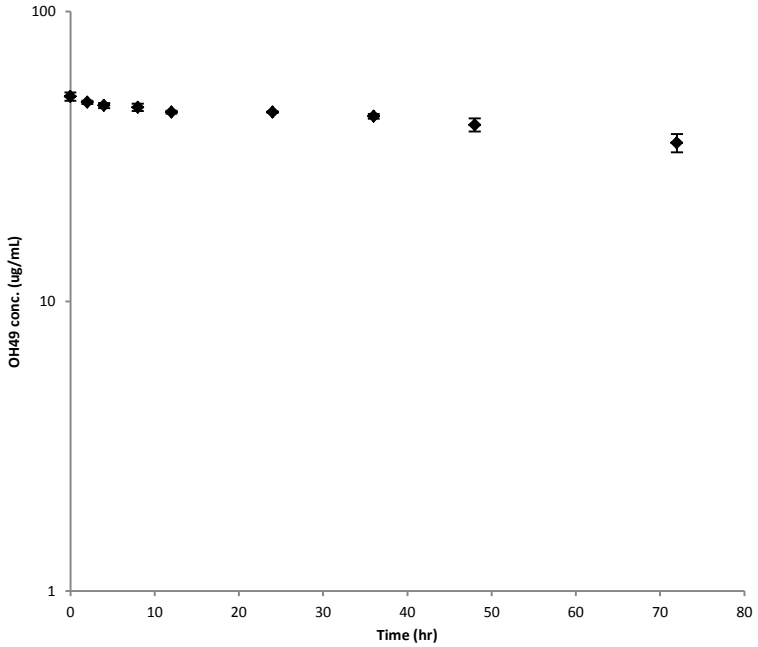

Figure 4.7. The concentration-time profile of OH49 incubated in mouse plasma at 37°C

CHAPTER 5

HIGH-PERFORMANCE LIQUID CHROMATOGRAPHY (HPLC) METHOD DEVELOPMENT AND VALIDATION FOR SIMULTANEOUS QUANTIFICATION OF L-BHDUAND L-BVOddU IN RAT PLASMA*

* Li, Dawei; Catherine A. White. To be submitted to Journal of Chromatography B

ABSTRACT

A reverse phase high-performance liquid chromatography (HPLC) assay was developed and validated for simultaneous quantification of L-β-5-Bromovinyl-(2-hydroxymethyl)-1, 3-(dioxolanyl) uracil (L-BVOddU) and its pro-drug L-β-5-Bromovinyl-[2-(2'-amino-3'-methtyl-butanoyloxy)methyl]-1, 3-(dioxolanyl) uracil (L-BHDU) in rat plasma. This validated assay was applied to an *in vitro* stability study of L-BHDU in human, rat and mouse plasma. The stability study suggested that rat is a better animal model to perform further full *in vivo* pharmacokinetic study, compared to mouse.

Key word: L-nucleoside analog Pro-drug Simultaneous quantification HPLC assay Stability in plasma

INTRODUCTION

Since the first anti-viral nucleoside drug, idoxuridine, was discovered in 1959 [1], nucleoside analogs have played an important role in the battle against various cancers and viral infections. More than 20 anti-viral nucleosides and nucleoside analogs are currently available. The mechanism of action of nucleoside analogs depends on their ability to mimic natural nucleosides, which can interact with viral or cellular enzymes as a competitive inhibitor or an alternate substrate, thus preventing further nucleic acid chain elongation. In biological systems, DNA and RNA are composed of β-D-nucleosides as proteins are composed of L-amino acids. For this reason, it has been widely accepted that only natural D-nucleosides could effectively interact and inhibit metabolic enzymes and exhibit biological activities, owing to the stereospecificity of enzymes in living systems [2, 3]. In the beginning of the 90s, this paradigm was proven not to be true with the discovery of lamivudine (3TC) as a therapeutic agent, which exhibited more potent anti-viral activity compared to the D-counterparts while exhibiting less toxicity [4-7]. This discovery sparked interest to explore the L-nucleosides as potential ant-viral agents. Since then, a large number of L-nucleoside analogs have been synthesized and evaluated for their anti-viral activities [8-12]. From this work, L-nucleoside analogs exhibit favorable features as therapeutic agents, including comparable or greater anti-viral activities than their D-counterparts, more favorable toxicological profiles and better metabolic stability. In the past several years, L-nucleosides have drawn great attention and significant progress has been made in battle against viral infections. Currently, some L-nucleoside analogs, such as lamivudine, emtricitabine and telbivudine, have been applied as treatment for HBV or HIV infections. Others, such as clevudine, elvucitabine,

maribavir, troxacitabine, and valtorcitabine are in clinical trials [13-18]. Most of these reported L-nucleosides focused on the treatment of HIV, HBV or HCV. Little attention has been paid to develop L-nucleosides for treatment of other viruses.

L-β-5-Bromovinyl-(2-hydroxymethyl)-1, 3-(dioxolanyl) uracil (L-BVOddU, Fig. 5.1) is an L-nucleoside analog exhibiting anti-viral activity against HSV-1 and varicella zoster virus (VZV) [19]. In 1994, Bednarski et al. initially synthesized L-BVOddU, which displayed significant activity against HSV-1[20]. L-BVOddU is also the first L-nucleoside that shows potent anti-VZV activity in cell culture with an EC50 value of approximately 0.07 ng /ml, which is about 80-fold greater than acyclovir (ACV) [19, 21]. Some studies suggest that L-BVOddU acts as substrate of virus-encoded thymidine kinase (TKs), and can be phosphorylated only by viral TKs but not by human cytosolic TKs. The monophosphate metabolite inhibits viral DNA synthesis by incorporating into viral DNA as an alternative substrate, which results in the termination of DNA strand elongation and cell death. The inhibitory mechanism of L-BVOddU may be unique and different from other anti-viral nucleoside analogs, which are converted to triphosphate metabolites for anti-viral activities. The high selection of L-BVOddU against VZV depends on the virus-encoded TKs, which phosphorylate the parent compound into active monophosphate metabolite [19]. To improve the conversion rate of L-BVOddU into the active monophosphate metabolite, a valine ester pro-drug L-β-5-Bromovinyl-[2-(2'-amino-3'-methtyl-butanoyloxy)methyl]-1, 3-(dioxolanyl) uracil (L-BHDU, Fig. 5.1) was designed and synthesized. The purpose of this study was to develop and validate an accurate, sensitive and reproducible HPLC method for the quantification of L-BHDU and L-BVOddU simultaneously in rat plasma. The HPLC assay was applied successfully to

study the *in vitro* stability of L-BHDU in human, rat and mouse plasma, which can be used to choose a suitable animal model for further *in vivo* pharmacokinetic evaluation.

EXPERIMENTAL

Chemicals and Reagents

L-BVOddU and L-BHDU were provided by College of Pharmacy, UGA. The chemical structures of L-BVOddU and L-BHDU were identified by nuclear magnetic resonance and mass spectrometry. HPLC grade Acetonitrile (ACN) was purchased from Fisher Scientific Inc. (Pittsburgh, PA, USA). Diazepam was used as the internal standard (IS), and was purchased from Sigma Aldrich (St. Louis, MO, USA). Potassium hydroxide (KOH), phosphoric acid (H3PO4) and monopotassium phosphate (KH2PO4) were obtained from J.T Baker Inc. (Philipsburg, NJ, USA). Heparin was manufactured by Baxter Healthcare Corporation (Deerfield, IL, USA). Water used throughout the study was purified with a Milli-Q water purification system from Millipore (Millipore, Bedford, MA, USA). Other reagents were analytical grade.

Preparation of stocks, Standard Solutions

Stock solutions of 10 mg/mL L-BVOddU, L-BHDU and the internal standard were individually prepared in acetonitrile. Standard solutions of L-BVOddU and L-BHDU were prepared from the stock solution by serial dilution with acetonitrile. The final concentrations of the standard solutions were 1000, 500, 100, 50, 10, 5 and 1 μg/ml for L-BVOddU and 1000, 500, 100, 50, 10, 5 and 2.5 μg/ml for L-BHDU. Quality control solutions with concentrations of high (600 ug/mL), medium (60 ug/mL) and low (6 ug/mL) were prepared in duplication from 10 mg/ml stock with. The internal standard solution was prepared by mixing and diluting the appropriate amounts from the stock

solutions with acetonitrile. The final concentration was 1 mg /mL. All of the solutions were stored in brown glass bottles at -80°C until use. Fresh standard solutions were prepared each day for analysis and validation.

Preparation of standards, quality control samples

Blank Sprague-Dawley rat plasma was purchased from Innovative Research (Novi, MI, USA). Calibration standards of plasma were prepared by spiking 10 μL of the L-BVOddU and L-BHDU standard solutions and the internal standard working solution to 100 μL of blank plasma. The calibration curve of plasma was in the range of 0.1-100 ug/mL of L-BVOddU and 0.25-100 ug/mL of L-BHDU, with an internal standard concentration in each sample of 100 μg/mL. Quality-control samples (QCs) were prepared with blank plasma at low (0.6 ug/mL), medium (6 ug/mL) and high (60 ug/mL) concentrations. The calibration standards and QCs were extracted on each day of the analysis with the procedure described below.

Sample Preparation

To each standard, blank and QC sample, 3 volumes of ice cooled acetonitrile were added for protein precipitation and extraction. After mixing vigorously on a vortex shaker for 10 min, the samples were centrifuged at 13000 rpm for 10 min at 4°C. The clear supernatants were collected, and 40 uL of the solution was injected for HPLC analysis.

Chromatographic System

HPLC analysis was performed an Agilent 1100 series system (Santa Clara, CA, USA) equipped with a variable wavelength UV detector, an on-line degasser, a quaternary gradient pump, an autosampler and a column oven. A Phenomenex Luna C18 column (250 x 4.6 mm, 5u particle size), protected by a Phenomenex C18 guard column

(Torrance, CA, USA) was used to achieve chromatographic separation. Data acquisition was performed using the chemstation chromatography software package.

Chromatographic Conditions

The column temperature was held at room temperature. The mobile phase was comprised of solution A (20 mM KH2PO4, pH= 7.0) and solution B (acetonitrile). Initially, the mobile phase was kept isocratic for 3 min with the composition 59:41 (v/v) of solutions A/B, and was changed linearly to 25:75 (v/v) from 3 min to 5 min, then kept the composition until 7 min. From 7 to 8 min, the mobile phase was changed to the initial composition, and kept for 3 min before the next injection. The mobile phase flow rate was 1.0 ml/min and the UV detection wavelength was set at 260 nm. The HPLC run time for each sample was 11 min. L-BVOddU, L-BHDU and the internal standard eluted at 4.2 min, 6.6 min, and 9.5 min, respectively.

Method validation

Linearity, Precision and accuracy

The linearity of the HPLC method for the quantification of L-BVOddU and L-BHDU were evaluated by a calibration curve for rat plasma with the range of 0.1-100 μg/mL and 0.25-100 ug/mL. Calibration curves were constructed by the plotting peak area ratio (y-axis) of the analyte to the internal standard versus the nominal concentrations (x-axis) with a weighting (1/y) least-squares linear regression.

To evaluate the precision and accuracy, QC samples (n = 5) at low (0.6 ug/mL), medium (6 ug/mL), and high (60 ug/mL) concentrations were processed and injected on a single day (intra-day) and on three consecutive days (inter-day). Each day, a freshly prepared calibration curve was constructed when the QC samples were extracted. The

precision was reported as the relative standard deviation (RSD %) which was calculated by the ratio of standard deviations of replicates to the mean concentrations. The accuracy was expressed as the relative error (RE %) which is the % bias of theoretical versus calculated concentrations. For a validated method, the precision of all the measurements should be less than or equal to15%, and the accuracy should be within the limits of ±15%.

Recovery and LLOQ

The absolute recoveries of L-BVOddU and L-BHDU from rat plasma were determined by comparing the peak area of the analyte extracted from QC samples to those of pure compound in the mobile phase at the same concentration. Five repetitions were carried out on QC samples spiked with LLOQ, low, medium and high concentration of analytes. The lower limit of quantification (LLOQ) was defined as the lowest concentration on the calibration plot with a precision of less than 20% and an accuracy (RE %) within ± 20% [22].

Stability

Autosampler stability (25°C, 8 h), bench-top stability (4°C, 4 h) and freeze-thaw stability (3 freeze-thaw cycles, -80°C, 72 h) in plasma were tested for the analyte at both low (0.6 ug/mL) and high (60 ug/mL) concentrations (n = 5).The bench-top stability of spiked plasma stored at 4°C was evaluated for 4 h. The freeze-thaw stability was investigated by comparing the stability samples following three freeze-thaw cycles, against freshly spiked samples. The autosampler stability was evaluated by comparing the extracted plasma or tissue samples that were injected immediately, with the samples that were re-injected after storage in the autosampler for up to 8 h.

Stability of the pro-drug (L-BHDU) in mouse, rat and human plasma

The stability of the pro-drug in mouse, rat and human plasma (Bioreclamation LLC, Westbury, NY, USA) was investigated by a modified method described previously [23, 24]. Briefly, 1.0 mL of plasma (n=3/species) were pre-incubated for 30 min at 37 °C followed by spiking of 10 μL of a 5.0 mg/mL stock solution of L-BHDU. Aliquots (50 μL) were withdrawn at 0, 10, 30, 60, 90, 120, 180, and 360 min and immediately quenched with 150 uL of ice cooled acetonitrile for protein precipitation. After mixing vigorously on a vortex shaker for 10 min, the samples were centrifuged at 13000 rpm for 10 min at 4°C. The clear supernatants were collected and stored at -80°C until analyzed. The samples were analyzed for L-BHDU concentration by using the HPLC method described above. The concentration-time profile of L-BHDU in mouse, rat and human plasma were plotted, which was used to evaluate the stability of the pro-drug in different plasma.

RESULTS AND DISCUSSION

Chromatographic method development

To perform pharmacokinetic or other *in vitro* and *in vivo* studies of L-BHDU, an accurate, sensitive and reproducible HPLC method for quantification of L-BHDU and L-BVOddU simultaneously was necessary. When developing the HPLC assay, different sample preparation processes, columns, mobile phase and gradient programs were evaluated. By comparing the chromatographic factors including good peak shapes, high sensitivities, and totally separation of analytes, the internal standard and endogenous components, the method was ultimately optimized as the condition described above. Fig. 5.2 shows the typical chromatograms of blank and spiked rat plasma. By comparing the

blank and spiked chromatograms, no interfering peaks from endogenous components were observed where L-BVOddU, L-BHDU and the internal standard were eluted, indicating good specificity and selectivity for this assay. Under these chromatographic conditions, L-BVOddU, L-BHDU and the internal standard were well separated, and eluted at 4.2 min, 6.6 min, and 9.5 min, respectively.

L-BHDU is a valine ester pro-drug, which is sensitive to the hydrolysis activity of esterases in plasma. The hydrolyzation of L-BHDU would greatly affect the precision and accuracy for quantification of the pro-drug and the parent compound. To prevent hydrolyzation of the valine ester pro-drug, all processes were kept on ice and maintained at 4°C, when sample preparation was performed.

Method validation

Linearity and range

The linearity of the calibration curves for L-BVOddU and L-BHDU were calculated using a least square regression method. The linear range of L-BVOddU and L-BHDU were 0.1-150 ug/mL and 0.25-150 ug/mL, respectively. As shown in Table 5.1, the coefficient of determination (R^2) of L-BVOddU and L-BHDU calibration curves in rat plasma are greater than 0.999; the coefficient of variations of slopes for all calibration curves are less than 5%. These results suggested a high precision of the present assay.

Precision and accuracy

The intra- and inter-day precision and accuracy of the assay were calculated from 3QC standard and LLOQ samples. Precision is reported as percent relative standard deviation (RSD %) and accuracy is reported as relative error (RE %). RSD and RE values for L-BVOddU and L-BHDU are shown in Table 5.2. The intra-assay RSD and RE for

all QC standard and LLOQ samples are less than15%, which met the FDA requirements and suggested the high reliability and reproducibility of the assay.

Recovery

The absolute recoveries of L-BVOddU and L-BHDU from plasma are listed in Table 5.3. For L-BVOddU, at the concentration range of 0.1-60 ug/mL, more than 95% of L-BVOddU is recovered after the sample preparation. For L-BHDU, at the concentration range of 0.25-60 ug/mL in plasma, the absolute recoveries were 95.9-98.2%. The coefficient of variations of the recoveries are less than 5% for each concentration.

Stability

Stability of L-BVOddU and L-BHDU in plasma was investigated under a variety of storage and processing conditions, including bench-top stability (4°C, 4 h) freeze-thaw stability (3 freeze-thaw cycles, -80°C, 72 h) and autosampler stability (25°C, 8 h). As shown in Table 5.4, the RSD % and RE % of all samples are less than 15%, which indicates L-BVOddU and L-BHDU in mouse plasma and tissue homogenates are stable in terms of autosampler, bench-top and freeze-thaw stability.

In-vitro stability of L-BHDU in mouse, rat and human plasma

L-BHDU is a valine ester pro-drug, which is sensitive to the hydrolysis activity of esterases that are widely distributed in tissues, especially in the intestine, liver and plasma. Previous studies suggested that esterases play a major role in drug metabolism and pro-drug activation [25-28], and exhibit significant species difference [29-31]. It is necessary to evaluate the stability of L-BHDU in plasma of different species *in vitro*. The concentration-time profile of L-BHDU incubated in mouse, rat and human plasma up to

360 min are shown in Fig. 5.3. The concentration of L-BHDU declined quickly in mouse plasma; while the concentration-time profiles of L-BHDU in rat and human plasma exhibited relatively similar pattern. This result suggests that mouse plasma presents the highest esterase activity and rat plasma has higher esterase activity than human plasma, which is consistent with published data (30-32). Other studies demonstrated that the esterase activity in the liver and intestine from mouse, rat and human have a similar pattern with that of plasma (29, 30). The hydrolysis of L-BHDU by esterase may affect the pharmacokinetics of this compound. There are significant species differences of esterase activity in different tissues. Therefore, when choosing a pre-clinical animal model to perform pharmacokinetic study, the rat should be considered as preferred animal model compared to mouse. The data also showed that L-BHDU is relatively stable in human plasma in vitro, which is a desired property for anti-viral activity. L-BHDU is designed to be more easily metabolized into the active monophosphate metabolite. Once hydrolyzed into L-BVOddU by esterase *in vivo*, it will be more difficult to be converted into active metabolite. The stability of L-BHDU in human plasma may improve its conversion rate, resulting in increased efficacy of the compound.

CONCLUSIONS

A rapid HPLC method was developed for quantification of the pro-drug (L-BHDU) and the parent compound (L-BVOddU) simultaneously in rat plasma. This method showed high sensitivity, reliability, and specificity, with a total run time of 11 min per sample. This method was successfully applied to evaluate the *in vitro* stability of L-BHDU in mouse, rat and human plasma. The *in vitro* stability study showed that the stability profile of L-BHDU in rat plasma is more similar to that in human plasma, which

suggested that for this compound, rat is a better animal model to perform further *in vivo* pharmacokinetic study compared to mouse.

REFERENCES

1. Prusoff, W.H. Synthesis and biological activities of iododeoxyuridine, an analog of thymidine. Biochim Biophys Acta. 1959. 32(1): 295-6.

2. Focher F, Spadari S, Maga G. Antivirals at the mirror: the lack of stereospecificity of some viral and human enzymes offers novel opportunities in antiviral drug development. Curr Drug Targets Infect Disord. 2003. 3(1):41-53.

3. Jaeger KE, Eggert T. Enantioselective biocatalysis optimized by directed evolution. Curr Opin Biotechnol. 2004. 15 (4): 305-13.

4. Coates JA, Cammack N, Jenkinson HJ, Mutton IM, Pearson BA, Storer R, Cameron JM, Penn CR. The separated enantiomers of 2'-deoxy-3'-thiacytidine (BCH-189) both inhibit human immunod-eficiency virus replication *in vitro*. Antimicrob. Agents Chemother. 1992;36:202-5.

5. Furman, P. A., Davis, M., Liotta, D. C., et al. The anti-hepatitis B virus activities, cytotoxicities, and anabolic profiles of the (-) and (+) enantiomers of cis-5-fluoro-1-[2-(hydroxymethyl)-1,3-oxathiolan-5-yl]cytosine (FTC). Antimicrob. Agents Chemother. 1992. 36:2686-92.

6. Furman, P. A., Wilson , J. E., Reardon , J. E., Painter, G. R. The effect of absolute configuration on the anti-HIV and anti-HBV activity of nucleoside analogs. Antiviral Chem. Chemother. 1995. 6:345-355.

7. Jarvis B, Faulds D. Lamivudine. A review of its therapeutic potential in chronic hepatitis B. Drugs. 1999. 58(1):101-41.

8. Balakrishna Pai S, Liu SH, Zhu YL, Chu CK, Cheng YC. Inhibition of hepatitis B virus by a novel L-nucleoside, 2'-fluoro-5-methyl-beta-L-arabinofuranosyl uracil. Antimicrob Agents Chemother. 1996. 40(2):380-6.

9.Le Guerhier F, Pichoud C, Jamard C, Guerret S, Chevallier M, Peyrol S, Hantz O, King I, Trépo C, Cheng YC, Zoulim F. Antiviral activity of beta-L-2',3'-dideoxy-2',3'-didehydro-5-fluorocytidine in woodchucks chronically infected with woodchuck hepatitis virus. Antimicrob Agents Chemother. 2001. 45(4):1065-77.

10. Chen H, Pai SB, Hurwitz SJ, Chu CK, Glazkova Y, McClure HM, Feitelson M, Schinazi RF. Antiviral activity and pharmacokinetics of 1-(2,3-dideoxy-2-fluoro-beta-L-glyceropent-2-enofuranosyl)cytosine. Antimicrob Agents Chemother. 2003. 47(6):1922-8.

11. Jessel S, Meier C. Carbocyclic L-nucleoside analogs as potential antiviral agents. Nucleic Acids Symp Ser (Oxf). 2008. (52): 615-6.

12. Zhang HW, Deto rio M, Herman BD, Solomon S, Bassit L, Nettles JH, Obikhod A, Tao SJ, Mellors JW, Sluis-Cremer N, Coats SJ, Schinazi RF. Synthesis, antiviral activity, cytotoxicity and cellular pharmacology of l-3'-azido-2',3'-dideoxypurine nucleosides. Eur J Med Chem. 2011. 46(9):3832-44.

13. Lalezari JP, Aberg JA, Wang LH, Wire MB, Miner R, Snowden W, Talarico CL, Shaw S, Jacobson MA, Drew WL. Phase I dose escalation trial evaluating the pharmacokinetics, anti-human cytomegalovirus (HCMV) activity, and safety of

1263W94 in human immunodeficiency virus-infected men with asymptomatic HCMV shedding. Antimicrob Agents Chemother. 2002. 46(9):2969-76.

14. S.G. Lim, C.L. Lai, M. Myers, M.F. Yuen, C.T. Wai, D. Lloyd, K. Pietropaolo, X.J. Zhou, G. Chao, N.A. Brown. Final Results of a Phase I/II Dose Escalation Trial of Valtorcitabine LdC) in Patients with Chronic Hepatitis B. Presented at the 40th Annual Meeting of the European Association for the Study of the Liver. Paris, France. 2005. April 13-17.

15. Vose JM, Panwalkar A, Belanger R, Coiffier B, Baccarani M, Gregory SA, Facon T, Fanin R, Caballero D, Ben-Yehuda D, Giles F. A phase II multicenter study of troxacitabine in relapsed or refractory lymphoproliferative neoplasms or multiple myeloma. Leuk Lymphoma. 2007. 48(1):39-45.

16. Chan HL, Heathcote EJ, Marcellin P, Lai CL, Cho M, Moon YM, Chao YC, Myers RP, Minuk GY, Jeffers L, Sievert W, Bzowej N, Harb G, Kaiser R, Qiao XJ, Brown NA; 018 Study Group. Treatment of hepatitis B e antigen positive chronic hepatitis with telbivudine or adefovir: a randomized trial. Ann Intern Med. 2007. 147(11):745-54.

17. DeJesus E, Saple D, Morales-Ramirez J, et al. Elvucitabine phase II 48 week interim results show safety and efficacy profiles similar to lamivudine in treatment naive HIV-1 infected patients with unique pharmacokinetic profile [abstract H-892]. Presented at the 48th Annual ICAAC/IDSA 46th Annual Meeting. Washington, DC: 2008. Oct 25-28

18. Kim SB, Song IH, Kim YM, Noh R, Kang HY, Lee HIe, Yang HY, Kim AN, Chae HB, Lee SH, Kim HS, Lee TH, Kang YW, Lee ES, Kim SH, Lee BS, Lee HY. Long-term treatment outcomes of clevudine in antiviral-naive patients with chronic hepatitis B. World J Gastroenterol. 2012. 18(47):6943-50.

19. Li L, Dutschman G E., Gullen E A., Tsujii E, Grill S P., Choi Y, Chu C K., and Cheng Y (2000) Metabolism and mode of inhibition of varicella-zoster virus by L- β -5-bromovinyl-(2-hydroxymethyl)-(1,3-dioxolanyl)uracil is dependent on viral thymidine kinase, Mol Pharmacol 58:1109-14.

20. Bednarski K, Dixit D, Wang W, Evans CA, Jin H, Yuen L and Mansour TS. Inhibitory activities of herpes simplex virus type 1 and 2 and human cytomegalovirus by stereoisomers of 29-deoxy-39-oxa-5(E)-(2-bromovinyl) uridines and their 49-thio analogues. Bioorg Med Chem Lett. 1994. 4:2667-72.

21. Choi Ys. Li L, Grill S, Gullen E, Lee CS, Gumina G. Structure-activity relationships of (E)-5-(2-bromovinyl)uracil and related pyrimidine nucleosides as ant-viral agents for herpes viruses. J Med Chem. 2000. 43:2538-46.

22. U. S. Department of Health and Human Services, Food and Drug Administration, Guidance for Industry, Bioanalytical Method Validation, May 2001, http://www.fda.gov/CDER/GUIDANCE/4252fnl.pdf.

23. Zhimeng Wu, John C. Drach, Mark N. Prichard, Milka Yanachkova, Ivan Yanachkov, Terry L. Bowlin, Jiri Zemlicka: L-Valine Ester of Cyclopropavir - a New Ant-viral Prodrug. Antivir Chem Chemother. 2009. 20(1): 37-46.

24. McDonnell ME, Vera MD, Blass BE, Pelletier JC, King RC, Fernandez Metzler C, Smith GR, Wrobel J, Chen S, Wall BA and Reitz AB. Riluzole prodrugs for melanoma and ALS: Design, synthesis, and *in vitro* metabolic profiling. Bioorg Med Chem. 2012. 20(18):5642-8.

25. Kamendulis LM, Brzezinski MR, Pindel EV, Bosron WF, Dean RA. Metabolism of cocaine and heroin is catalyzed by the same human liver carboxylesterases. J Pharmacol Exp Ther. 1996. 279(2):713-7.

26. Ettmayer, G. L. Amidon, B. Clement, and B. Testa. Lessons learned from marketed and investigational pro-drugs. J. Med. Chem. 2004. 47:2393-2404

27. Liederer BM, Borchardt RT. Enzymes involved in the bioconversion of ester-based prodrugs. J Pharm Sci. 2006. 95(6):1177-95.

28. Watanabe A, Fukami T, Takahashi S, Kobayashi Y, Nakagawa N, Nakajima M, Yokoi T. Arylacetamide deacetylase is a determinant enzyme for the difference in hydrolase activities of phenacetin and acetaminophen. Drug Metab Dispos. 2010. 38(9):1532-7.

29. Inoue M, Morikawa M, Tsuboi M, Sugiura M. Species difference and characterization of intestinal esterase on the hydrolizing activity of ester-type drugs. Jpn J Pharmacol. 1979. 29(1):9-16.

30. Berry LM, Wollenberg L, Zhao Z. Esterase activities in the blood, liver and intestine of several preclinical species and humans. Drug Metab Lett. 2009. 3(2):70-7.

31. Bahar FG, Ohura K, Ogihara T, Imai T. Species difference of esterase expression and hydrolase activity in plasma. J Pharm Sci. 2012. 101(10):3979-88.

32. Rudakova EV, Boltneva NP, Makhaeva GF. Comparative analysis of esterase activities of human, mouse, and rat blood. Bull Exp Biol Med. 2011 Nov; 152(1):73-5.

Table 5.1. Linear regression equations generated from validation data of L-BVOddU and L-BHDU in rat plasma; slope (mean± s.d.), intercept (mean± s.d.), coefficient of determination (mean± s.d.).

Analyte	Slope	Intercept	R^2
L-BVOddU	111.7 ± 0.9	-0.2 ± 0.1	0.9998 ± 0.0002
L-BHDU	177.8 ± 0.3	-0.04 ± 0.008	0.9996 ± 0.0002

Table 5.2. Intra-day (n=5) and Inter-day (n=15) precision (RSD %) and accuracy (RE %) of the HPLC assay for quantification of L-BVOddU and L-BHDU in rat plasma.

L-BVOddU Conc. (ug/mL)	Intra-day (n=5)			Inter-day (n=15)		
	Conc. observed (ug/mL)	RSD (%)	RE (%)	Conc. observed (ug/mL)	RSD (%)	RE (%)
0.1	0.10 ± 0.009	9.10	3.13	0.10 ± 0.009	8.45	2.76
0.6	0.65 ± 0.03	5.06	8.68	0.62 ± 0.04	6.13	3.62
6	6.16 ± 0.04	0.62	2.75	6.09 ± 0.11	1.85	1.58
60	59.12 ± 0.92	1.56	-1.46	59.85 ± 1.25	2.08	-0.25

L-BHDU Conc. (ug/mL)	Intra-day (n=5)			Inter-day (n=15)		
	Conc. observed (ug/mL)	RSD (%)	RE (%)	Conc. observed (ug/g)	RSD (%)	RE (%)
0.25	0.26 ± 0.01	3.28	4.67	0.26 ± 0.01	4.59	3.22
0.6	0.61 ± 0.03	5.25	2.19	0.64 ± 0.03	4.58	6.09
6	5.96 ± 0.05	0.86	-0.67	6.04 ± 0.11	1.79	0.64
60	57.64 ± 0.42	0.73	-3.94	58.81 ± 1.24	2.12	-2.00

Table 5.3. Absolute recoveries of L-BVOddU and L-BHDU from rat plasma (mean ± s.d., n=15).

L-BVOddU Conc. (ug/mL)	Absolute recovery (%)	L-BHDU Conc. (ug/mL)	Absolute recovery (%)
0.1	97.9 ± 1.2	**0.25**	98.2 ± 2.0
0.6	97.0 ± 0.3	**0.6**	97.3 ± 2.3
6	96.5 ± 3.0	**6**	95.9 ± 2.3
60	95.6 ± 1.0	**60**	96.5 ± 2.3

Table 5.4. Autosampler stability (n = 5), bench-top stability (n = 5) and freeze-thaw stability (n =5) of L-BVOddU and L-BHDU at 0.6 and 60.0 ug/mL concentrations in rat plasma.

L-BVOddU:

Stability	Spiked conc. (ug/mL)	Conc.observe (ug/mL)	RSD %	RE %
Three freeze-thaw cycles	0.6	0.62 ± 0.04	5.8	3.5
	60	61.9 ± 1.4	2.3	3.2
Bench-top (4h)	0.6	0.61 ± 0.04	6.8	2.5
	60	63.4 ± 2.1	3.3	5.7
Auto-sampler (8h)	0.6	0.6 ± 0.03	5.6	0.7
	60	62.8 ± 4.7	7.5	4.8

L-BHDU:

Stability	Spiked conc. (ug/mL)	Conc.observe (ug/mL)	RSD %	RE %
Three freeze-thaw cycles	0.6	0.58 ± 0.04	7.1	-2.9
	60	60.4 ± 2.4	4.0	0.7
Bench-top (4h)	0.6	0.63 ± 0.04	6.5	5.4
	60	60.4 ± 3.0	4.9	0.7
Auto-sampler (8h)	0.6	0.59 ± 0.05	8.0	-1.2
	60	58.6 ± 3.3	5.6	-2.2

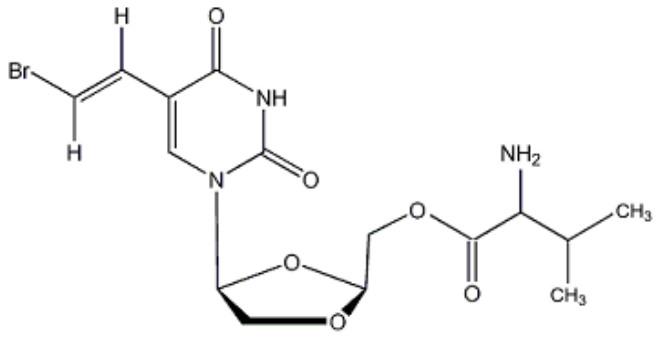

L-BHDU

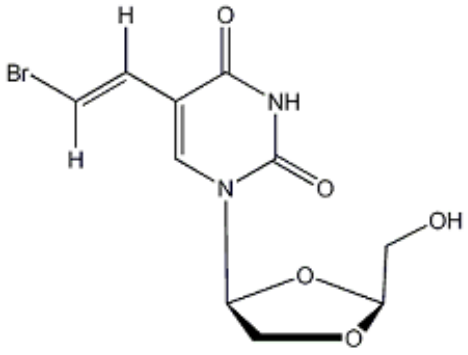

L-BVOddU

Figure 5.1. Chemical structure of L-BVOddU and L-BHDU

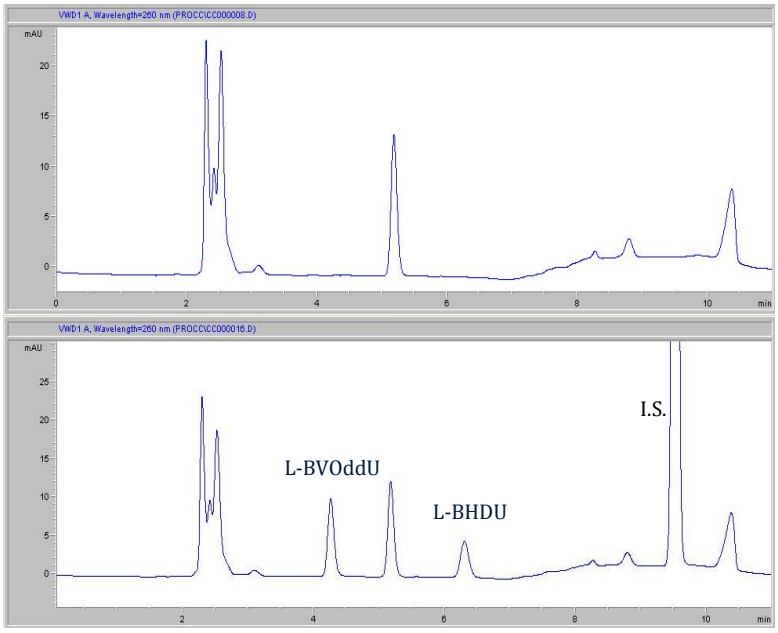

Figure 5.2. Representative HPLC chromatograms of blank (top) and spiked* (bottom) rat plasma.

*plasma was spiked with 2 ug/mL L-BVOddU, L-BHDU and 100 ug/mL IS

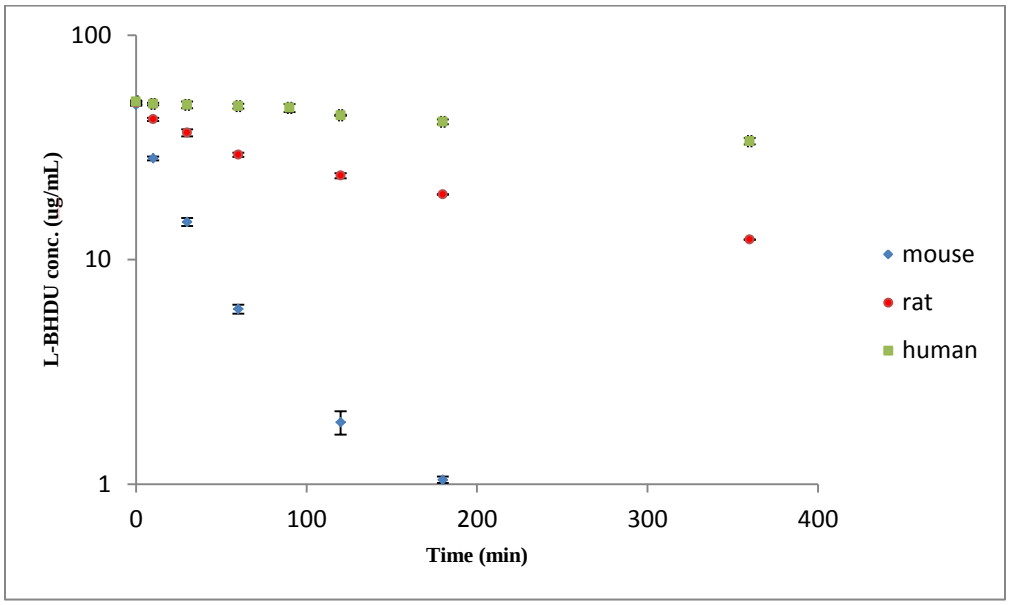

Figure 5.3. Concentration vs. time profiles of L-BHDU in mouse, rat and human plasma incubated at 37°C

CHAPTER 6

CONCLUSIONS

Pharmacokinetics is one of the most important attributes of a drug. Suboptimal pharmacokinetics is stated to be one of main reasons for failures during drug development. It has been estimated that about 40% of candidate compounds failed in clinical trials due to poor pharmacokinetic behavior. Therefore, it is important to perform pharmacokinetic evaluations at the earliest possible stages of drug discovery before entering costly full development programs in clinical testing.

Traditionally, "preclinical pharmacokinetics" refers to pharmacokinetics in animals. To date, the definition has expanded to all *in vivo* and *in vitro* pharmacokinetic activities supporting drug development. These preclinical pharmacokinetic activities include *in vitro* pharmacokinetic evaluations at the discovery stage that facilitates selection of lead compounds and preclinical pharmacokinetic studies in animals. The goal of these pharmacokinetic activities is to improve failure detection in the early stages of drug discovery which will significantly reduce the total R&D costs of drug development.

Preclinical pharmacokinetic and tissue distribution study of (1-Decyl) triphenylphosphonium bromide (dTPP) following oral, IV and subcutaneous administration was performed. A simple, rapid and sensitive HPLC assay was developed and validated for the quantification of dTPP in mouse plasma and tissues. This assay was successfully used to determine the pharmacokinetic characteristics of dTPP in mice. The pharmacokinetic studies indicated that dTPP has a fairly low bioavailability and was rapidly cleared from plasma. dTPP is extensively distributed in tissues such as, brain,

heart, intestine, kidney, liver, lung, muscle, and spleen after IV and subcutaneous administration. Therefore, oral administration may be used to treat intestinal infection caused by parasites. IV and subcutaneous injections may work as alternative routes of administration to treat systemic infections.

A preclinical pharmacokinetic and tissue distribution study of 2-(Hydroxymethyl)phenylboronic acid cyclic monoester (OH49), an aryl boronic acid analog, with anti-tuberculosis activity was conducted. A simple, rapid and sensitive HPLC assay was developed and validated for quantification of OH49 in mouse plasma and tissues. The pharmacokinetic and tissue distribution studies were performed in mice following oral and IV administration to evaluate the pharmacokinetic characteristics of OH49. The results suggested that OH49 was rapidly absorbed after oral administration, had a bioavailability of 28.3%, a short elimination half-life, rapid clearance from the body and wide tissue distribution. The *in vitro* study suggested that OH49 was stable in mouse plasma, which is mainly due to the stable oxaborole ring and boron-carbon bond of this compound.

L-β-5-Bromovinyl-[2-(2'-amino-3'-methtyl-butanoyloxy)methyl]-1, 3-(dioxolanyl) uracil (L-BHDU) is a pro-drug of an anti-viral agent, L-β-5-Bromovinyl-(2-hydroxymethyl)-1, 3-(dioxolanyl) uracil (L-BVOddU), which is a L-nucleoside analog. This pro-drug was designed to improve the conversion rate of L-BVOddU into the active monophosphate metabolite by coupling a valine ester group. A simple, rapid and sensitive HPLC assay was developed and validated for quantification of L-BHDU and L-BVOddU simultaneously in rat plasma. An *in vitro* stability study of L-BHDU was performed in human, rat and mouse plasma by using the validated HPLC assay. The

stability study suggested that the rat was a better animal model to perform further pharmacokinetic evaluations for this compound.